NASA-CR-195501

NASW-4435

NAVAL POSTGRADUATE SCHOOL
Monterey, California

(NASA-CR-195501) CONCEPTUAL DESIGN PROPOSAL: HUGO GLOBAL RANGE/MOBILITY TRANSPORT AIRCRAFT (Naval Postgraduate School) 116 p

N94-24787

Unclas

G3/05 0204252

CONCEPTUAL DESIGN PROPOSAL

GLOBAL MOBILITY PLATFORM

" HUGO "

GLOBAL TRANSPORT, INC.

March 1993

Project Advisor: Prof. C. F. Newberry

AIAA/McDonnell Douglas

Graduate Team Aircraft Design Competition

HUGO Global Range/Mobility Transport Aircraft

Global Transport, Inc.

Design Team

	AIAA #
LCDR Tom Johnston	(107280)
LT Dave Perretta	(107283)
LT Doug McBane	(107281)
LT Greg Morin	(107277)
LT Greg Thomas	(107275)
LT Joe Woodward	(107278)
LT Steve Gulakowski	(107282)

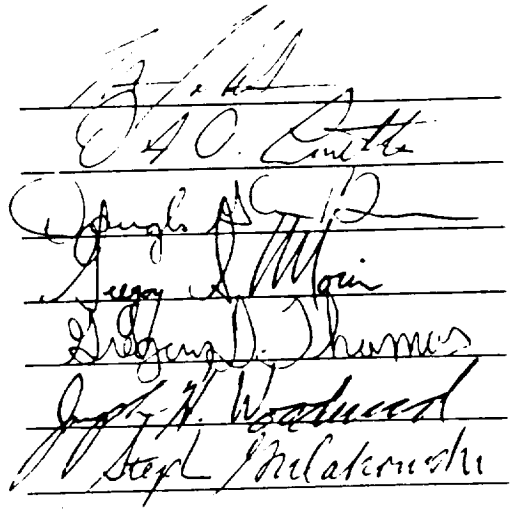

Project Advisor: C. F. Newberry

Faculty Advisor: M. F. Platzer

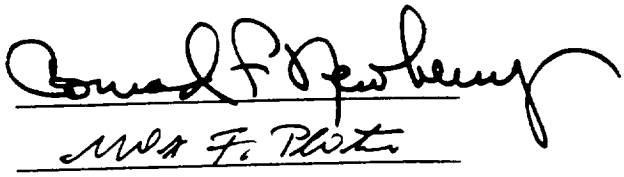

TABLE of CONTENTS

I. OVERVIEW

A. BACKGROUND

With the collapse of the former Soviet Union and the emergence of the United Nations actively pursuing a peace keeping role in world affairs, the United States has been forced into a position as the world's leading peace enforcer. It is still a very dangerous world with seemingly never ending ideological, territorial and economic disputes requiring the U.S. to maintain a credible deterrent posture in this uncertain environment. This has created an urgent need to rapidly transport large numbers of troops and equipment from the Continental United States (CONUS) to any potential world trouble spot by means of a global range/mobility transport aircraft. The most recent examples being Operation Desert Shield/Storm and Operation Restore Hope.

To meet this challenge head-on, a Request for Proposal (RFP) was developed and incorporated into the 1992/1993 AIAA/McDonnell Douglas Corporation Graduate Team Aircraft Design Competition. The RFP calls for the conceptual design and justification of a large aircraft capable of power projecting a significant military force without surface transportation reliance.

B. REQUEST FOR PROPOSAL (RFP)

1. Requirements and Restraints

The following specifications were required by the RFP.

a. Maximize the amount of material that could be transported in 72 hours of continuous operation by a fleet of global transports based in the United States to any location in the world.

b. Minimize the delivery cost.

c. Minimum unfueled range should be 6,000 nautical miles.

d. Minimum payload should be 400,000 pounds at a Minimum maneuver load factor of 2.5 g's.

e. Must be able to operate from existing domestic airbases and be able to use existing airbases or sites of opportunity at the destination.

(1) Critical U.S. field length is 10,000 feet.

(2) Critical destination field length is 8,000 feet, 4,000 foot elevation, and 95°F.

f. The aircraft must meet all MIL-SPEC and FAR Part 25 requirements.

g. Technology available date (TAD) would be 2010.

h. Planned initial operational capability (IOC) would be 2015.

2. Primary Mission Profile.

The RFP design mission profile, Figure I-1, consisted of:

a. Warm-up and 15 minute taxi.

b. Takeoff and climb to best cruise altitude.

c. Cruise at best altitude and Mach # to destination.

d. Descend on course and land.

(1) Only one aircraft on deck at a time to minimize attack risk.

e. Taxi/Idle for 30 minutes.

(1) Offload full payload and load 15% of full payload.

f. Takeoff and climb to best cruise altitude.

g. Return at best cruise altitude and Mach.

h. Loiter 15 minutes (15 minutes reserve fuel).

i. Descend, land, and 10 minutes taxi.

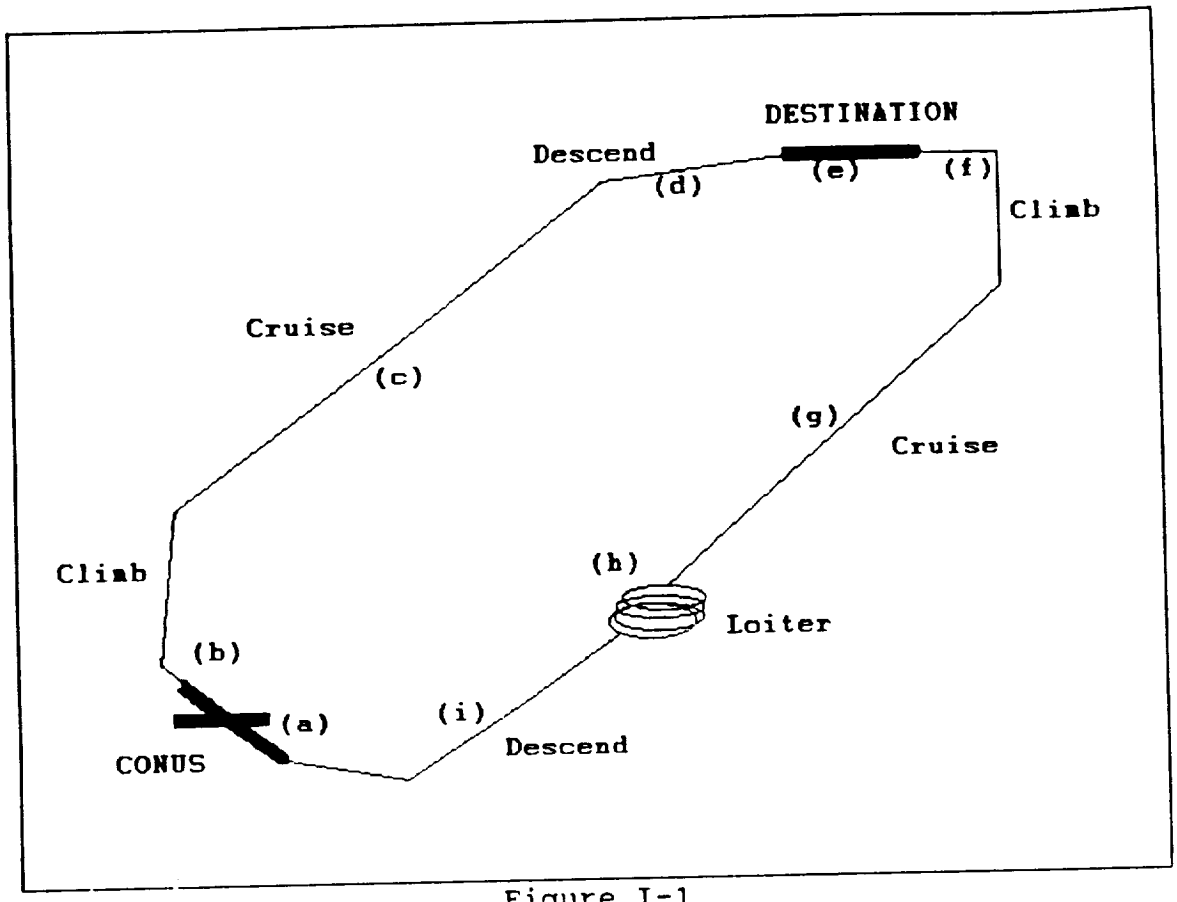

Figure I-1
Primary Mission Profile

C. DESIGN TEAM ORGANIZATION

A design team was established at Global Transport, Inc. with the objective of exploring the effect on varying basic performance specifications for a global range military transport aircraft. The team eventually decided on HUGO as the design concept. The teams organization and areas of responsibility are indicated in Figure I-2.

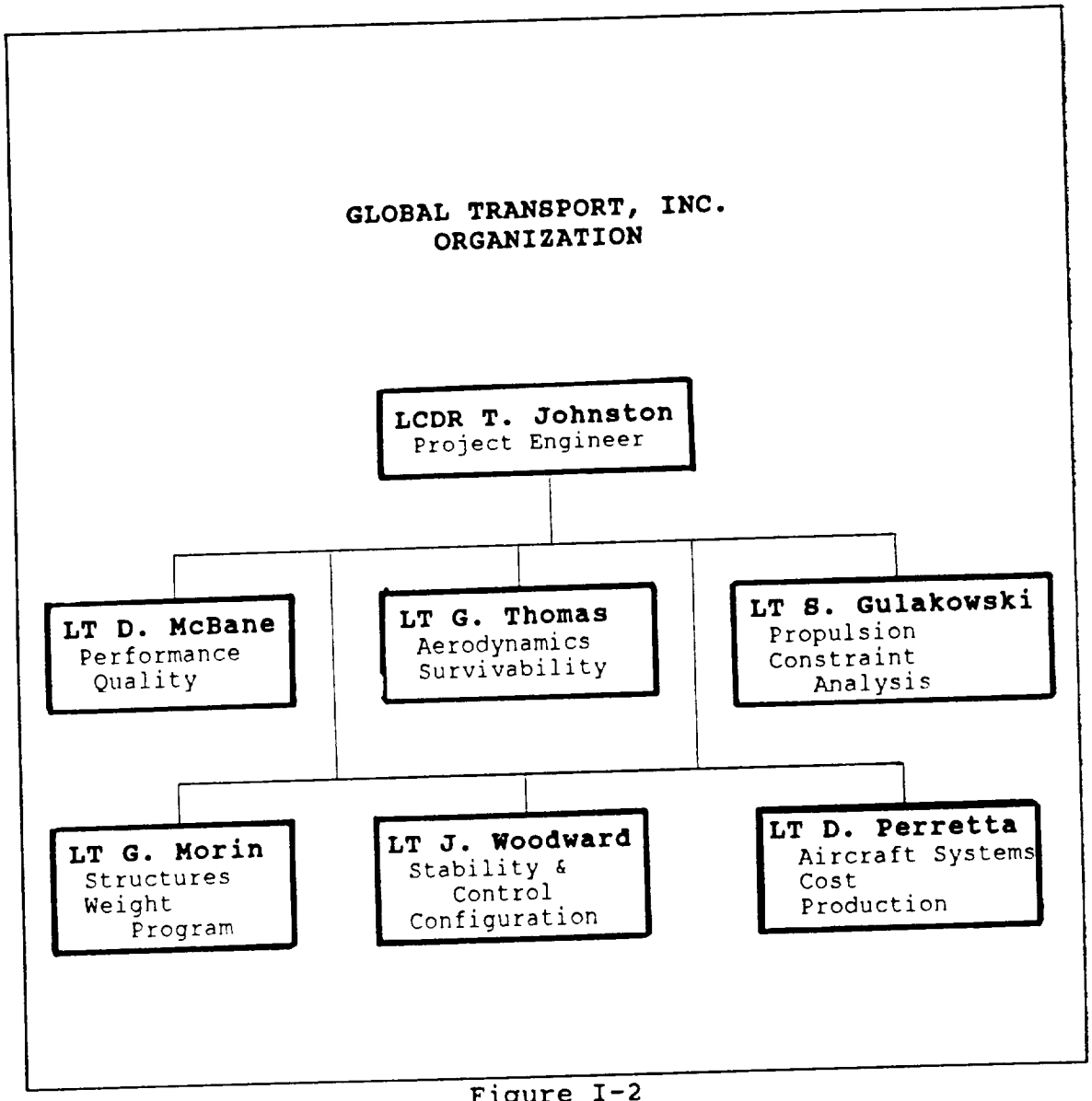

Figure I-2
Design Team Organization

D. DESIGN OBJECTIVES and STRATEGY.

The design was driven to meet or exceed all RFP requirements and restraints. Interrelationships between Product Characteristics and Design and Manufacturing Requirements were investigated through Quality Function Deployment methods. Figures I-3, I-4 and I-5 display house of quality results. These investigations drove the team to the following guiding philosophies:

1. Emphasize systems commonality with commercial freight transports to reduce costs. This could provide the Air Force MAC with a possible surge capability through mutually beneficial arrangements.
2. Utilize state of the art manufacturing techniques and hardware already applied to current generation transports to reduce development costs.
3. Maximize mission effectiveness by requiring high reliability and maintainability to meet the expected 'real world' short-fuzed war time situations and improve sortie generation during any extended surge period.
4. Utilize advanced technologies that offer potential for significant improvements in performance and operating economics without excessive technological risk.

a. Laminar Flow Control (LFC) to increase flight efficiency. Lange and Bradley, Reference 16, concluded that LFC:

- Reduces TSFC by 24-29%
- Increases Cruise Lift-to-Drag by 30%
- Decreases engine thrust by 21%
- Decreases ramp weight by 13%
- Decreases required block fuel by 29%
- Would increase RDT&E and operating costs

b. Sophisticated high lift devices for improved low speed aerodynamics. Kruegar LE and triple slotted Fowler TE flaps.

c. Utilize affordable, advanced composites in the primary and secondary structure to reduce aircraft weight by 26% (Forsch, Reference 8). Minimize required repair due to battle damage (Wollaston, Reference 28).

d. Utilize ultra-high bypass ratio turbofan engines to decrease TSFC and with acoustic treatment to comply with increasing environmental constraints. (Meese, Reference 19).

e. Digital fly-by-wire flight controls. All surfaces hydraulically actuated.

Product Characteristics

House of Quality

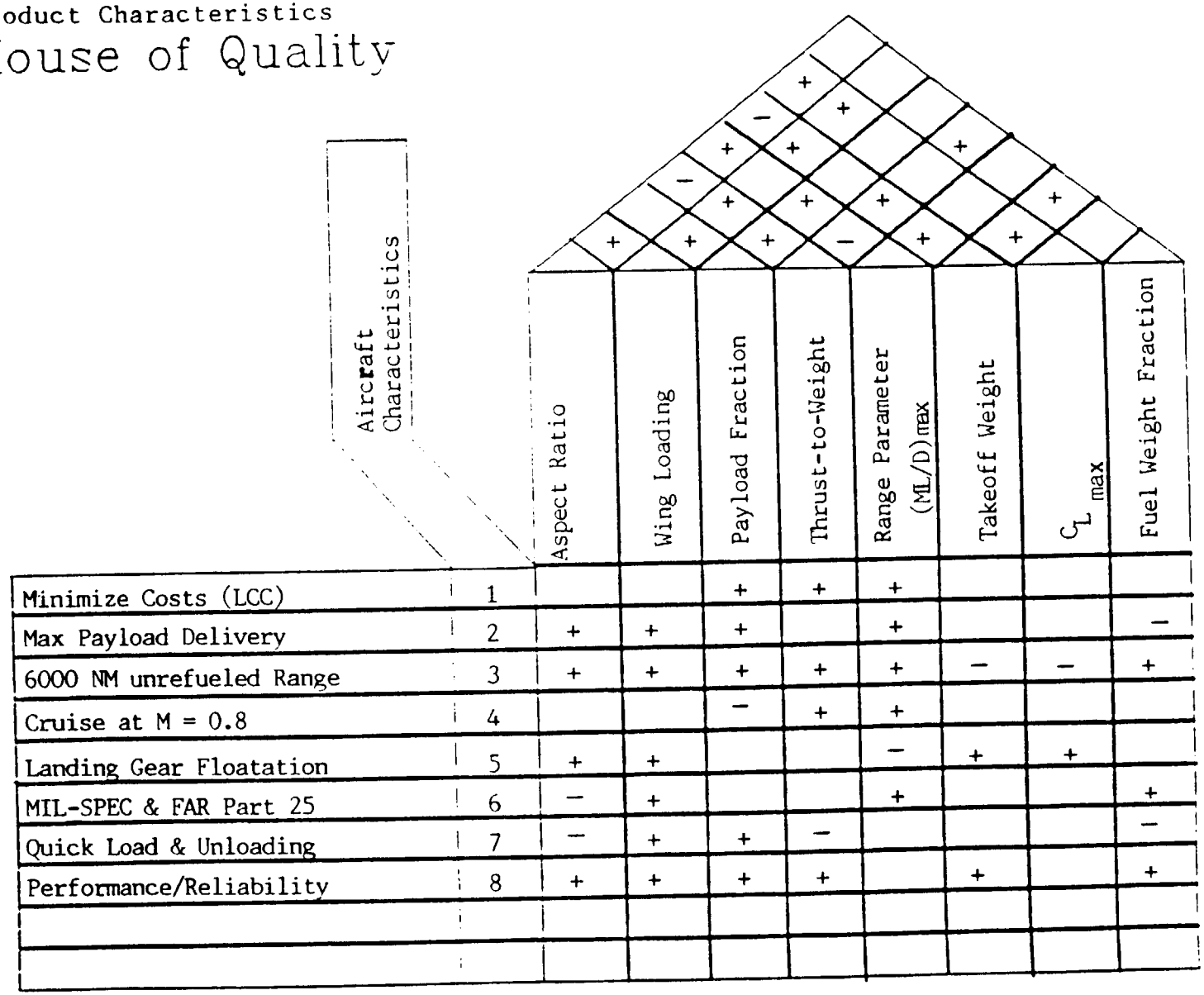

Figure I-3

Product Characteristics

Design Requirements

House of Quality

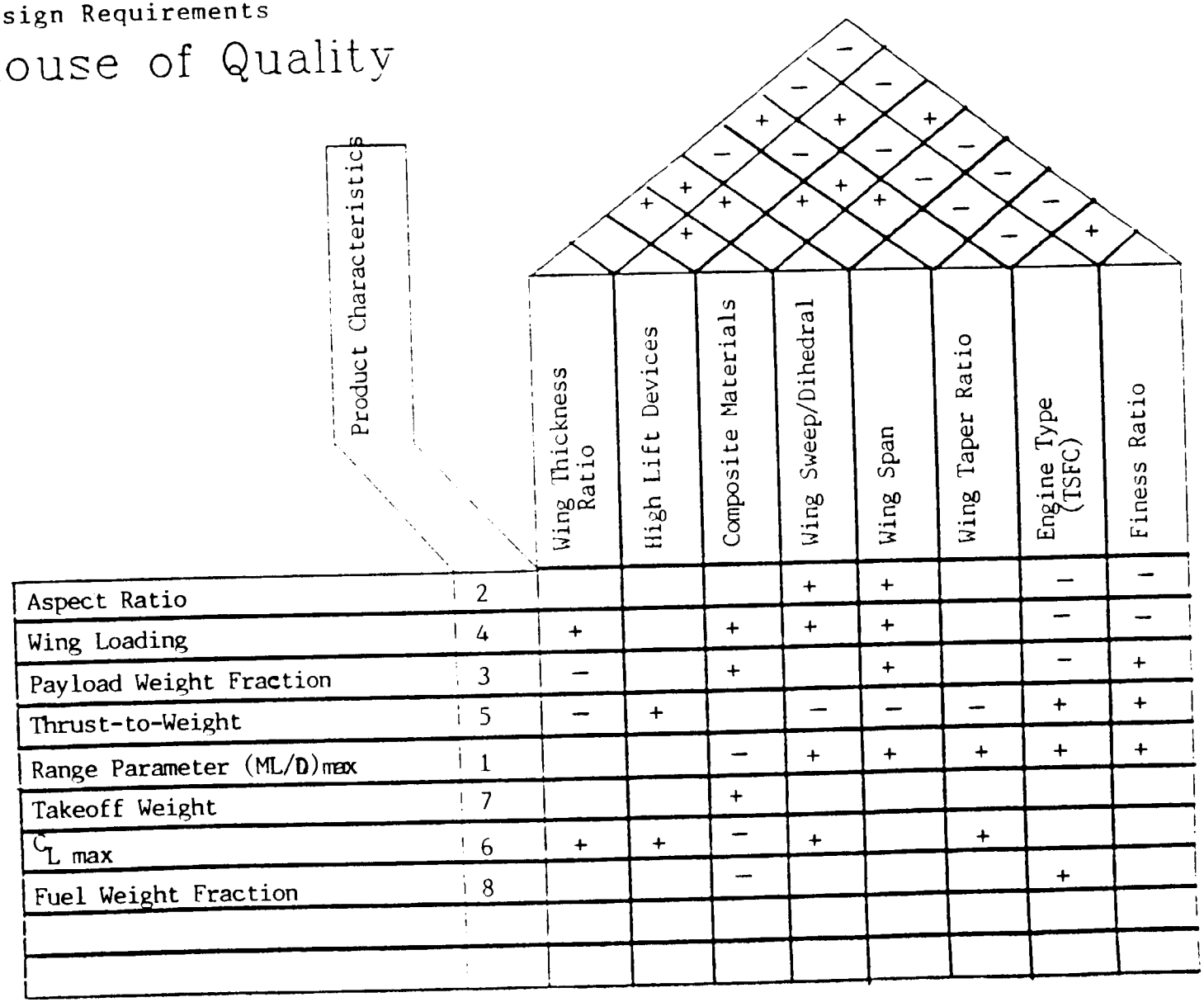

Figure I-4

Design Requirements

Manufacturing Requirements

House of Quality

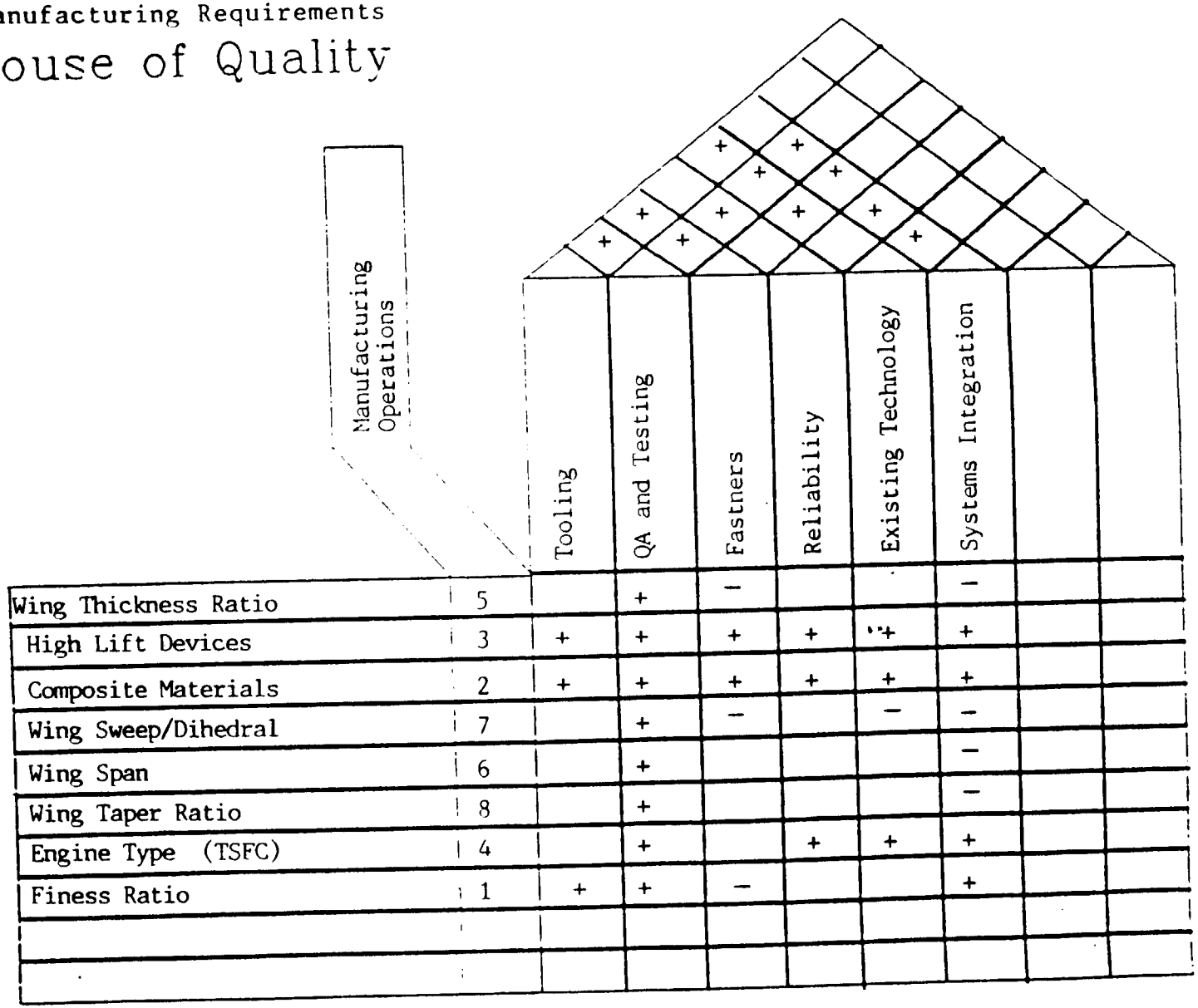

Figure I-5

Manufacturing Requirements

E. FUNDAMENTAL PERFORMANCE ISSUES

This strategy focused the design on the following fundamental performance issues as outlined by Lange and Bradley, Reference 16.

- **Cost Affordability, Reliability,** and **Maintainability**
- Payload: **Cargo Bay Compartment size** and Quick loading/unloading capability
- **Range**
- **Speed**
- Takeoff and Landing Performance (High Lift Augmentation)
- Landing Gear Flotation
- Internal Pressurization to 8000 feet

F. CARGO BAY OPTIMIZATION

1. Design Point

A U.S. Mechanized Division was used as the typical military payload design point. The following payload combinations were analyzed: M1A Abrahms Battle Tank, CH-53E Super Sea Stallion helicopter, 2.5 ton truck, Missile/artillery launchers, and Civilian/Military cargo pallets.

The following assumptions were made as outlined in Torenbeek, Reference 27: 85% loading efficiency; Average cargo density of 12 lb/ft^3; A maximum floor loading of 1200 lb/ft^2, evenly distributed, and a 10,000 lb, local load; Quick loading/unloading via forward and aft Access capabilities, and

Electrical traveling cranes in bay roof with two lifting points.

Load multiples of Abrahms Tanks, Super Sea Stallion, and civilian/military cargo pallets resulted in cargo bay width being dictated by civilian containers, and bay height being dictated by military pallets.

2. Optimumization Results

Optimum cargo bay capacity (Chapter III) was found to be (with 150 troops above forward cargo compartment):

- Sixty, 8'x 8'x 10' military pallets or Eight, 9'x 10'x 20' civilian containers
- Three M1A Abrahms Tanks and Twelve, 8'x 8'x 10' cargo pallets
- Three CH-53E Super Sea Stallion helicopters

Optimum cargo bay dimensions (Chapter III) were determined to be: Payload weight of 430,000 pounds, Length of 160 feet, Width of 35 feet, and a Height of 13.5 feet.

G. CONCEPT EXPLORATION

1. Current and Planned Transport Aircraft

Performance requirements, design objectives, and Torenbeek, Reference 27, led to the following optimizing parameters:

- Aspect Ratio (**AR**)
- Wing Loading at takeoff $(W/S)_{T/O}$
- Payload weight ratio (W_P/W_{TO})

- Thrust-to-Weight ratio at takeoff $(T/W)_{T/O}$
- Fuel/Range parameter $(ML/D)_{MAX}$

To get a feel for these parameters, a review of current large transport aircraft and AIAA future studies was conducted and characteristic trends are displayed in Table I-1.

TABLE I-1
CURRENT and AIAA STUDIES for TRANSPORT AIRCRAFT
(Optimized Aerodynamic Parameters)

	AR	W/S	W_P/W_{TO}	$(T/W)_{TO}$	$(L/D)_{CR}$	$(ML/D)_{MAX}$	b (ft)
Lockheed C-5	7.75	124	.27	.22	19.5	14.9	222
Boeing 747-400	6.96	141	.15	.27	15.1	12.1	213
C-141	8	100	.19	.26	15.6	12.1	161
DC-10	7.21	153	.19	.26	15.2	11.75	162
AN-225 Dream	8.64	136	.41	.23	16.1	8.1	254
AN-124 Condor	8.56	132	.37	.23	16.8	12.8	240
[1]**Lange IOC 1985**	8.2	130	.36	.25	20	17	241
[1]**Lange IOC 1995 Turbulent Flow**	10.3	140	.14	.32	23.1	19.6	417
[1]**Lange IOC 1995 Laminar Flow**	11.6	132	.17	.29	30.1	25.5	424
[2]**Barber IOC 1985**	10	136	.27	.22	24.2	19.6	329
McDonnell Douglas C-17A	7.2	152	.30	.28	15.4	11.6	171

(1) Lange and Bradley, Reference 16.
(2) Barber, Noggle, and Rettie, Reference 3.

2. Configuration Studies.

A configuration study using Garrard, Reference 9 and Torenbeek, Reference 27 revealed the following trends.

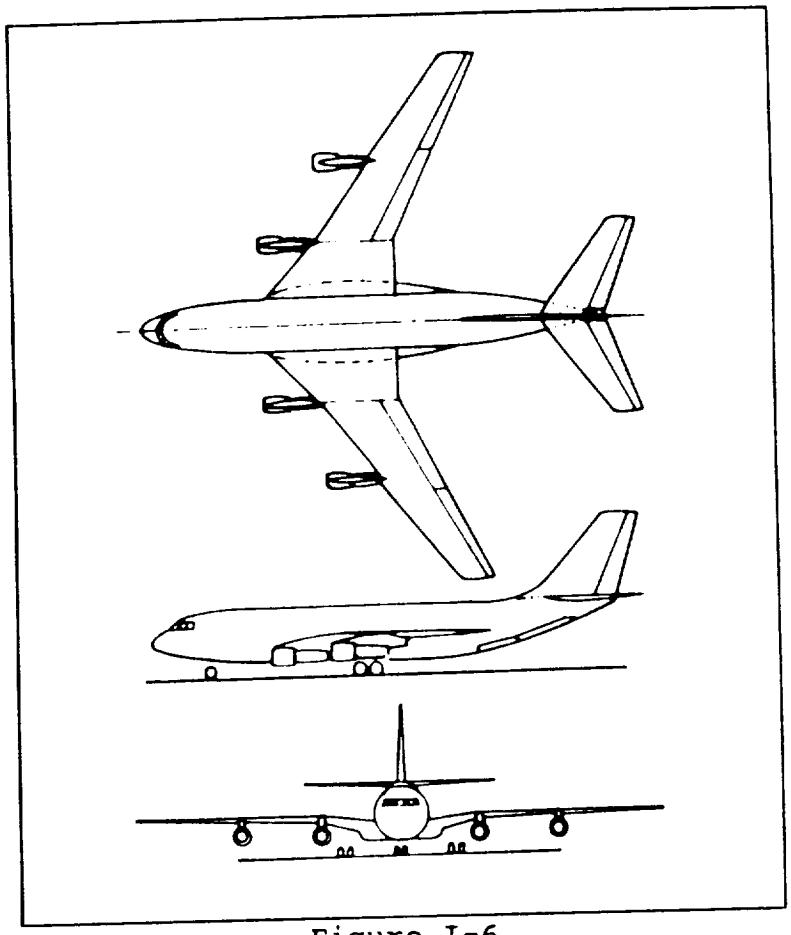

Figure I-6
Low Wing Configuration

a. Low/Medium Wing

- Requires kneeling landing gear for loading/unloading
- Requires cranked wing for engine ground clearance when aircraft is lowered
- Large energy absorbing mass during forced landing. A potential fire hazard
- Ground effect (reduction in vortex-induced drag) results in decreased takeoff and increased landing distances
- Greater elevator deflection required for takeoff rotation due to nose down pitching moment caused by a decrease in downwash at the horizontal tail

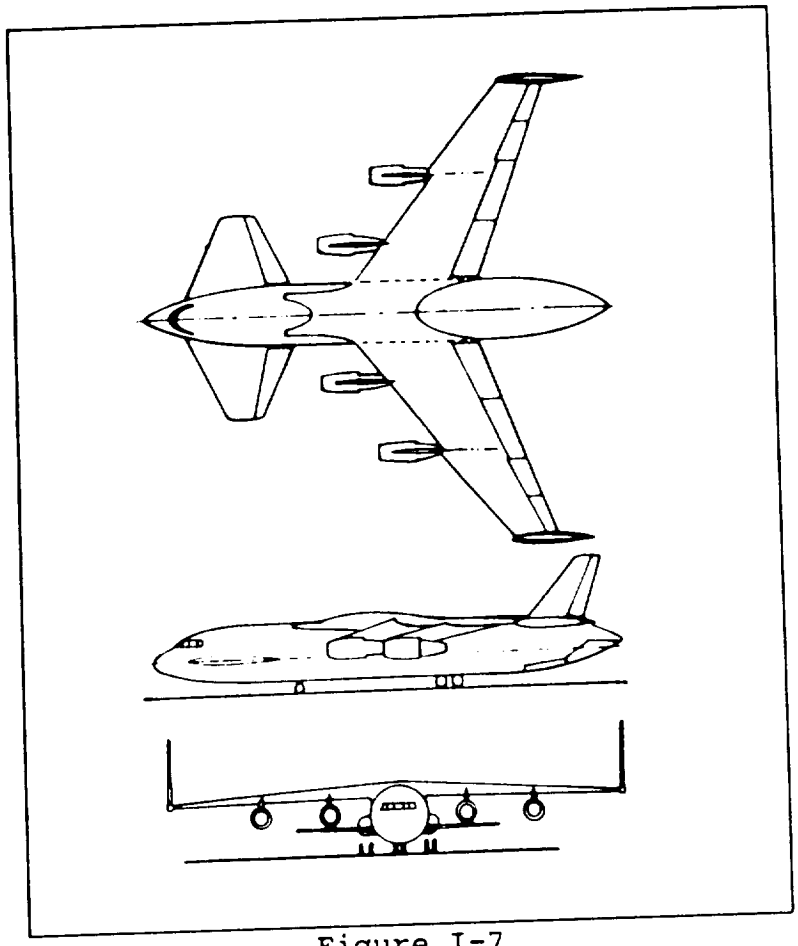

Figure I-7
Canard Configuration

b. Canard.

- The longitudinal control surface is out of the wing downwash
- Higher C_{Lmax} and Reduced trim drag
- The main wing must have a low AR so the canard can produce a higher C_{Lmax} to produce a larger CG spread
- Somewhat shorter wing span - Has shared wing loading with the canard
- Possible aerodynamic interference from canard onto the main wing at high angles of attack

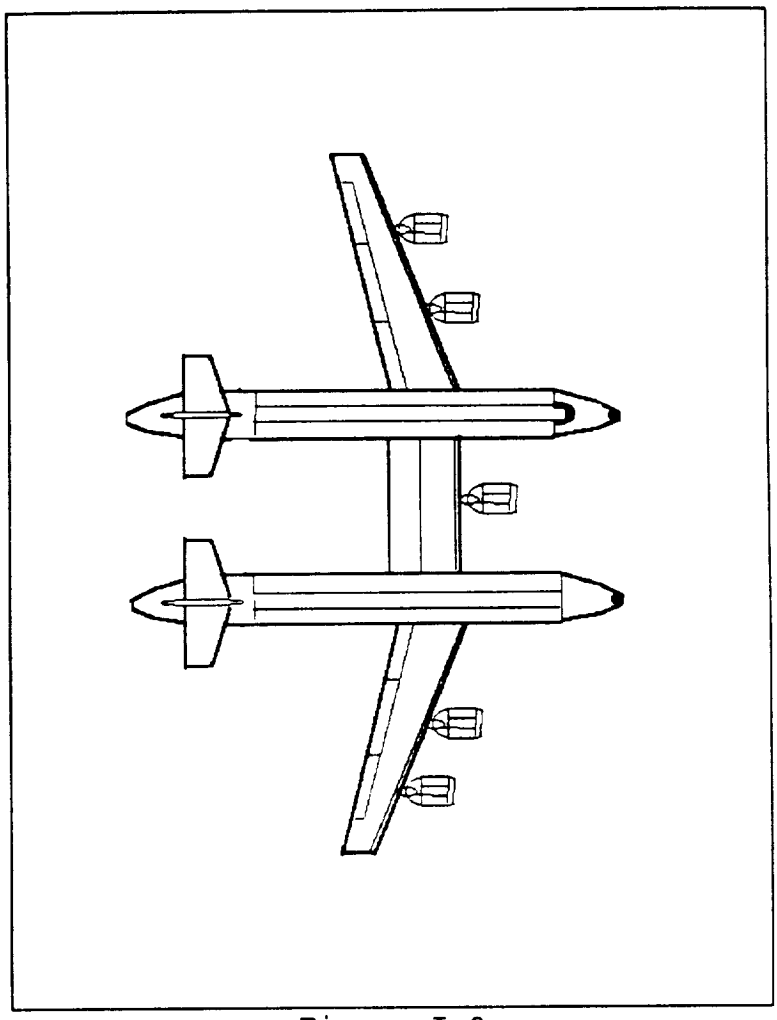

Figure I-8
Twin Fuselage Configuration

c. Twin-Fuselage.

- Longer unsupported wing span achievable
- Increased cargo volume and weight
- One fuselage unpressurized
- Better weight distribution
- Higher Cdo, $C_D = .025 + .041\ C_L^2$
- Flutter problems aft between the two fuselages

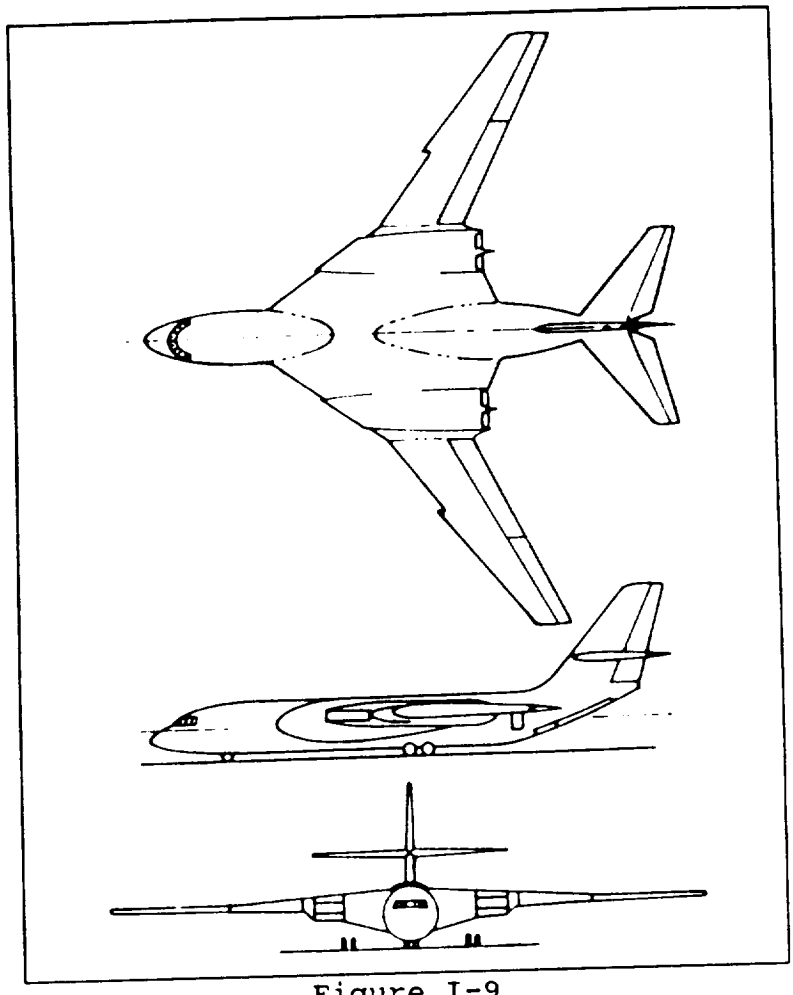

Figure I-9
Supersonic Configuration

d. Supersonic - Highly swept Wing

- Unable to carry effective landing flaps
- Low AR with a very large area is required to get sufficient lift for landing
- Large approach angles and speeds required
- Low wing problems
- Much heavier, much more costly
- $C_D = .035 + .22\ C_L^2$
- TSFC = 1.5 to 2 $lb_m/lb_f/HR$

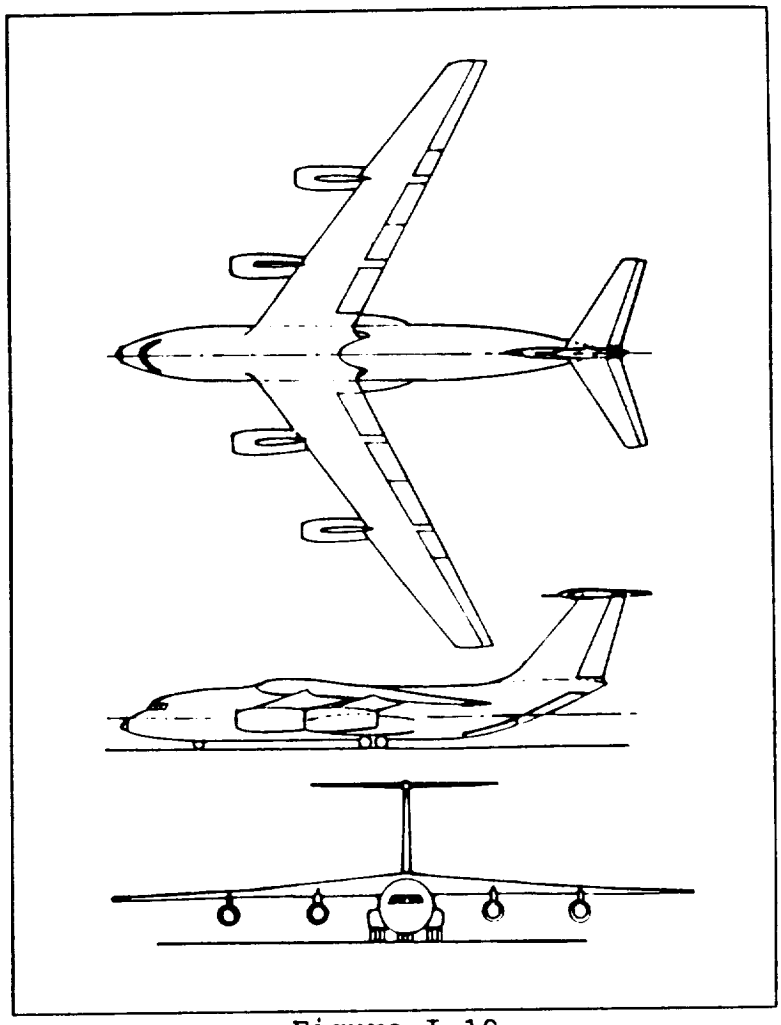

Figure I-10
High Wing Configuration

e. High Wing

- Allows lowest possible cargo floor height
- Outstanding ground clearance -- Quick load/unload
- Lowest C_{do} @ .02
- Required to mount main gear in fuselage. Requires increased structure for transmission of bending and impact loads. It is difficult to obtain a sufficiently wide track.

3. Response Time and Rate of Delivery Optimization.

A trade-off study was completed maximizing the amount of material that could be transported in a 72 hour period by continuous transport operation from CONUS. The calculated results are compiled in Table I-2. The study revealed there was very little overall gain in going to the supersonic speed range. The following assumptions were made in this evaluation:

- 3000 NM trip each way
- Best cruise altitude/speed
- W_F = 450,000 pounds for all aircraft
- An 80% availability rate. CONUS turn-around requires four hours to complete maintenance and refueling
- Ground speed (ktgs=knots ground speed) allows for an average 15 knots head wind
- Supersonic time allows for acceleration to M = 2.5

TABLE I-2
RESPONSE TIME & RATE OF DELIVERY OPTIMIZATION

Concept Design	Cruise Time (HRs)	Trip Time (HRs)	MIN # REQ A/C	MIN # Buy	Ave Trips/ A/C	Total # Trips	Total Tons moved
SUBSONIC (331 ktgs @ M = .6 @ 35 Kft, TSFC=.41)	9.07	22.81	46	58	2.7	125	28,125
SUBSONIC (446 ktgs @ M = .8 @ 35 kft, TSFC=.47)	6.72	18.11	37	46	3.5	130	29,250
SUPERSONIC (1419 ktgs @ M = 2.5 @ 60 kft, TSFC = 1.9)	2.5	9.67	20	25	6.9	138	31,050

4. Life Cycle Cost (LCC) Comparison.

A Life Cycle Cost analysis was completed for the three design concepts. Results are compiled in Table I-3. The lowest LCC was determined to be the medium subsonic, single fuselage concept.

TABLE I-3
LIFE CYCLE COST COMPARISON (Millions 1993 Dollars)

	SUBSONIC TWIN FUSELAGE	SUBSONIC SINGLE FUSELAGE	SUPERSONIC LOW AR HIGH SWEEP
Airframe	1280	1067	4889
Development	502	419	2826
Flight Test A/C	2414	2012	10060
Flight Test Operations	236	197	985
Total DT&E	**4434**	**3696**	**18760**
Engine & Avionics	1316	1197	598
Manufacturing	3348	3044	3285
Material	663	603	663
Engineering	1926	1751	1926
Tooling	1905	1732	1905
QA	595	541	595
Total Production	**9754**	**8871**	**8972**
Fuel	261	234	371
Maintenance	25	22	32
Crew	15	15	11
One Year O&M Total	301	271	414
20 Year O&M Total	6020	5420	8280
Total LCC	**$ 20,200**	**$ 18,000**	**$ 36,000**

5. Payload-Range Analysis.

Each design concept's Range and Endurance as a function of Mach Number and Payload weight are summarized in Figures I-11 through I-16. Assuming Mach 0.8 and a payload weight of 450,000 pounds, the Twin Fuselage has a 6500 NM range and a 17 hour endurance, and the Single Fuselage has a 7500 NM range and an 18 hour endurance. The Supersonic concepts range and endurance, with the same payload weight, are an order of magnitude less than the subsonic concepts.

6. HUGO Constraint Analysis.

Using Nicolai, Reference 22, and Mattingly, Reference 18, a Takeoff Thrust Loading vs. Wing Loading Constraint Analysis was completed and is presented in Figure I-17. The following constraint cases were analyzed:

- Constant Altitude/Speed Cruise
- Constant Altitude/Speed Turn
- Constant Speed Climb and Service Ceiling
- Takeoff Ground Roll
- Braking Roll

The Takeoff Ground Roll and the Braking Roll proved to be the most constraining cases.

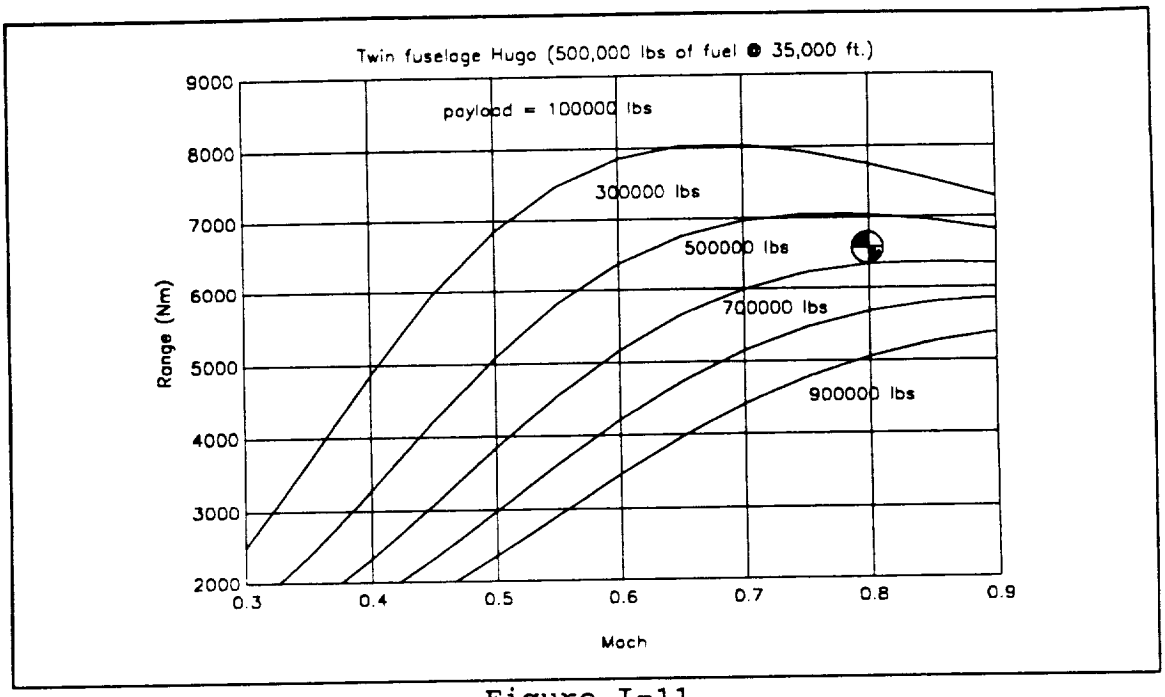

Figure I-11
Twin Fuselage Range

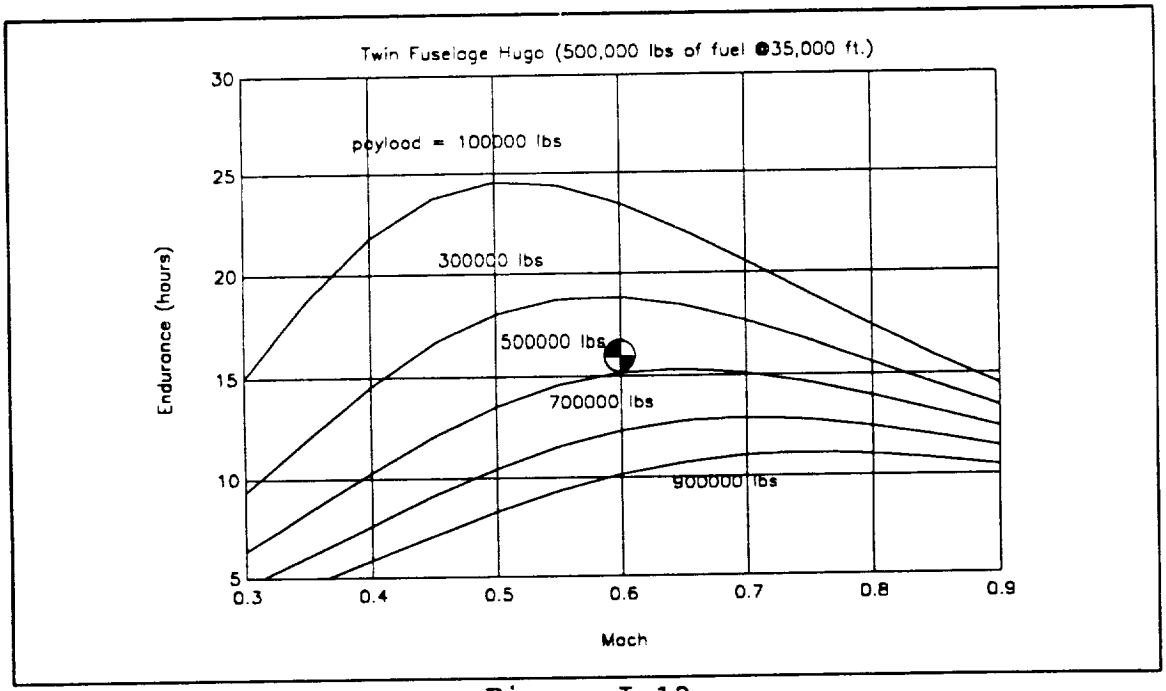

Figure I-12
Twin Fuselage Endurance

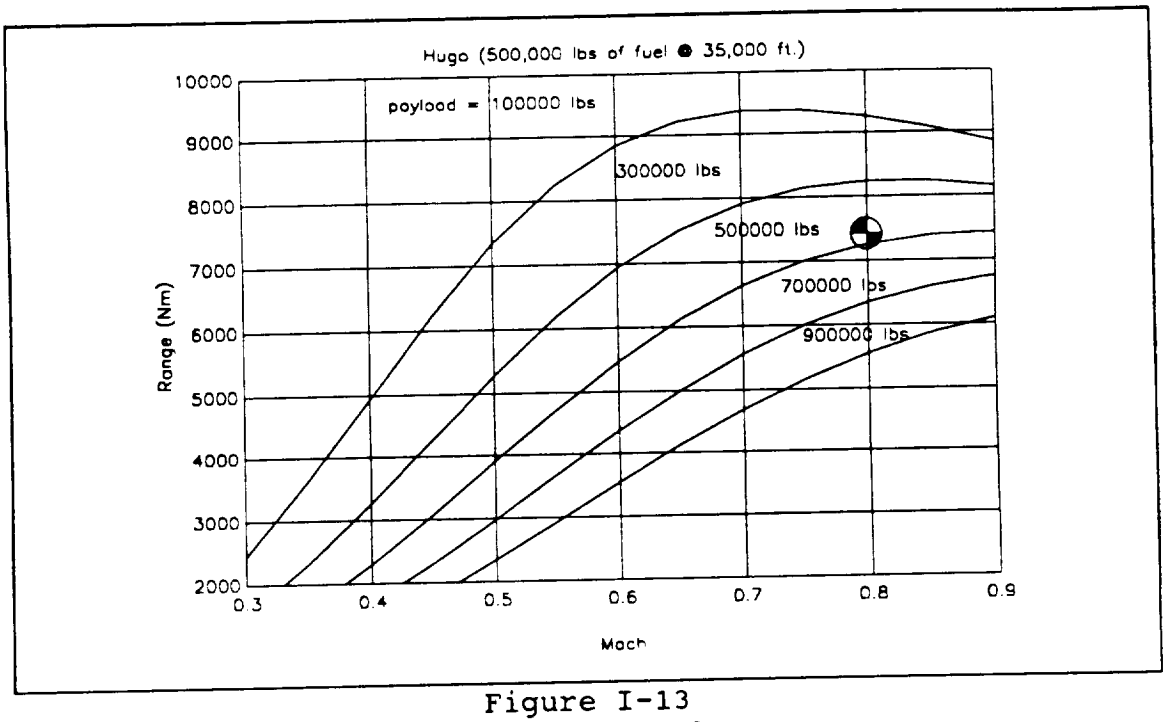

Figure I-13
Single Fuselage Range

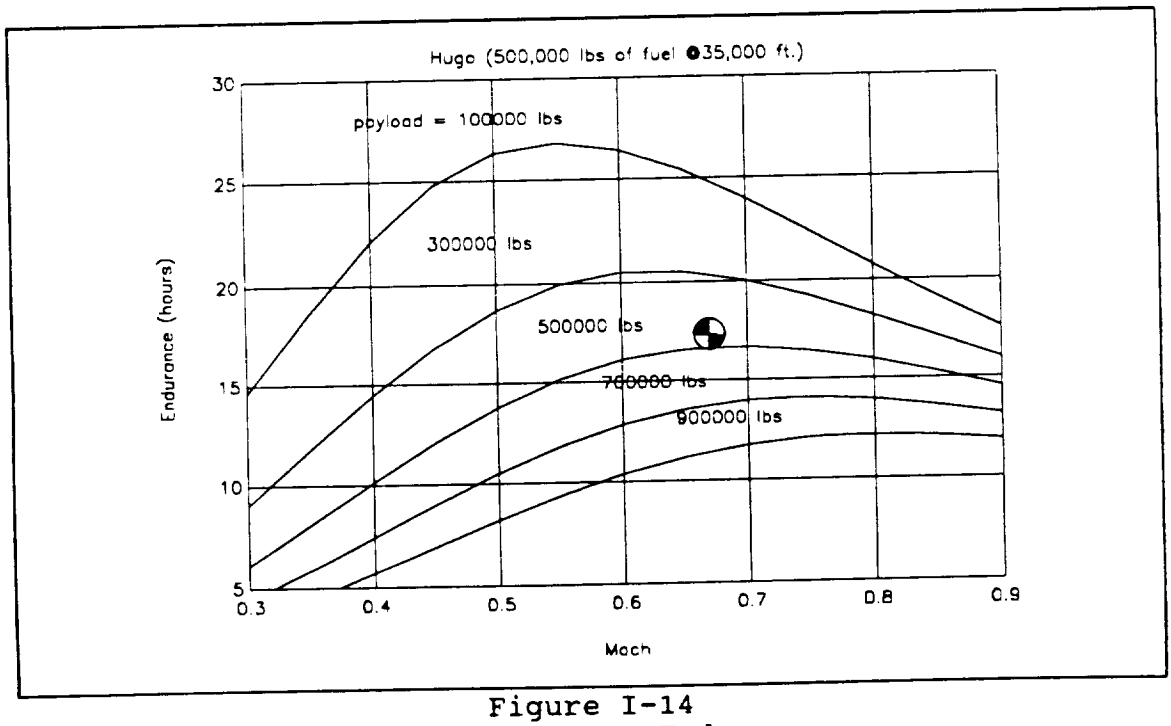

Figure I-14
Single Fuselage Endurance

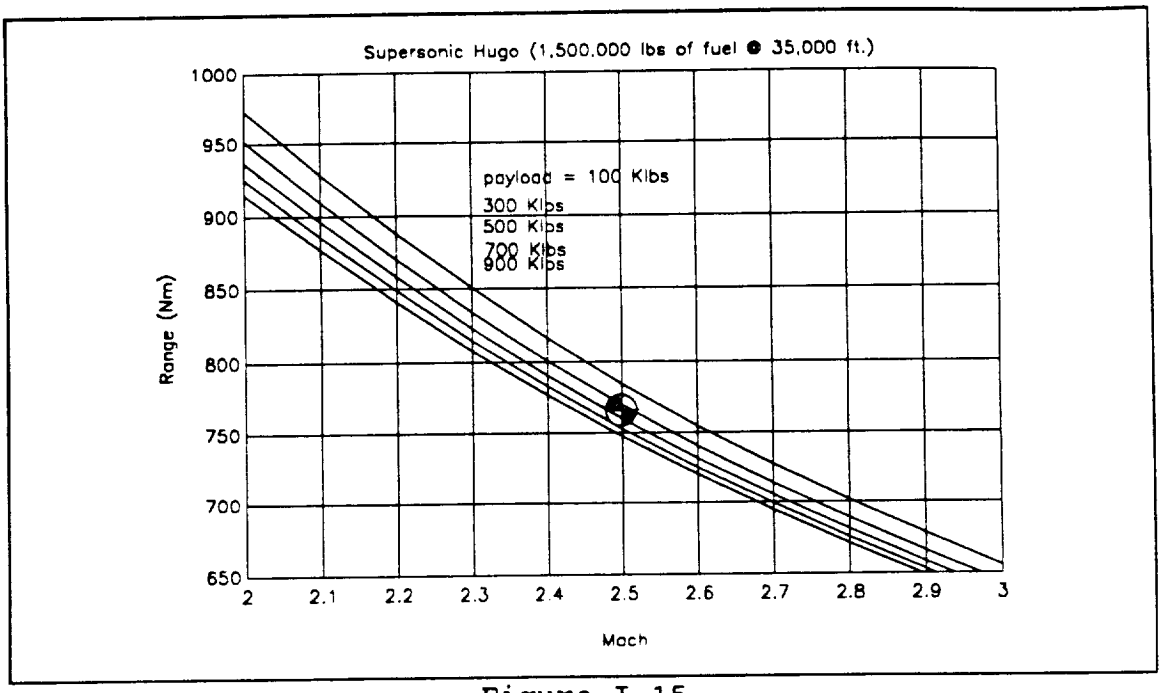

Figure I-15
Supersonic Range

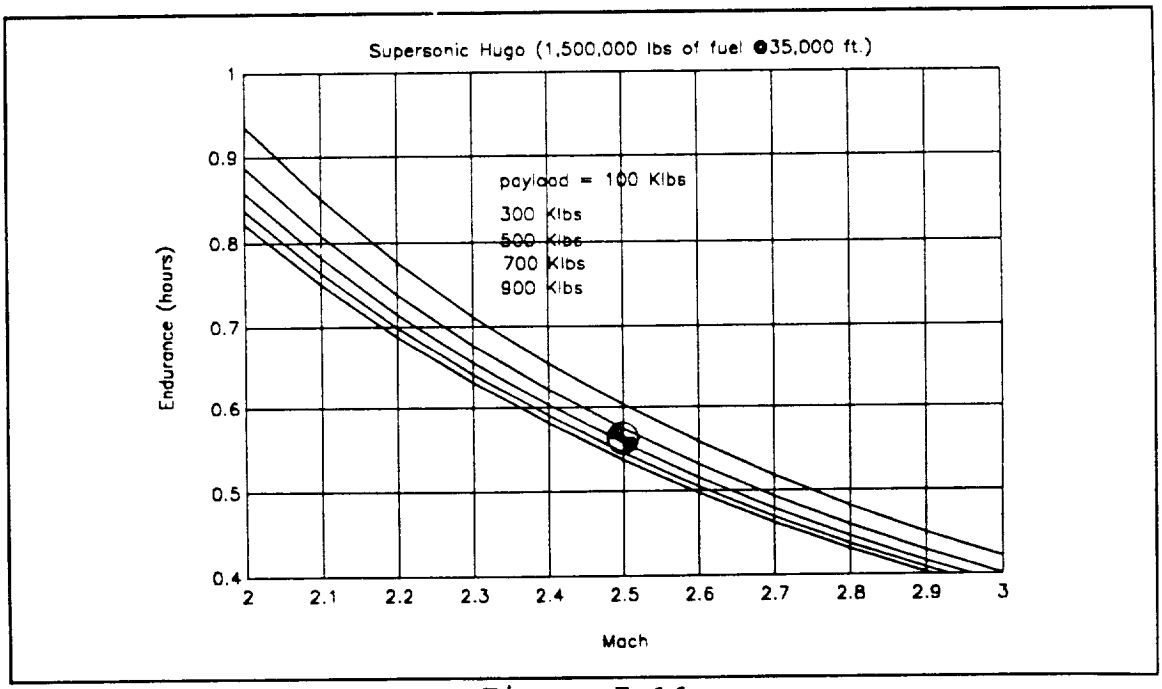

Figure I-16
Supersonic Endurance

The following design point was chosen based on the previous optimization analysis and using Kirkpatrick, Reference 14 and Kuchemann, Reference 15:

- Aspect Ratio **(AR)** = **8.9**
- Wing Loading $(W/S)_{T/O}$ = **135 lb/ft²**
- Payload Fraction $(W_P/W_{T/O})$ = **.33**
- Minimum Thrust-to-Weight $(T/W)_{T/O}$ = **.265**
- Range Parameter $(ML/D)_{MAX}$ = **17**

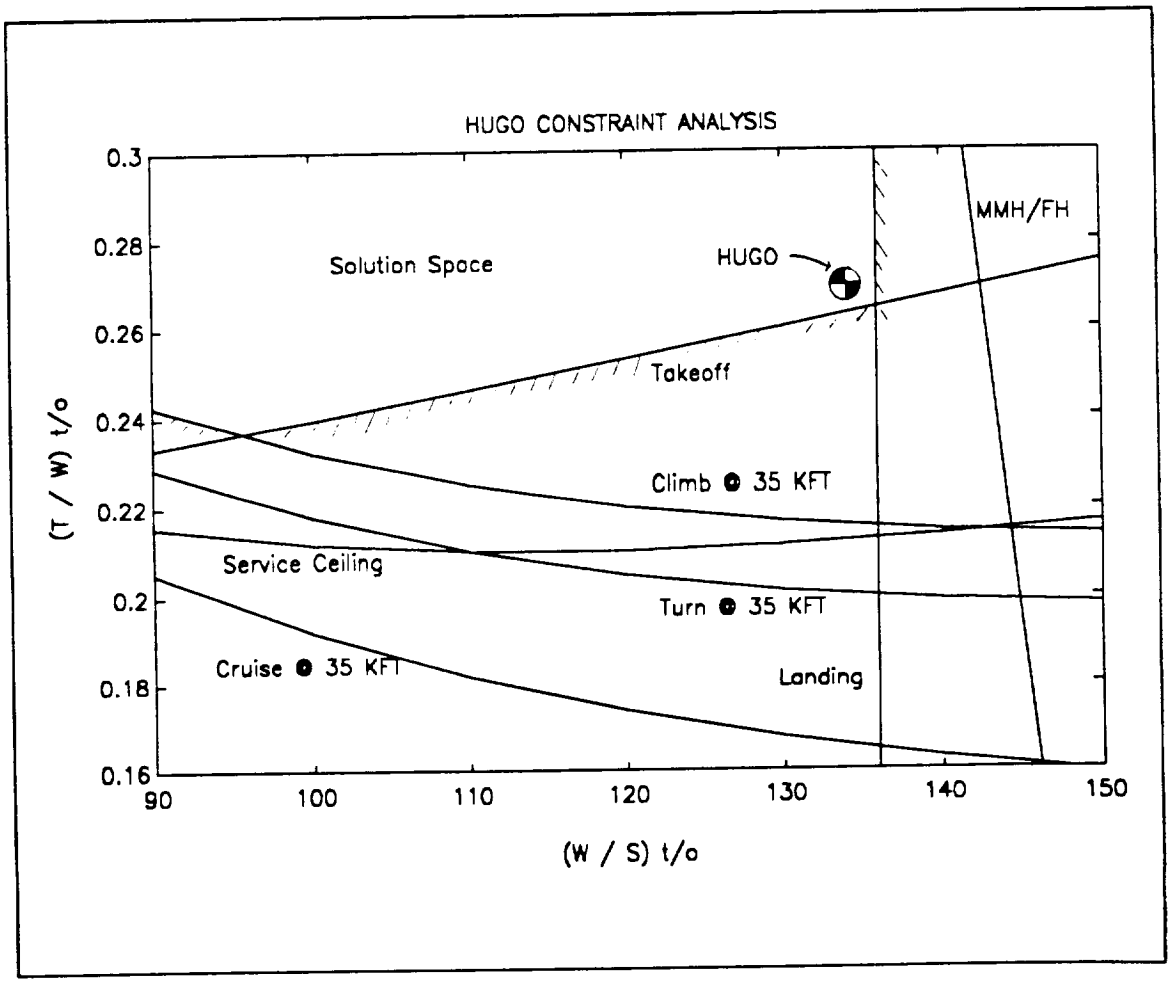

H. HUGO CONFIGURATION

1. Chosen Configuration

The optimum concept based on the previous analysis proved to be a High Wing but Low Horizontal Tail concept as shown in Figure I-18. HUGO's characteristics are:

a. Weight:

Takeoff	1,367,000 pounds
Payload	450,000 pounds
Fuel	500,000 pounds
Empty	417,000 pounds

b. Cruise Design Point:

Mach Number	0.8
Altitude	35,000 feet
$(ML/D)_{MAX}$	17

c. Cargo Bay

Length	160 feet
$Height_{MAX}$	13.5 feet
$Width_{MAX}$	35 feet

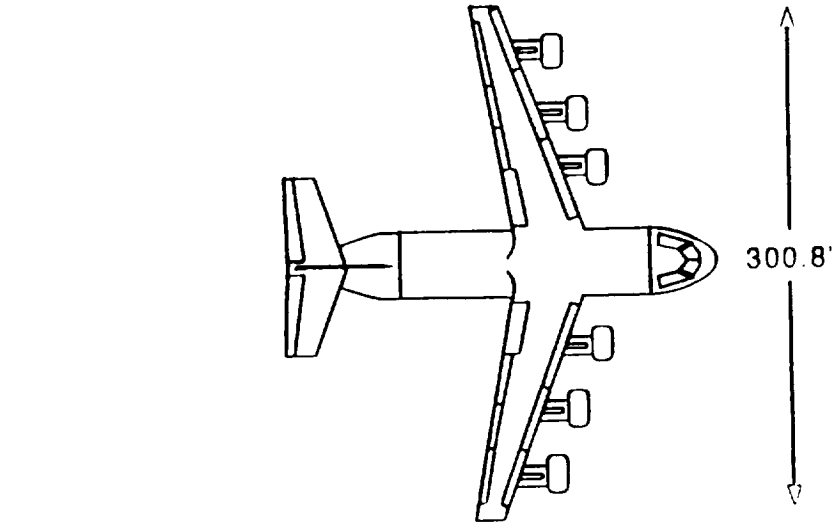

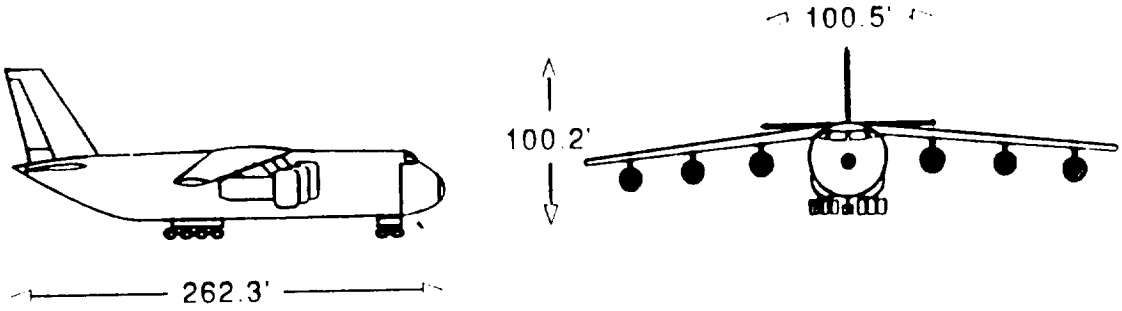

Wing:
b = 300'
S = 10080 ft^2
AR = 8.93
ct = 18'
cr = 48'
taper ratio = .38
mac = 35.27'
LE sweep = 25°
TE sweep = 15°
c/4 sweep = 22.6°

Horizontal Tail:
b = 100'
S= 2100 ft^2
AR = 4.76
ct = 15'
cr = 31'
taper ratio = .48
LE sweep = 20°
TE sweep = 2°
Vh = .08
Se/Sh = .2

Vertical Tail:
h = 60'
S = 1745 ft^2
AR = 2.06
ct = 21'
cr = 41'
taper ratio = .51
LE sweep = 32°
TE sweep = 15°
Vv = .07
Sr/Sv = .2

Figure I-18
HUGO Global Transport

2. Fuselage

The fuselage sizing was driven by cargo bay optimum size requirements (Chapter III) and an optimum fineness ratio (l/d) of 6.5 (Chapter V) to minimize profile drag.

a. Landing Gear

The landing gear flotation is designed to operate out of paved runways and unprepared fields (unpaved strips). The nose gear and the rear half of the main gear is steerable to provide a minimum ground turning radius. Carbon, anti-skid brakes are used.

b. Loading Schemes

Quick loading and unloading is achieved by a hydraulically operated, visor type, cargo bay door forward with an upward hinged nose, and a simultaneously extending folding nose loading ramp; and by a rear fuselage ramp/door with a simultaneously extending loading ramp. The aircraft nose gear is capable of hydraulically kneeling the nose down to extendable feet.

c. Maintainability

Numerous access doors and panels are built into the design allowing ease of maintenance. A maintenance passage/inspection way is under the cargo bay floor. An access Tunnel is placed in the vertical tail for routine maintenance. Extensive use is made of maintenance monitoring systems and built in tests.

3. Wing Planform

The wing planform is based on optimization of Aspect Ratio, Thickness Ratio, Sweep, and Taper ratio to achieve maximum range, L/D, and Drag Divergence Mach Number (Chapter II). Spoiler augmentation supplements both high and low speed ailerons to prevent aileron reversal (high speed) and to increase roll authority (low speed). Laminar Flow Control (LFC) applied along the wing span from root to tip and 90% of the chord improves range and fuel performance (Lange and Bradley, Reference 16).

a. High Lift Devices

Krueger leading edge flaps and triple slotted Fowler trailing edge flaps provide the required $C_{L_{max}}$.

4. Empennage

The single vertical tail is highly swept with a low aspect ratio. The horizontal tail is low mounted to prevent drag losses from miss-aligned super velocities and flutter problems encountered with the conventional C-5 "T" tail. LFC is also applied to much of the empennage.

5. Engines

Six, 100,000 pound installed thrust, high by-pass turbofan, AIAA ATF engines are utilized and mounted on pods below the wing. The design point is at 35,000 feet, 0.8 Mach, and a TSFC of 0.46. Thrust reversers, capable of inflight or ground operations, are incorporated into the design.

6. Materials

Multiple path structures are used preventing catastrophic failures due to a single element failure (fail safe through redundancy). The aircraft is designed using composite materials for the primary and secondary structure to the greatest possible extent. The cargo bay floor is titanium and attached mobily to the lower fuselage structure allowing temperature changes. The structure is fatigue resistant. Long term structural integrity is assured by designing to meet:

- 30,000 operating flight hours
- 12,000 landings
- 20,000 pressurizations

II. AERODYNAMICS

A. DESIGN REQUIREMENTS

A primary RFP requirement was to design the wing planform at high subsonic cruise speeds for optimum performance. This requirement meant balancing wing sweep angle with planform weight while considering other wing properties, since high sweep angle allows cruising at a higher Mach number. Too much sweep adds a significant weight penalty and reduces lift available for takeoff and landing. The secondary requirement was to design a wing that could generate sufficient lift for takeoff and landing.

B. DESIGN CHOICES

1. Wing Geometry

One RFP requirement for HUGO is the quick loading and unloading of infantry troops. HUGO also needed to carry a variety of cargo, such as two and one-half ton trucks, M-1 tanks and artillery vehicles, while providing space for personnel. Taking these requirements into consideration a high wing aircraft was chosen so that the wing root box did not interfere with cargo loading.

One of the most effective ways of delaying and reducing the effects of shock wave-induced flow separation is the use of wing sweep. Sweep-Back will increase the critical

Mach number, force divergence Mach number, and the Mach number at which the drag rise will peak. Sweep will also delay the onset of compressibility effects as shown in Figure II-1, which shows the affects of sweep angle on the minimum wing-drag coefficient. A disadvantage of wing sweep is the decrease in wing lift curve slope, which affects the L/D ratio for the aircraft as shown in figure II-2.

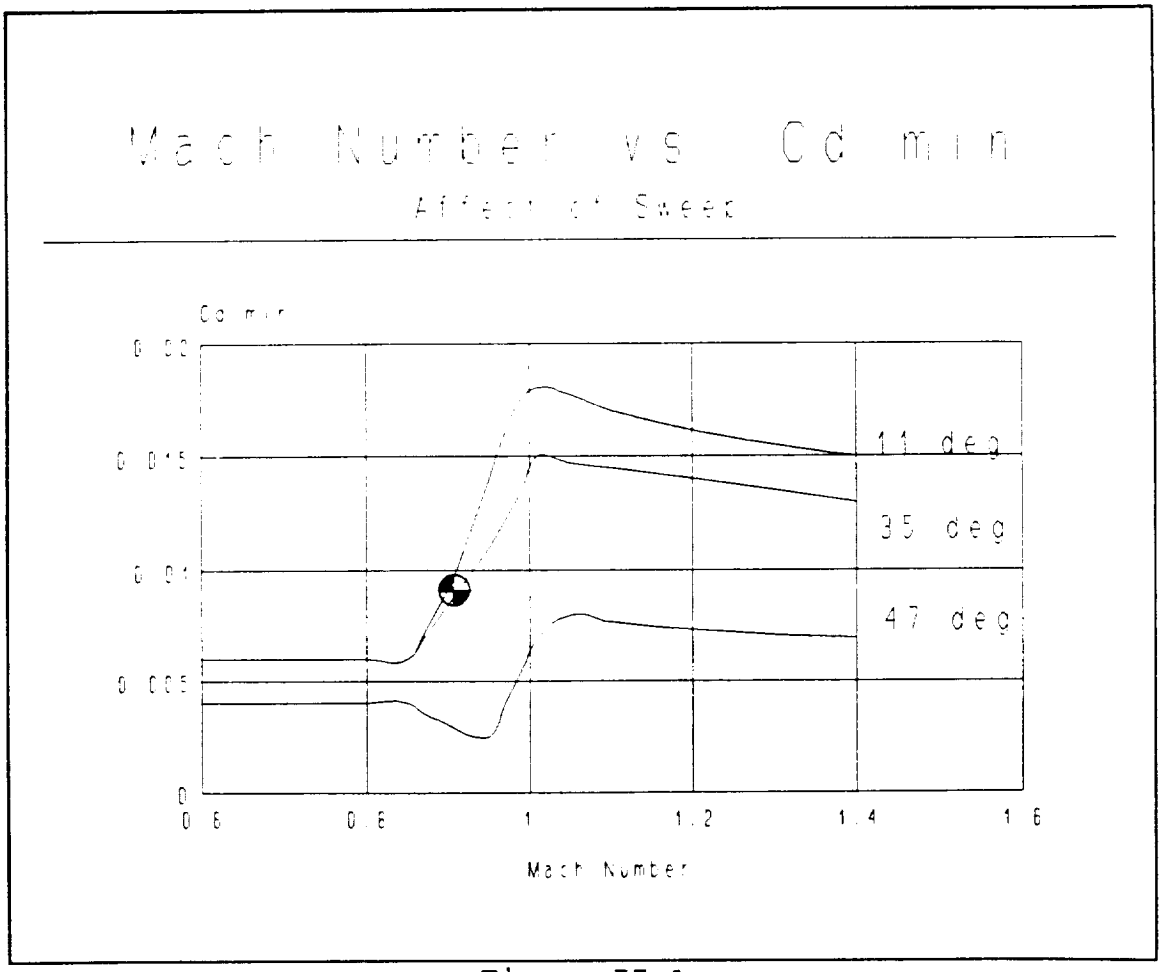

Figure II-1
Mach Number vs. C_{dmin}

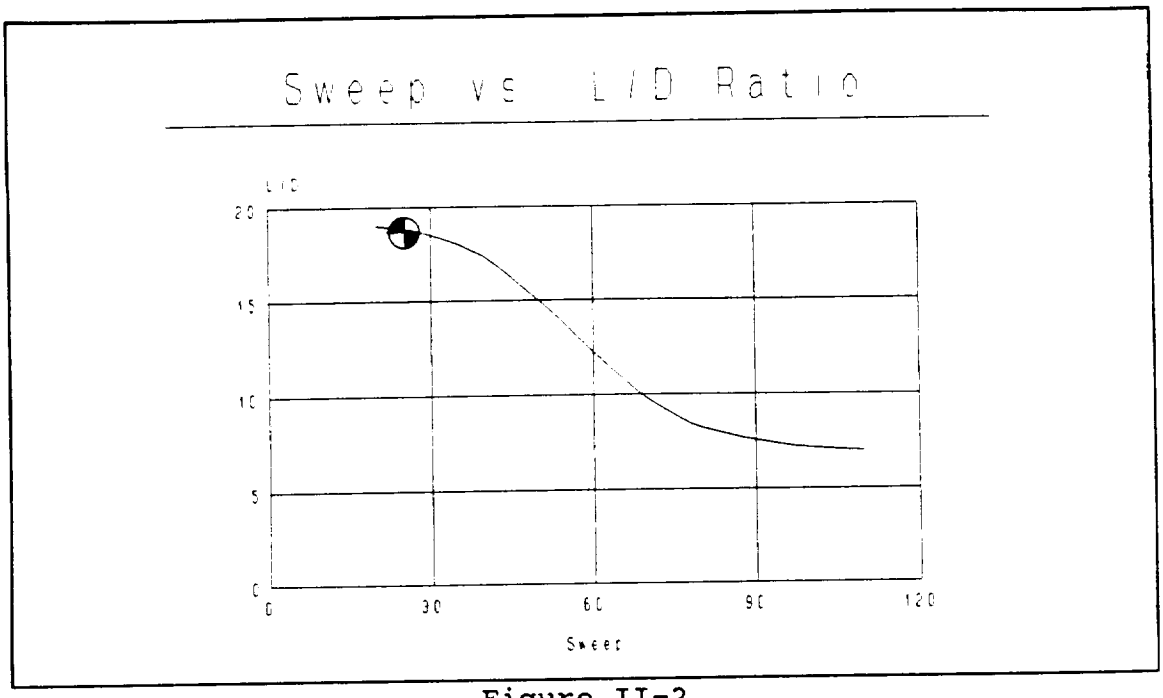

Figure II-2
Sweep vs. L/D

Other disadvantages to wing sweep are a reduction in C_L max and tip stall. The early flow separation at the tip is due to the spanwise flow causing a thickening of the boundary layer near the tips and hastening flow separation. Trade studies were conducted to determine the optimum sweep angle for HUGO. As shown in Figure II-2, the optimum sweep angle was determined to be 25°.

Another way of delaying the drag rise due to shock wave induced separation is by using a supercritical airfoil section. The supercritical section has a much flatter shape on the upper surface that reduces both the extent and strength of the normal shock; and reduces the adverse pressure rise behind the shock, with corresponding reductions in drag. To

compensate for the reduced lift on the upper surface of the supercritical airfoil resulting from the reduced curvature, the airfoil has increased camber near the trailing edge. A second advantage of the supercritical airfoil is that for a given thickness ratio, the critical Mach number stays the same but the divergence Mach number can be delayed.

2. Sectional Properties

The NASA SC(3)-0615 supercritical airfoil was chosen for the section nearest the root and the NASA SC(3)-0609 series was chosen for the tip (Harris, Reference 12). These airfoils are designed for cruising at a C_l of .6, very close to HUGO's design C_l. The airfoil cross section is shown in Figure II-3.

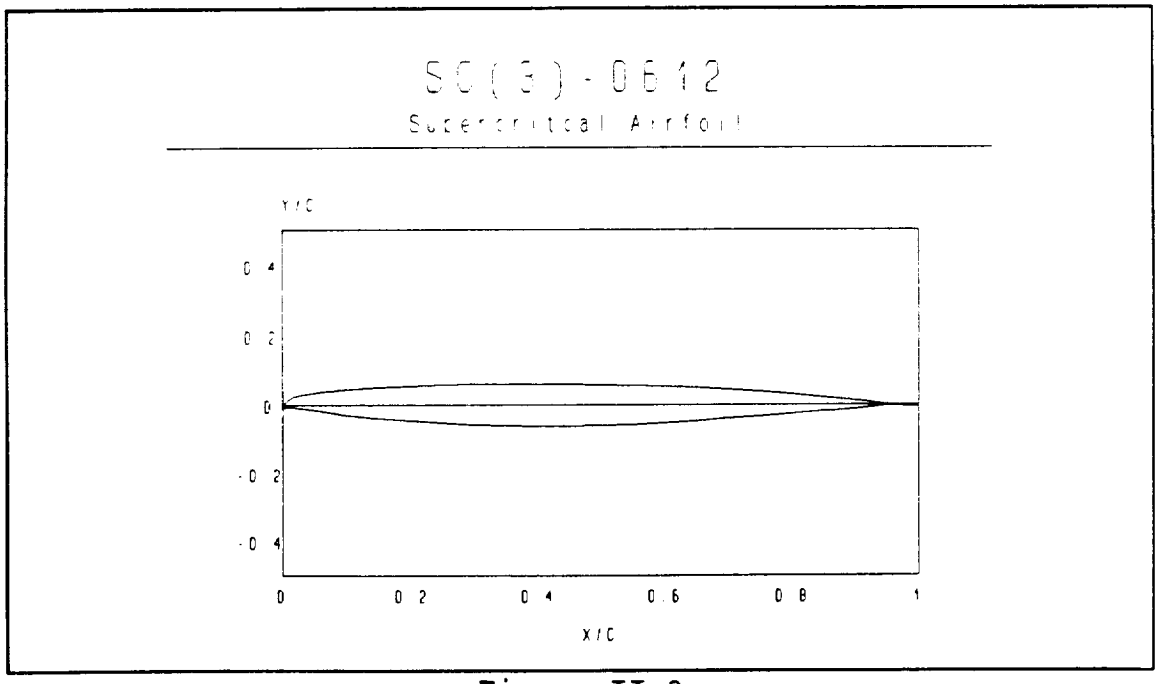

Figure II-3
Thickness-to-Chord vs. Chord

The thickness-to-chord ratio varies from root to tip on HUGO. At the root the t/c ratio is 15%, and at the tip it is 9.0%. The breakpoint for constant t/c ratio is the 40% semi-span point. From that point on it is a constant t/c of 9.5%. The extra thickness inside the 40% semi-span breakpoint is used to balance $M_{critical}$ across the span, to hold fuel, and match required bending moments. The span distribution can be seen in Figure II-4.

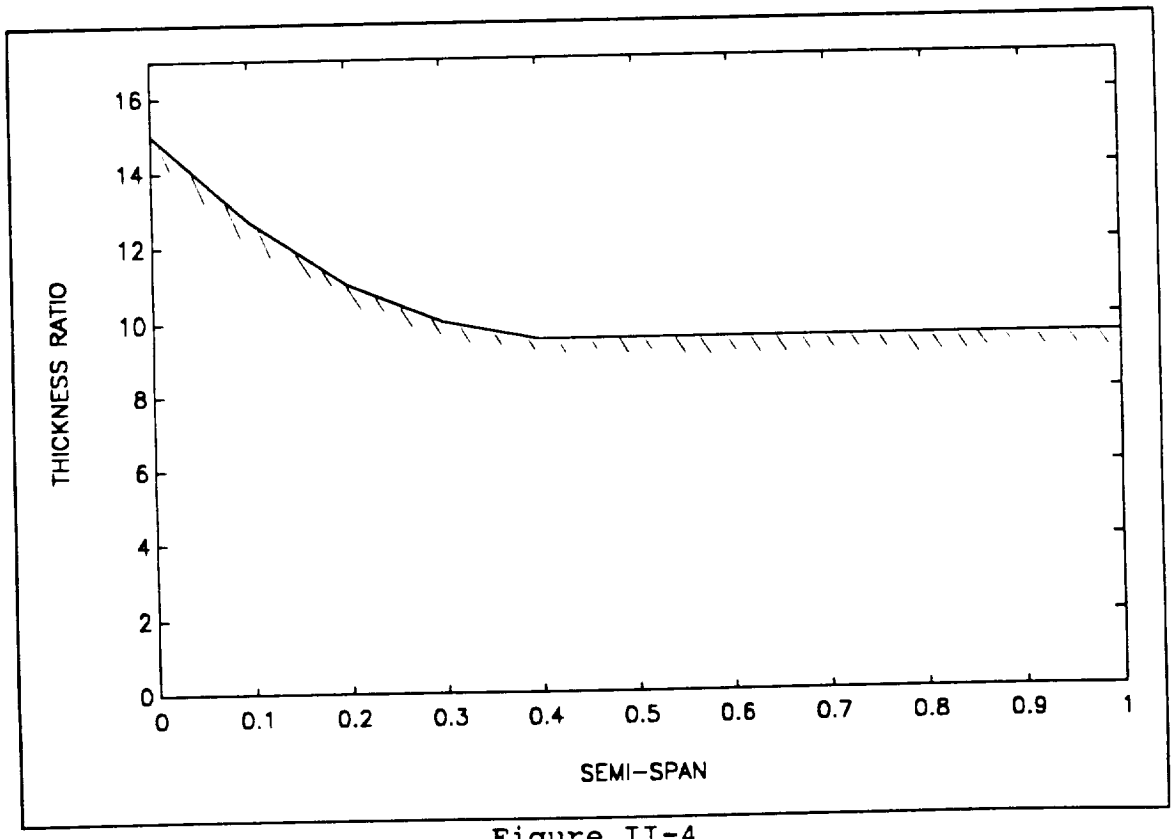

Figure II-4
Thickness Ratio vs. Semi-Span

3. HIGH LIFT DEVICES

To increase the lift of the wing, the circulation must be increased and/or separation prevented. The circulation may be increased by increasing α and by making the camber more positive in the region of the trailing edge. A trailing edge flap effectively increases the airfoil camber and increases the circulation resulting in an increase in C_l. This increase in circulation is observed as an increase in the magnitude of the angle for zero lift. Separation is prevented by reducing the adverse pressure gradient over the top of the airfoil or by stabilizing the layer with suction or blowing.

HUGO uses trailing edge flaps, which increase the circulation about the airfoil. Hugo also has leading edge Curved Krueger flaps which act as separation delay devices. The Krueger flaps are a two-position flap. One position for takeoff, and one for landing. The angle required was determined by the streamtube flowing over the leading edge in the given configuration.

The trailing edge flaps are triple slotted Fowler type flaps. These flaps, in conjunction with the leading edge flaps, will give a C_{Lmax} of 2.5. The flap effects can be seen in Figure II-5 (Waviness in linear region due to plotting). Torenbeek, Reference 27, provides a typical cargo aircraft C_{Lmax} of 2.3 and 3.0 for a takeoff and landing configuration, respectfully.

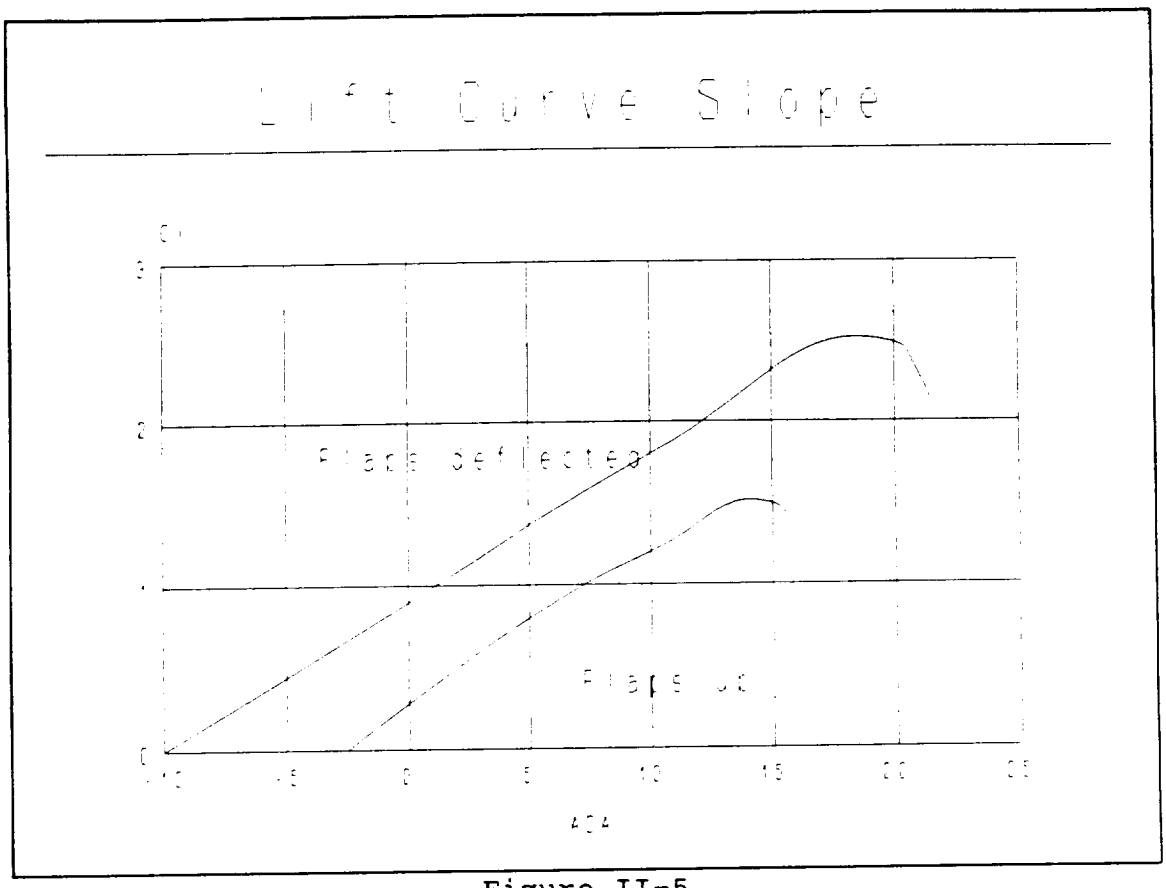

Figure II-5
Lift Curve Slope

The geometric configuration of the wing can be seen in Figure II-6. The position of the control surfaces were determined by the control power required to maneuver. The diagram shows:

- Inboard and Outboard Ailerons
- Air brakes and Ground Spoilers
- Leading Edge Krueger Flaps
- Triple Slotted Fowler Trailing Edge Flaps

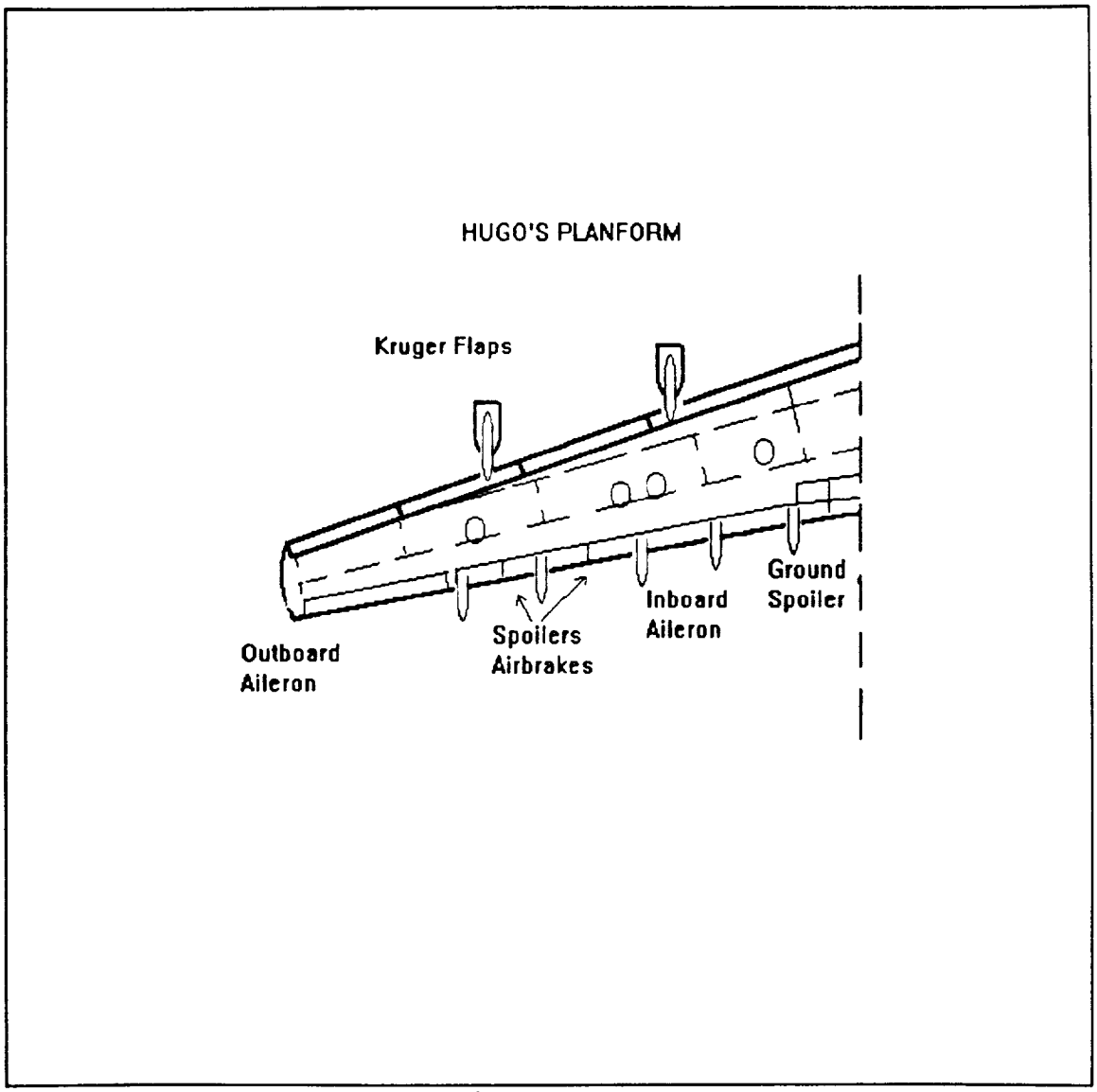

Figure II-6
Planform

III. STRUCTURAL ANALYSIS

Hugo's structural design has been optimized to meet or exceed both RFP and MILSPEC requirements. Structural technology has been elevated to obtain an aircraft capable of transporting a larger payload further than ever before. RFP requirements for a 400,000 pound minimum payload at a 2.5g maneuver load factor formed the initial structural design constraints. Optimization of the cargo bay to transport material in support of a mechanized infantry division and civilian applications provided sizing characteristics to optimize the cargo bay and fuselage. Using Forsch, Reference 8, innovative use of composite materials were used throughout the aircraft structure producing significant weight savings.

A. INTERNAL CONFIGURATION

Initial sizing of the fuselage was performed through optimization of the cargo bay for various military and civilian payloads. A study of current civilian and military cargo showed the cargo bay width to be driven by civilian cargo containers; while military cargo dictated height requirements. Optimum length was driven by both civil cargo containers and optimum fineness ratio. The driving factor in determining the design payload was the 126,000 pound M-1 tank.

Multiples of this weight provided additional input to the sizing study.

Once layout of the cargo bay was determined, various payload arrangements were devised as shown in Figure III-1. Both nose and rear loading capabilities were incorporated into the design to facilitate rapid cargo unloading. Frontal access is through a visor type nose, requiring placement of the cockpit above the cargo bay. The ability to carry wide items, such as the M2A2 Bradley and the LAV-25, side by side further increase the cargo versatility of HUGO.

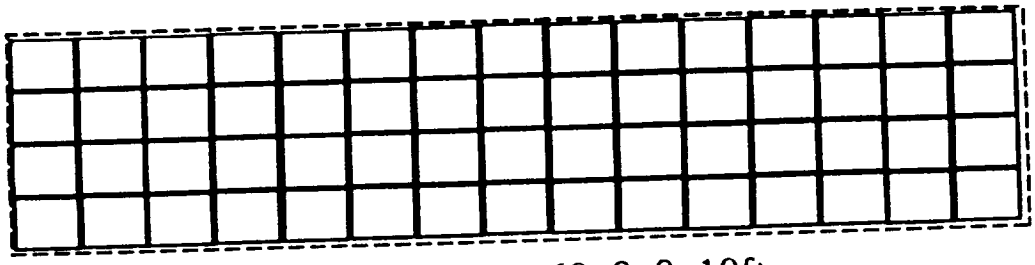

Military Pallets: 60 8x8x10ft
@111bs/ft^3=422,4001bs

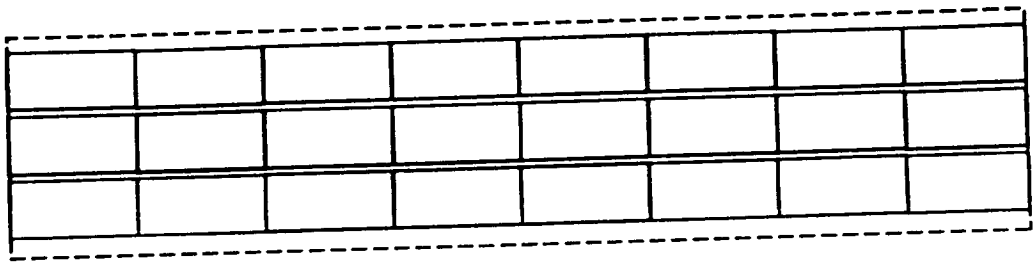

Civil Containers: 8 9x10x20ft
@101bs/ft^3=432,0001bs

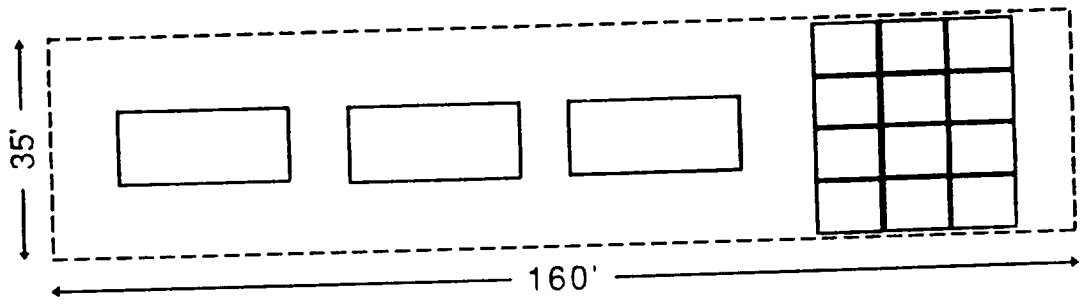

3 M-1 Abrams tanks and
12 8x8x10ft pallets @91bs/ft^3

35ft cargo bay allows
3 vehicles side by side

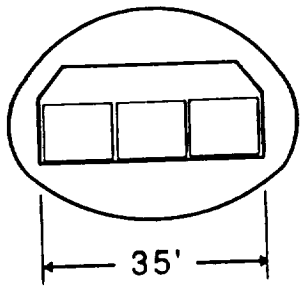

Figure III-I
Cargo Bay Loading Configurations

B. REFINED WEIGHT ANALYSIS

Upon completion of the initial configuration and sizing, a component weight analysis program was established. Multiple iterations through Nicolai's, Reference 22, weight analysis techniques provided the basic results. Reducing composite components by a nominal 20% resulted in the weights shown in Table III-1. Variation of component moment arms in Table III-1 provided a means to control CG travel. Keeping the static margin less than 15% (Raymer, Reference 23), the aircraft weight distribution was manipulated to produce a maximum CG travel of 15 feet or 23% MAC during flight operations as shown in Figure III-2. Final component placement resulted in mass moments of inertia, also shown in Table III-1, which provided input for control analysis.

SEGMENT	WEIGHT	X ARM	X MOM	Z ARM	Z MOM	Y ARM	Y MOM	Ixx	Iyy	Izz	Iyz	Ixy	Ixz
AIRFRAME													
Wing	1999040.0	119.0	21182000.0	45.0	8010000.0	51.0	9078000.0	484908425.0	83398441.7	524444016.7	0.0	0.0	-36714790.9
Fuselage	48814.0	130.0	6435000.0	17.0	841500.0	15.0	742500.0	25275599.4	16984176.5	13983577.1	0.0	0.0	6343352.5
Horiz Tail	17600.0	235.8	4291560.0	60.0	1092000.0	30.0	546000.0	28777792.4	187966800.5	191949008.1	0.0	0.0	46854775.9
Vert Tail	6340.0	235.8	1721340.0	50.0	365000.0	0.0	0.0	1892176.2	72312712.4	70420536.2	0.0	0.0	11543312.4
Main Gear	20775.0	135.0	2804625.0	6.0	124650.0	15.0	311625.0	20846122.9	18310318.3	4812945.4	0.0	0.0	1496972.2
Nose Gear	7400.0	15.0	111000.0	5.0	37000.0	0.0	0.0	6180657.4	117376793.6	111196136.2	0.0	0.0	26215743.7
PAYLOAD	450000.0	167.0	75150000.0	25.0	11250000.0	5.0	2250000.0	46896435.9	425067780.9	400871345.1	0.0	0.0	-117819705.5
FUEL SYSTEM													
Wing Fuel	500000.0	124.0	62000000.0	40.0	20000000.0	20.0	10000000.0	218603525.8	110847650.3	292244124.5	0.0	0.0	-41425428.4
Wing Bladder	8500.0	121.0	1028500.0	40.0	340000.0	20.0	170000.0	3716259.9	2653625.0	5737365.0	0.0	0.0	-859776.1
PROPULSION													
STRBD Outbd Eng's	26000.0	114.6	2980359.2	35.0	910000.0	100.0	2600000.0	260031446.2	13729823.9	273698377.8	0.0	0.0	-656324.3
Nacelle/Duct	4000.0	114.0	456000.0	35.0	140000.0	100.0	400000.0	40004837.9	2229402.5	42224564.6	0.0	0.0	-103740.8
Wing Eng Ctrls	448.0	110.0	49060.0	35.0	15610.0	100.0							-13529.1
Starting Sys	900.0	110.0	99000.0	35.0	31500.0	100.0							-27300.8
STRBD Mid Eng's	26000.0	103.0	2677269.4	35.0	910000.0	75.0	1950000.0	146281446.2	31176943.0	177395496.8	0.0	0.0	-989649.8
Nacelle/Duct	4000.0	104.0	416000.0	35.0	140000.0	75.0	300000.0	22504837.9	4516014.1	27011178.2	0.0	0.0	-147731.2
Wing Eng Ctrls	448.0	98.0	43708.0	35.0	15610.0	75.0							-19415.0
Starting Sys	900.0	98.0	88200.0	35.0	31500.0	75.0							-39178.2
STRBD Inbd Eng's	26000.0	91.3	2374179.8	35.0	910000.0	50.0	1300000.0	65031446.2	55690479.2	120659033.1	0.0	0.0	-1322975.4
Nacelle/Duct	4000.0	92.0	368000.0	35.0	140000.0	50.0	200000.0	10004837.9	8315948.0	18311110.2	0.0	0.0	-200519.6
Wing Eng Ctrls	448.0	87.0	38802.0	35.0	15610.0	50.0							-24810.4
Starting Sys	900.0	87.0	78300.0	35.0	31500.0	50.0							-50065.8
UTILITIES													
Cockpit Indicators	365.0	15.0	5475.0	40.0	14600.0	6.0	2190.0	28720.6	5498254.9	5497814.3	0.0	0.0	-272919.4
AC/Anti-Ice	5750.0	91.3	525058.9	20.0	115000.0	50.0	287500.0	15485996.1	13420205.4	26884209.2	0.0	0.0	3698037.8
Oxy Sys	200.0	85.0	17000.0	20.0	4000.0	20.0	4000.0	118643.3	591630.3	832986.9	0.0	0.0	146182.3
Elec sys	3620.0	60.0	217200.0	20.0	72400.0	50.0	181000.0	9749444.5	22488466.4	30839021.9	0.0	0.0	3903871.4
APU	500.0	130.0	65000.0	15.0	7500.0	0.0	0.0	178609.6	207357.8	28748.3	0.0	0.0	71656.9
MISC.													
Pass Seats	3200.0	70.0	224000.0	37.0	118400.0	20.0	64000.0	1310747.2	14646471.8	15895724.6	0.0	0.0	-670367.6
Flt Dk Seats	220.0	20.0	0.0	23.0	5060.0	10.0	2200.0	48139.4	3067788.6	3063649.3	0.0	0.0	281969.4
Lav	510.0	50.0	25500.0	23.0	11730.0	1.0	510.0	61105.8	3972662.8	3912577.1	0.0	0.0	486882.7
TOTAL	1366962.0 pounds 42486.5 slugs		185472137.1		45700170.0		30389525.0	1407935253.5	1212467747.8	2361313544.4	0.0	0.0	-100515468.9

Xcg from nose	137.6	Ixx =	43760031.5
		Iyy =	37684708.5
Zcg ref 10" below fuselage	33.9	Izz =	73391979.4
		Ixy =	0.0
STATIC MARGIN %	14.7	Iyz =	0.0
		Ixz =	-3124121.0

Table III-1
Weight Analysis

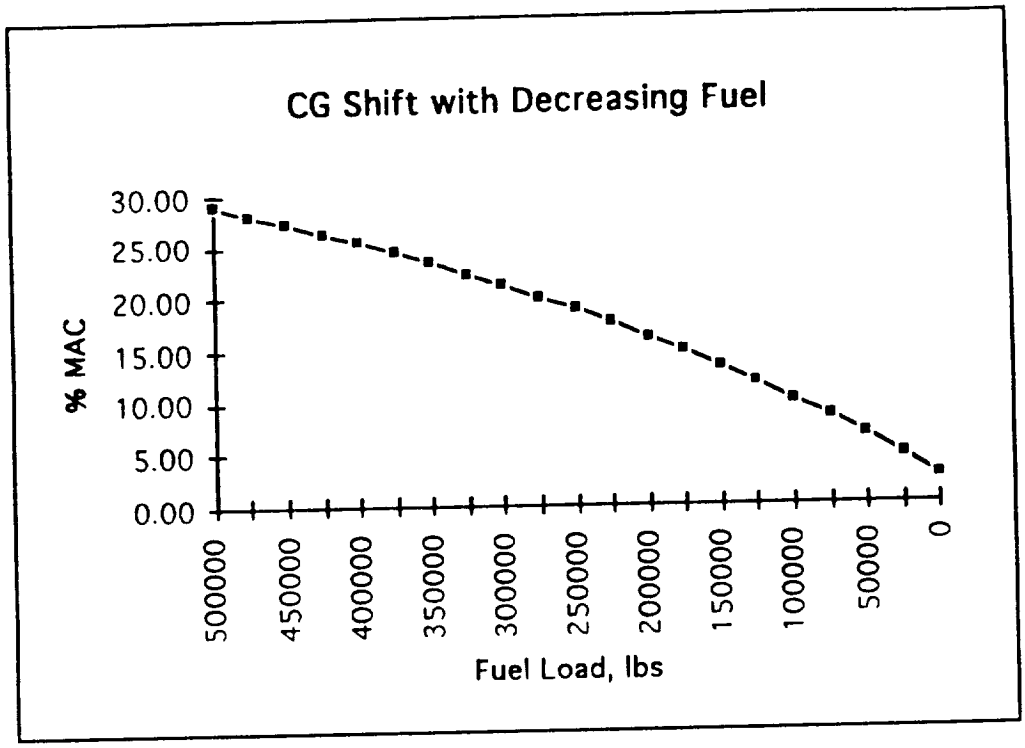

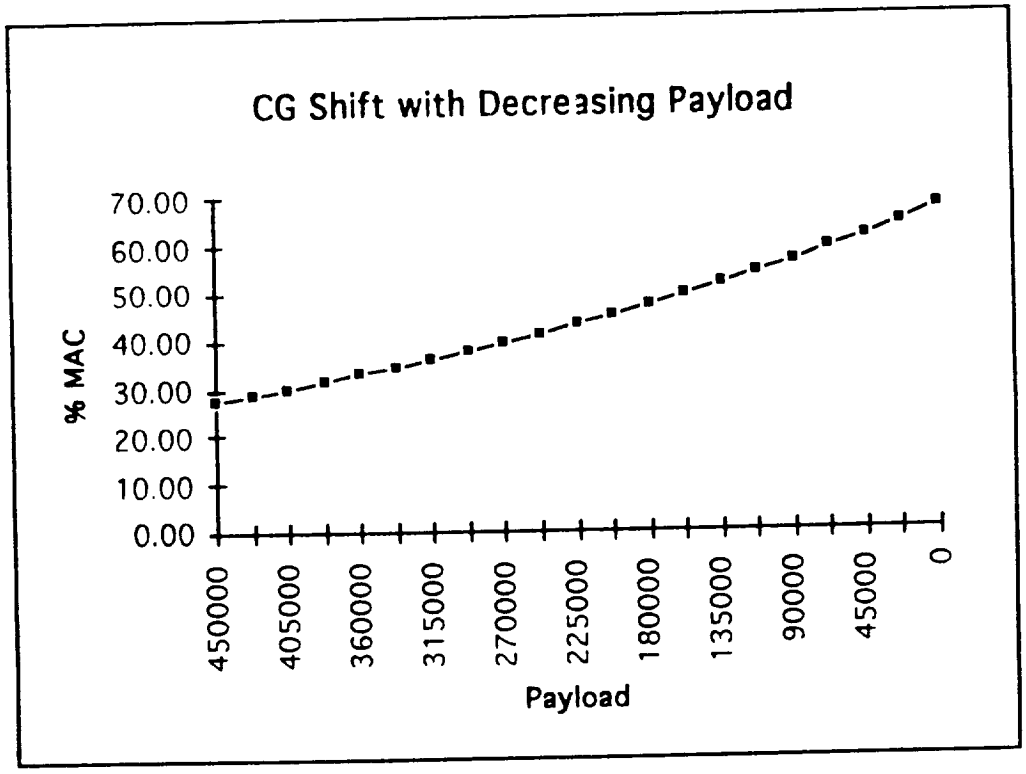

Figure III-2
Center of Gravity Shift

C. CONSTRUCTION MATERIALS

The material selection process was driven by the need to balance weight reduction and costs. Although the use of weight saving composite materials were most desirable, prohibitive costs and manufacturing concerns limited their use on a large scale. Improved aluminum alloys were chosen for use throughout the fuselage and internal wing structures.

Advanced composite materials were chosen for a variety of proven applications. Most significantly the wing skins, nose visor, landing gear doors and control surfaces were constructed from high strength graphite-epoxy. Efficient use of this material in areas of relatively low stress has helped produce considerable weight savings. Aramid-carbon layups, which achieve maximum weight reduction at minimum cost, were used with honeycomb cores in the engine nacelles, pylon fairings, and wing-fuselage fairings.

D. LOAD ANALYSIS

To facilitate analysis of in-flight loads, Hugo was modeled as a combination of simply supported components. Applied loads were studied at normal cruise, a safety factor of 1.5 times the limit load, and at sea level. Lifting loads were generated from the use of a vortex-panel computer code using the wing planform at cruise altitude. The wing was further modeled as a trapezoidal volume (Torenbeek,

Reference 27), allowing a study of the effects of fuel tank and engine placement, and in-flight loads experienced by the wing. Synthesis of the above data produced shear and moment diagrams for discussed load regimes and is displayed in Figure III-3. Note that as expected, the maximum shear and moment occurs at the wing root during the 3.75 g maneuver load at approximately 2.5 million pounds and 130 million ft-lbs, respectively. Internal construction of the wing and fuselage was designed to support these loads.

Problems associated with the effects of wing flutter were combated with a combination of aeroelastic tailoring of the wing and strategic placement of the outer engines.

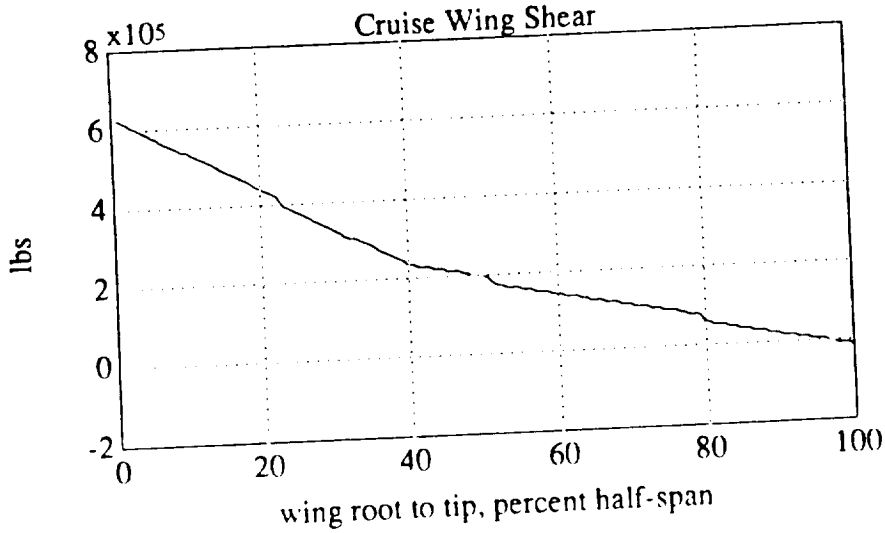

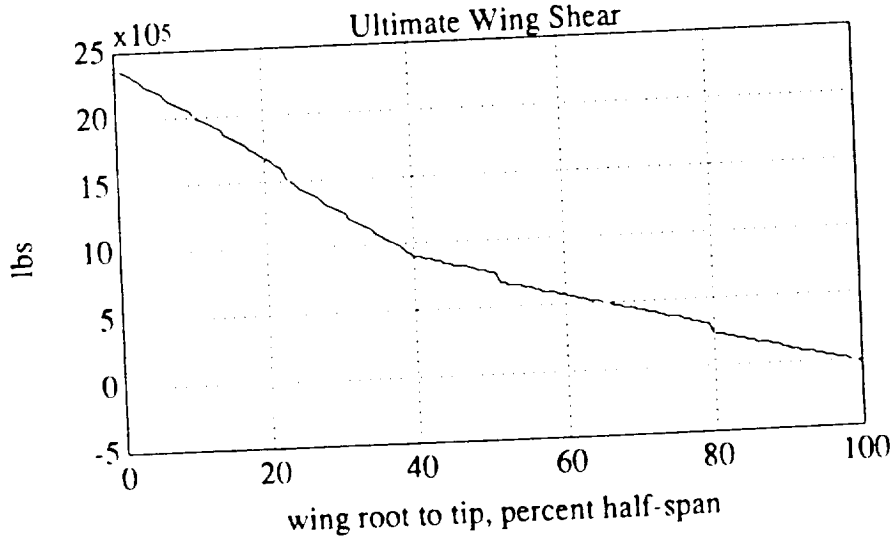

Figure III-3a
Wing Shear Loads

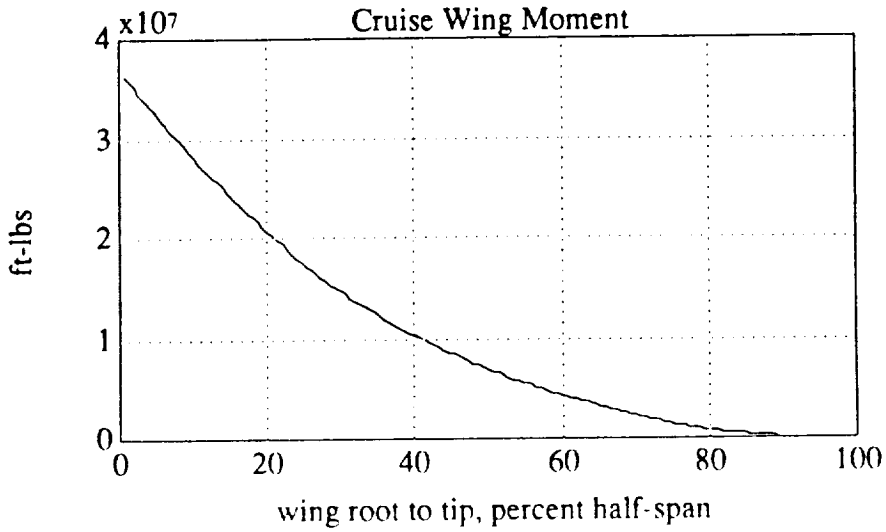

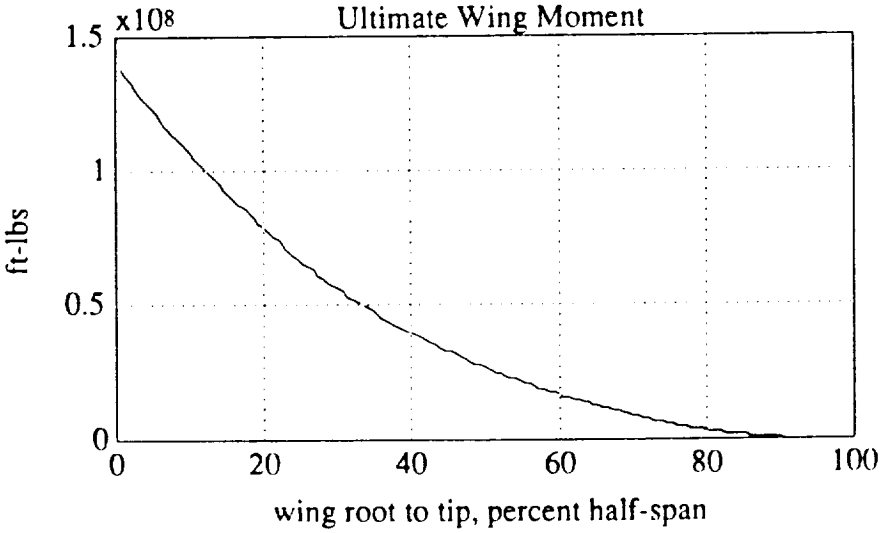

Figure III-3b
Wing Moment
Loads

E. Landing Gear

1. Configuration

Hugo's enormous size required the use of a multi-bogy landing gear configuration with the main gear having eight, three-wheeled trucks and the nose gear a single four-wheeled truck. Landing load and configuration analysis was performed according to Raymer, Reference 23 and Curry, Reference 4.

Longitudinal and lateral placements of the landing gear are shown in Figure III-4. Tip-back requirements resulted in longitudinal truck placement of 33.5 feet for the nose gear and 150.5 feet for the main gear. This produced a static taildown angle of 16° and a tip-back angle of 18°. Angle off the vertical from the main gear to the most aft CG is 22°, which is larger than the tip-back angle as required. Lateral placement of the main gear provides for an overturn angle of 27°. This configuration has the nose gear carrying a minimum of 6% and a maximum of 19% of the static gross weight of the aircraft, thus allowing for sufficient nose wheel steering capability.

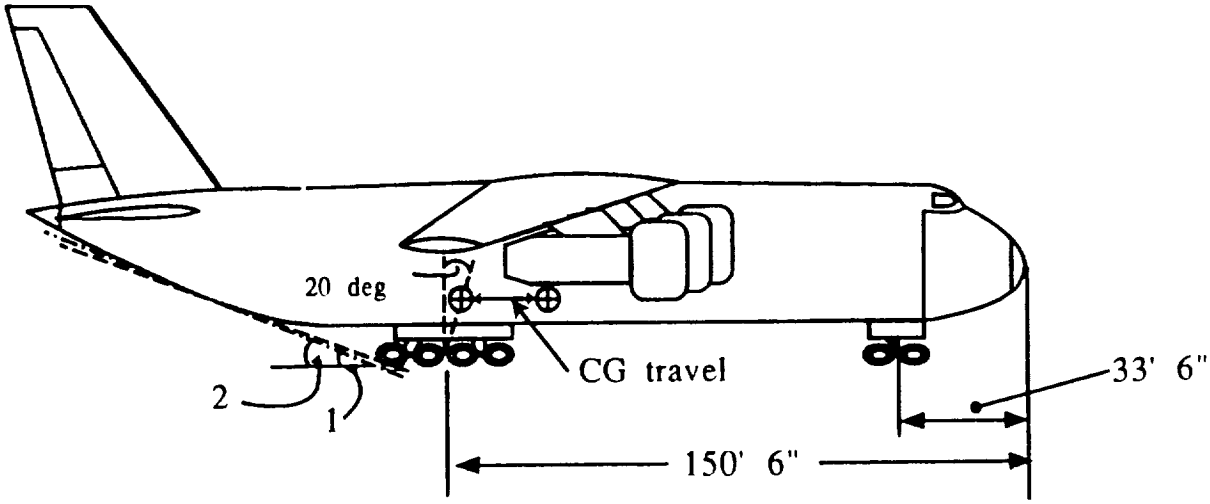

1. Static Taildown Angle = 16 deg
2. Tipback Angle = 18 deg

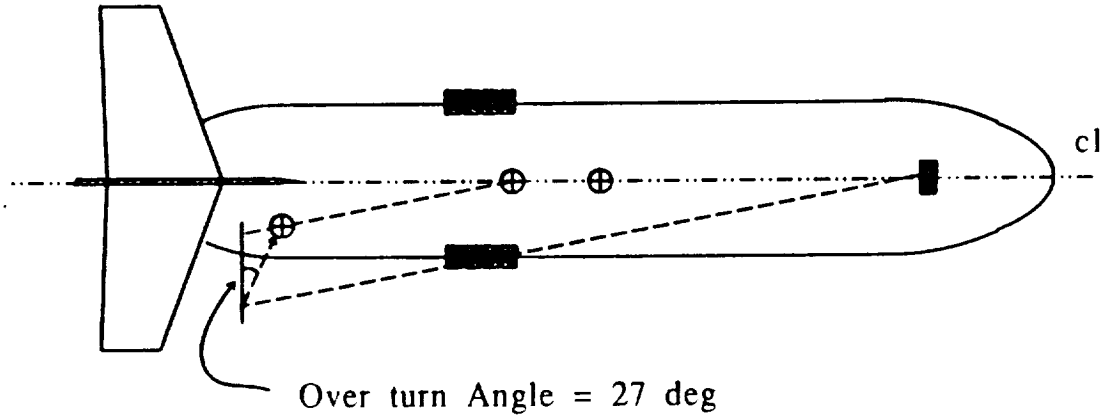

Figure III-4
Hugo Landing Gear Geometry

2. Tire Sizing

Tire selection for the desired configuration was based on loads calculated using Raymer, Reference 23, and are presented in Table III-2.

Table III-2
Tire Load Sizing

Max Gross Weight	1,400,000 pounds
Max Static Load	1,300,000 pounds
Max Static Load-Nose	400,000 pounds
Min Static Load	65,812 pounds
Dynamic Braking Load	37,161 pounds

In order to keep the number of nosewheels to a minimum, the same size tires are used throughout. Minimum calculated tire dimensions were calculated 50 inches diameter and 20 inches wide. These loads and dimensions correspond to several commercially available tires as shown in Raymer, Reference 23. Selected tire specifications are displayed in Table III-3.

Table III-3
Tire Specifications

Type	Three part name	Max Diameter	52.0 in
Size	52x20-23	Rolling Radius	21.3 in
Max Load	63,700 lbs	Wheel Diameter	23.0 in
Inflation	195 psi	Number of Plies	30
Max Width	20.5 in		

3. Stroke and Oleo Sizing

Calculations of the landing gear stroke used a vertical velocity of 12 feet per second at touchdown. A shock absorber stroke of 9.5 inches was calculated using an oleo efficiency of 0.8, gear load factor of 2.85, tire efficiency of 0.47, and tire data presented above (Raymer, Reference 23 for method). In order maintain efficient steering, the nosewheel stroke was set to 10.5 inches. The total oleo length is 17 inches for the main gear and 23 inches for the nose. Using an internal pressure of 2000 psi, the required oleo outer diameters are 18.7 inches for the main gear and 21.7 inches for the nose gear. Figure III-5 displays the structural configuration.

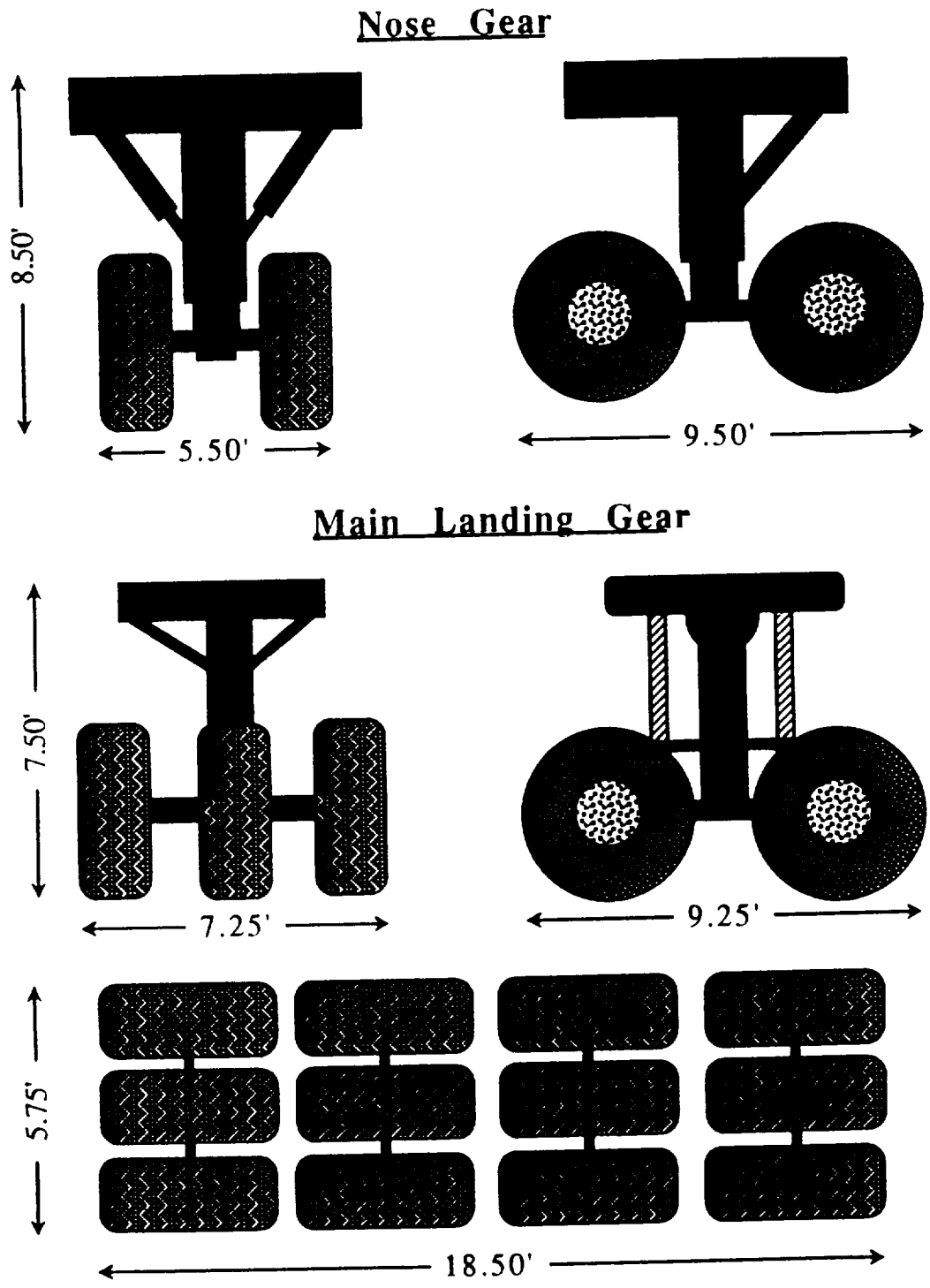

Figure III-5
Landing Gear Configuration

IV. PROPULSION

A. ENGINE SELECTION

Engine selection to maximize the amount of material that can be transported in 72 hours was based upon the selected flight profile. High subsonic and supersonic cruise profiles were the two explored. The low subsonic flight regime was eliminated due to the time period required to deliver the material.

The design point for the supersonic analysis was Mach 2.5 at 60,000 feet (Chapter I). On-design analysis for the supersonic engine was carried out using Mattingly's ONX program, Reference 18, for gas turbine engines. The engine cycles considered were turbojet with afterburner, mixed exhaust turbofan with afterburner and stoichiometric burning turbojets and turbofans. The minimum Thrust Specific Fuel Consumption(TSFC) attainable using this analysis was 1.6 per hour. This TSFC combined with the size and drag of the aircraft at Mach 2.5 eliminated the supersonic flight regime.

The design point for the high subsonic flight profile for the HUGO aircraft was Mach 0.8 at 35,000 feet. The four engine cycles considered were the turbojet, high bypass turbofan, unducted fan, and the AIAA Advanced Turbofan(ATF).

Figure IV-1 is a graph of TSFC versus Thrust at Mach 0.8 and 35,000 feet for all four engines. It can be shown from this graph that the two best cycles in terms of TSFC and Thrust are the UDF and the AIAA ATF engines. The final factor in deciding which engine would power the Hugo aircraft was the size of the engine. The UDF has a fan blade diameter of 21 feet whereas the ATF engine has a fan tip diameter of 12.5 feet. Due to the diameter of the UDF engine fan blades and the TSFC data, the AIAA ATF engine was selected for the HUGO aircraft.

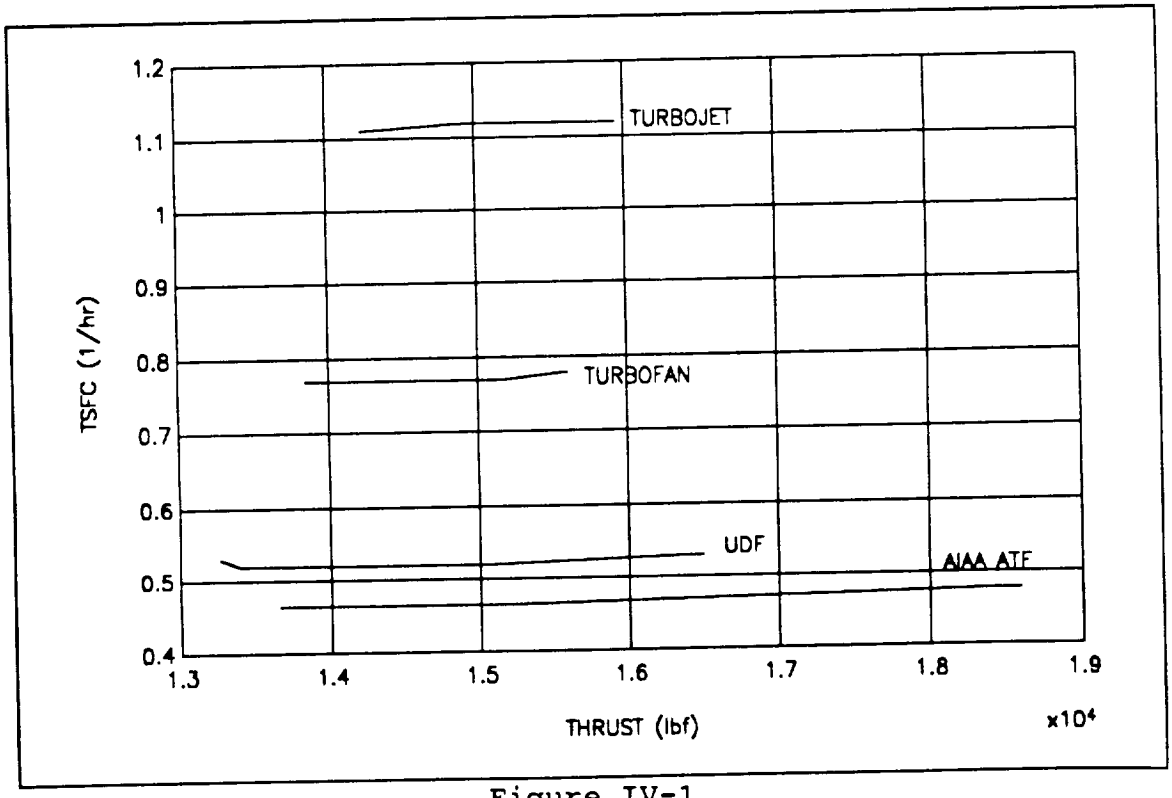

Figure IV-1
On-Design TSFC vs. Installed Thrust

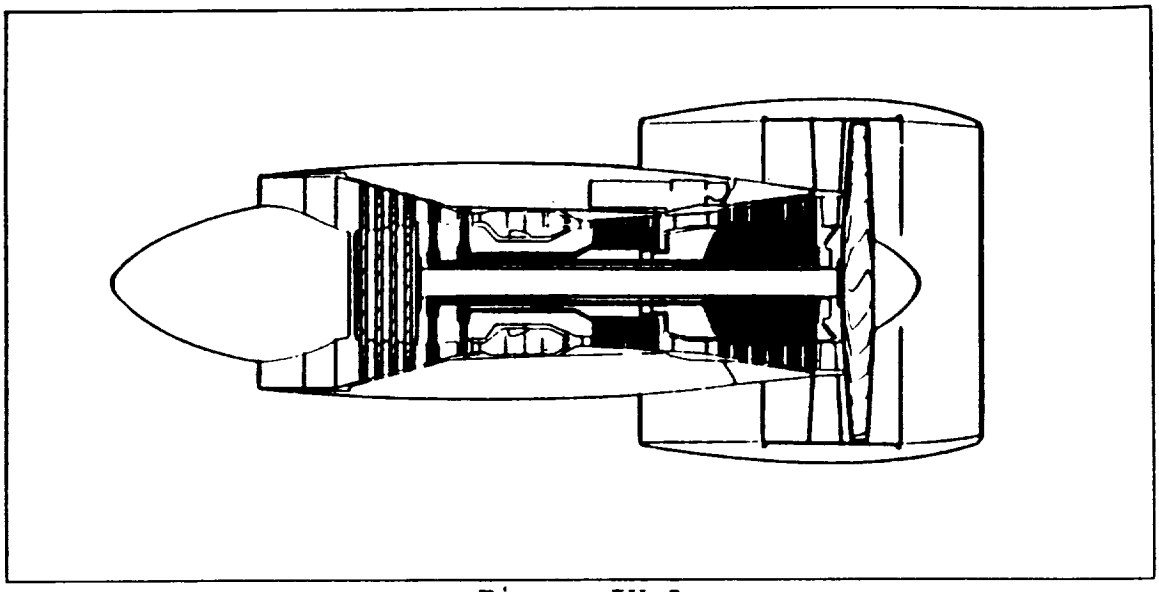

Figure IV-2
High Bypass Turbofan Engine

B. ENGINE DESIGN

The design of the ATF engine was carried out following the information given in Gouhin, Reference 10. Fan diameter, bare engine length, and bare engine weight were calculated using equations provided in Gouhin. Figure IV-2 is a schematic of a high bypass turbofan engine taken from Torenbeek, Reference 27. Figures of merit for the ATF engine are listed in Table IV-I.

C. ENGINE PERFORMANCE

Uninstalled performance (thrust, fuel flow, and ram drag) for the AIAA ATF engine was provided in Gouhin. Figure IV-3 is a plot of Uninstalled Thrust vs. Ram Drag. The

Uninstalled performance (thrust, fuel flow, and ram drag) for the AIAA ATF engine was provided in Gouhin. Figure IV-3 is a plot of Uninstalled Thrust vs. Ram Drag. The maximum uninstalled thrust available of 120,000 pounds occurs at Mach 0.4 and sea level. The maximum ram drag on the engine is at Mach 0.6 and 10,000 feet. Figure IV-4 is a plot of Ram Drag versus Mach Number at varying altitudes.

Table IV-1
ATF Figures of Merit

BARE ENGINE WEIGHT	13,500 lbs
BARE ENGINE LENGTH	11.7 ft
FAN DIAMETER	12.5 ft
OVERALL PRESSURE RATIO	100
BYPASS RATIO	20
CRUISE THRUST	18,418.4 lbf
CRUISE TSFC	0.46 1/hr
SEA LEVEL THRUST	100,000 lbf
SEA LEVEL TSFC	0.23 1/hr

Installed performance was calculated from the uninstalled data provided. Figures IV-5 and IV-6 are plots of Installed Thrust and TSFC (military power) versus Mach number and altitude respectively. Figure IV-7 is a carpet plot showing the variation of Thrust and TSFC with Mach Number and altitude.

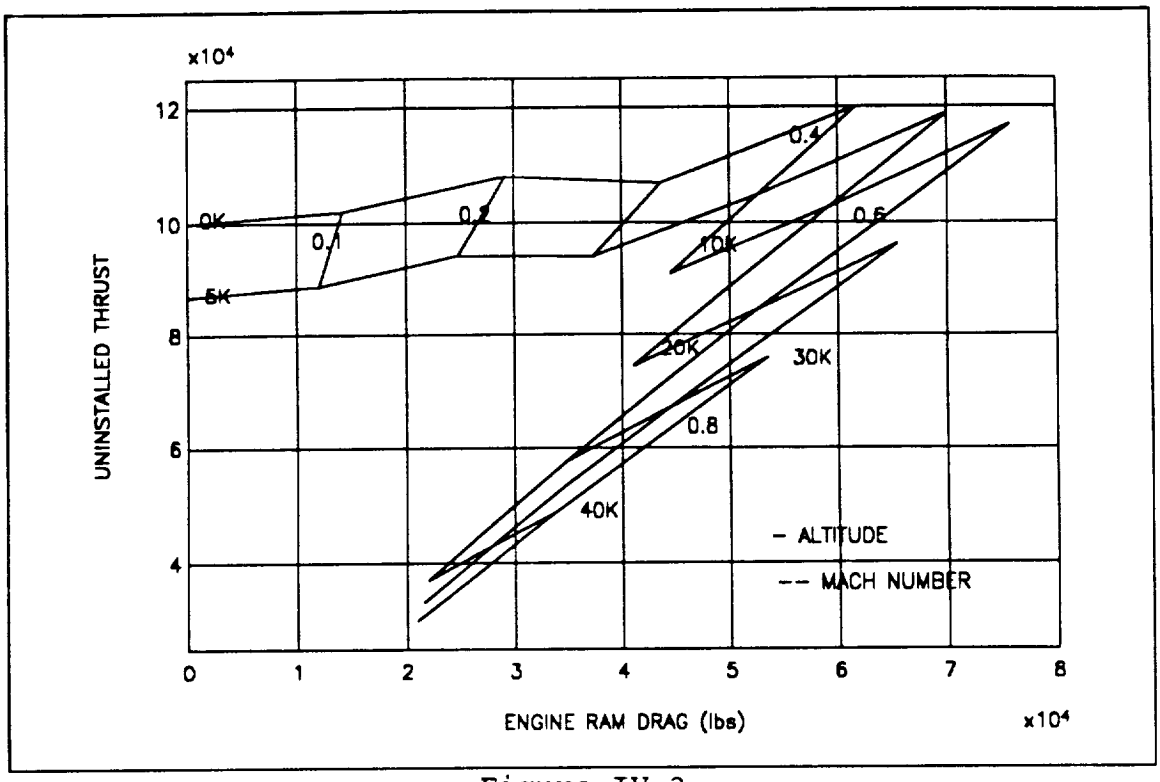

Figure IV-3
AIAA ATF Uninstalled Thrust vs. Ram Drag

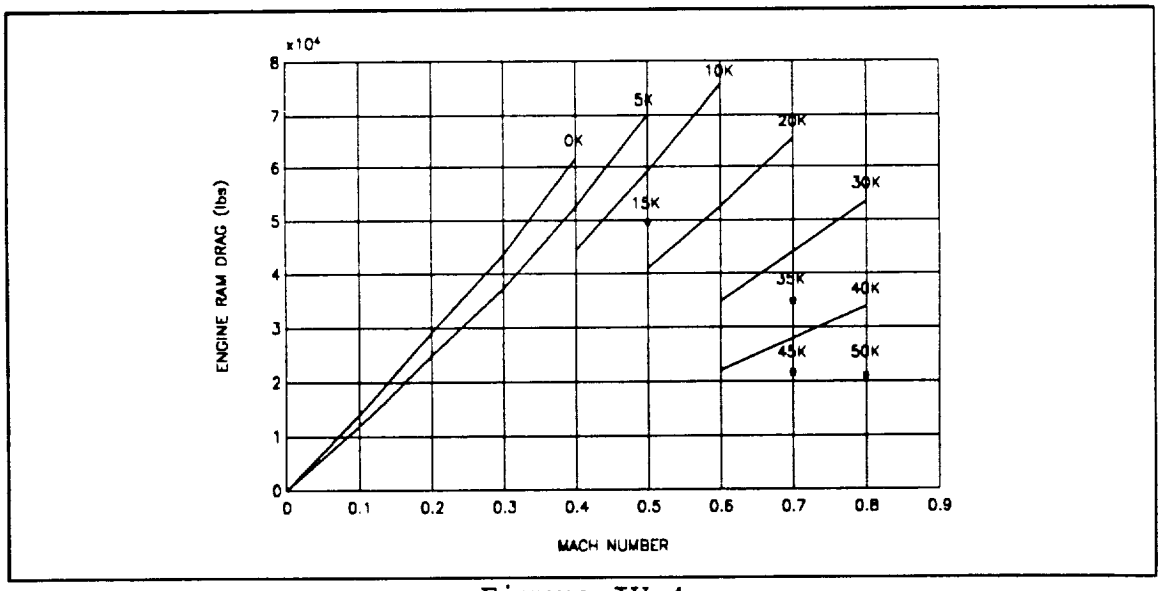

Figure IV-4
AIAA ATF Ram Drag vs. Mach

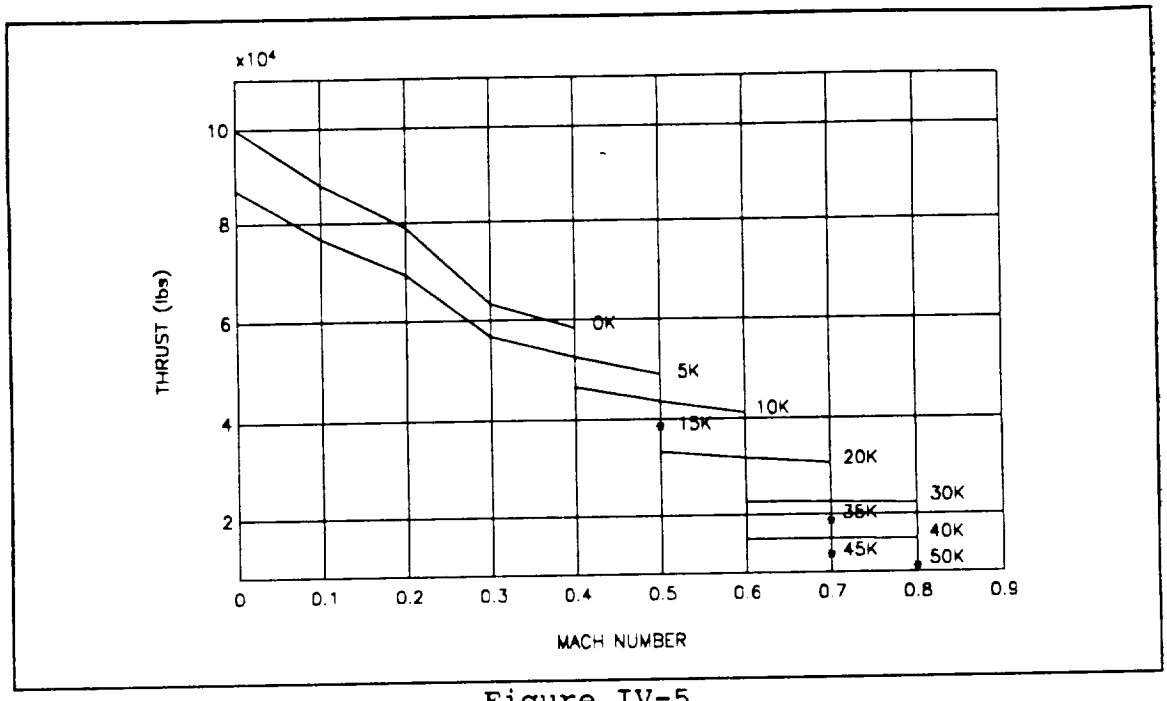

Figure IV-5
AIAA ATF Installed Thrust vs. Mach

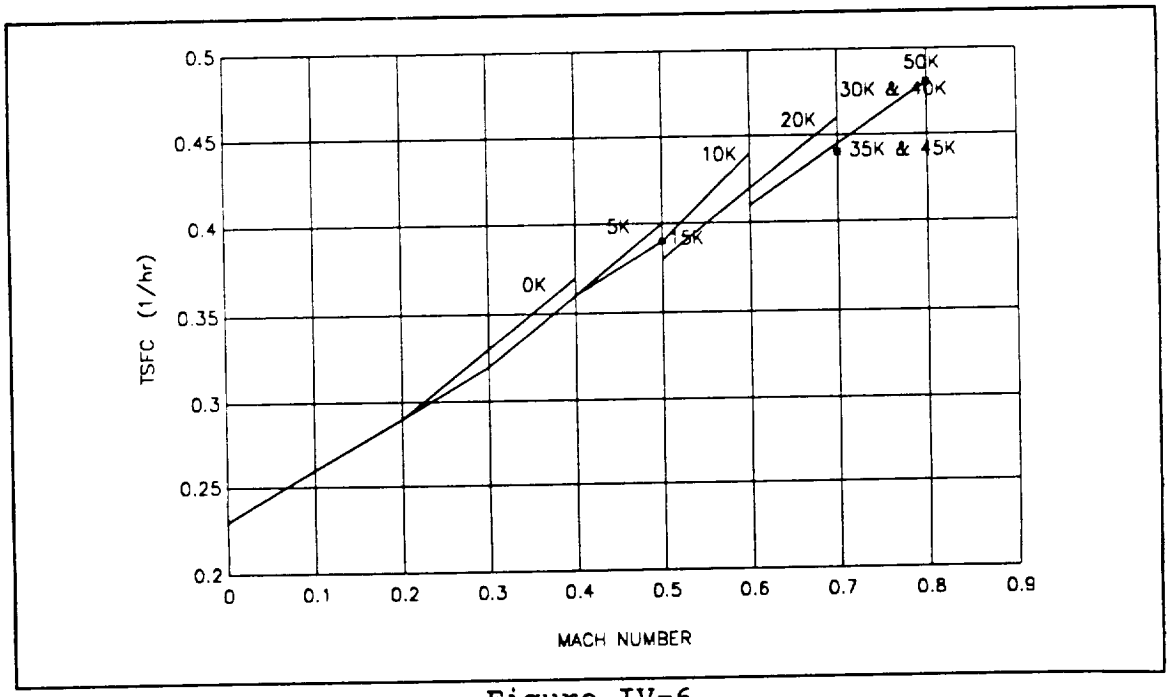

Figure IV-6
AIAA ATF Installed TSFC vs. Mach

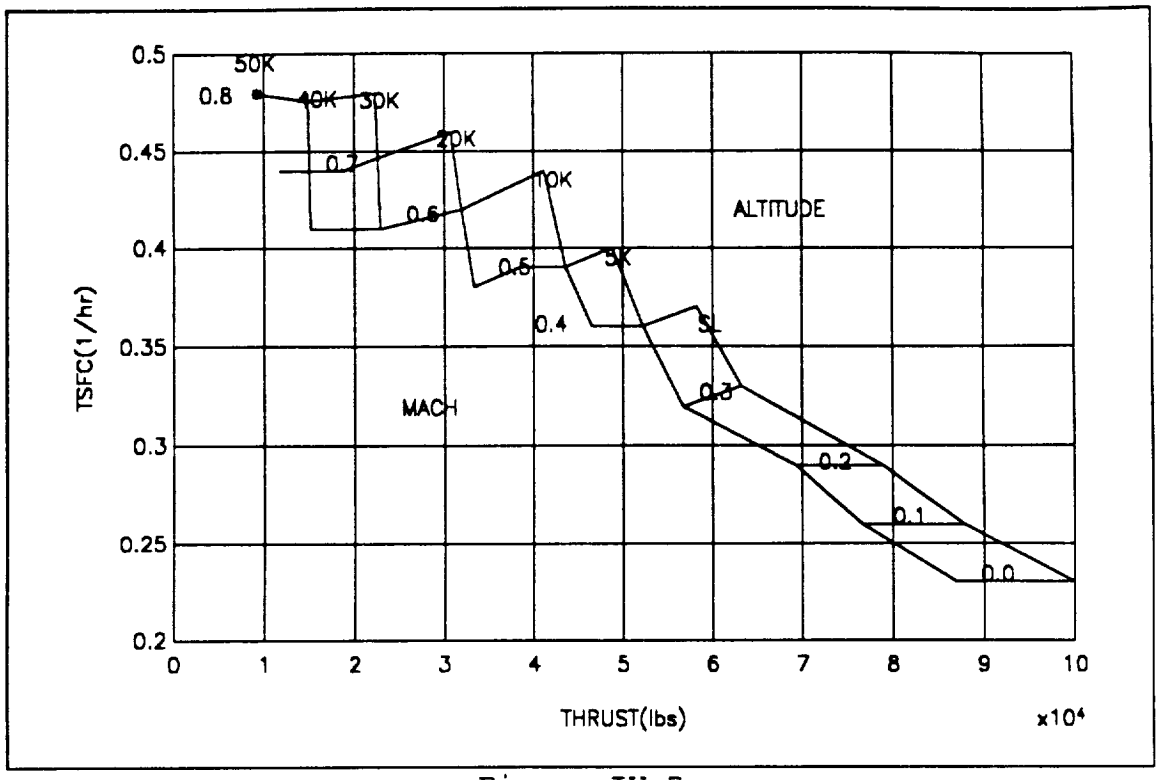

Figure IV-7
AIAA ATF Installed TSFC vs. Thrust/Mach/Altitude

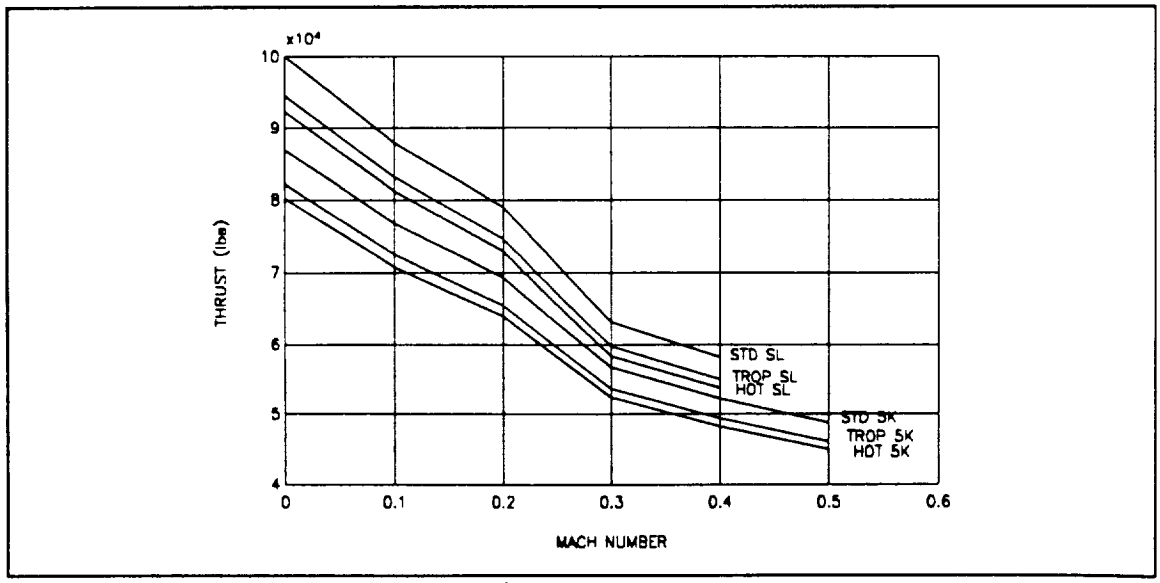

Figure IV-8
AIAA ATF Non-Standard Day Engine Data

The installed performance was also calculated using temperature ratios for hot (103 °F) and tropical (89.9 °F) days versus a standard day at sea level and at 5,000 feet. Figure IV-8 is a plot of this data.

D. INLET AND NOZZLE DESIGN

The inlet is a simple diverging duct designed to diffuse the oncoming streamtube of air from Mach 0.8 to Mach 0.4 at the face of the fan. This design was carried out using the corrected mass flow at the face of the fan and the inlet using equation 10.1 from Mattingly, Reference 18. MFP in equation 10.1 is the Mass Flow Parameter (0.5122). The face diameter of the inlet is 10.3 feet.

$$D_{th} = \frac{4}{\Pi} \frac{M_o\sqrt{T_{t0}}}{P_{t0}} \frac{1}{MFP\ @\ M=0.8} \qquad 10.1$$

Both the primary nozzle and the bypass nozzle are converging ducts designed to choke the flow at the exit at the on design condition. The analysis was conducted assuming the materials would be available for turbine construction to allow the combustor to operate stoichiometrically. Using this analysis the total exit area of the fan and core nozzles was calculated to be 60 square feet.

E. THRUST REVERSERS

The thrust reversal system will aid in reducing braking roll, especially on wet or icy runways. It is also useful in ground maneuverability.

The size and bypass ratio of the ATF engine make it impractical to use a conventional thrust reversal system. A conventional system would add up to 20% of the bare engine weight; therefore, the ATF has incorporated variable pitch fan (VPF) rotor blades. This VPF system will add a maximum of 7% of the bare weight. The variable pitch system also has a 15% increased reverse thrust rating over the conventional system (Torenbeek, Reference 27).

F. EMISSIONS

Engine emissions were estimated using the data from the Phase III Combustor S27E of the NASA/Pratt and Whitney Experimental Clean Combustor Program-Engine Test Results, (Roberts, Reference 24) on the JT9D-7A engine. This data was adjusted by 10% for advances in technology, based on sea-level takeoff, climb, and approach, and displayed in Table IV-2.

Table IV-2
Emissions (lb_m Pollutant/1000 lb_m Fuel/HR)

Nitrogen Oxides	2.4
Carbon Monoxide	2.9
Unburned Hydrocarbons	0.1
SAE Smoke Parameter	30

V. PERFORMANCE

A. PERFORMANCE CALCULATIONS

All performance calculations were performed using either a standard day (59 ^{o}F), tropical day (89.9 ^{o}F) or a hot day (103 ^{o}F) and are labeled accordingly. Subsonic theory was used for the calculations and is addressed in Anderson, Reference 1. All results reflect a clean cruise configuration with maximum payload and fuel. Exception to this can be found in the takeoff and landing calculations in which a takeoff C_L of 2.5 was used. In addition, a landing C_L of 3.2 was used with 100,000 pounds of fuel.

1. Fuselage Characteristics

Because of the large size of the aircraft and its design parameters, innovative ideas were considered including a way to minimize the drag contribution from the body. The dominating parameter in this calculation according to USAF DATCOM was the fineness ratio of the body (length/diameter). The drag contribution of the body versus fineness ratio can be seen in Figure V-1. From Figure V-1, a fineness ratio of about five appears ideal which agrees with Nicolai, Reference 22; however, it is not practical from a cargo standpoint and,

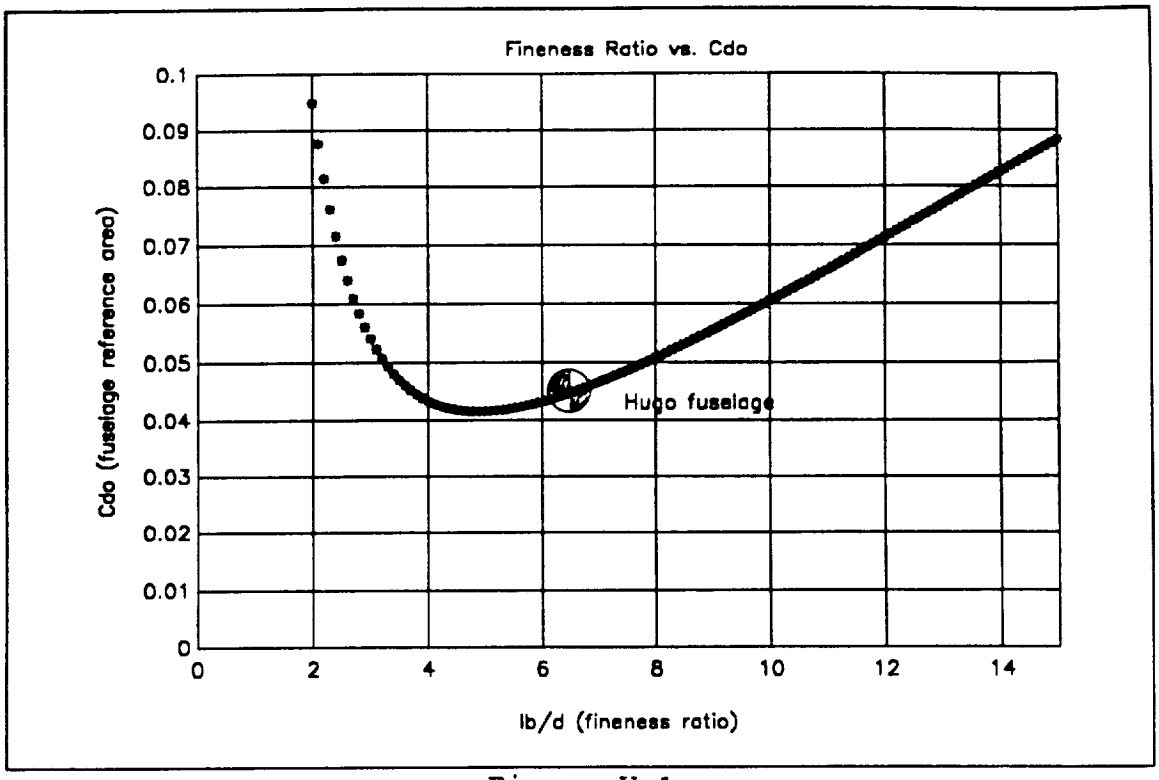

Figure V-1
Cdo vs. Fineness Ratio

more importantly, a stability and control standpoint. A fineness ratio of 6.5 was used to obtain a sufficient moment arm for the empennage.

2. Aircraft Drag Characteristics

After the general configuration and dimensions had been determined, several drag polers were calculated for use in other essential performance calculations. Two drag polers, a typical cruise configuration and a typical landing configuration, can be seen in Figure V-2 and were calculated using USAF DATCOM methods.

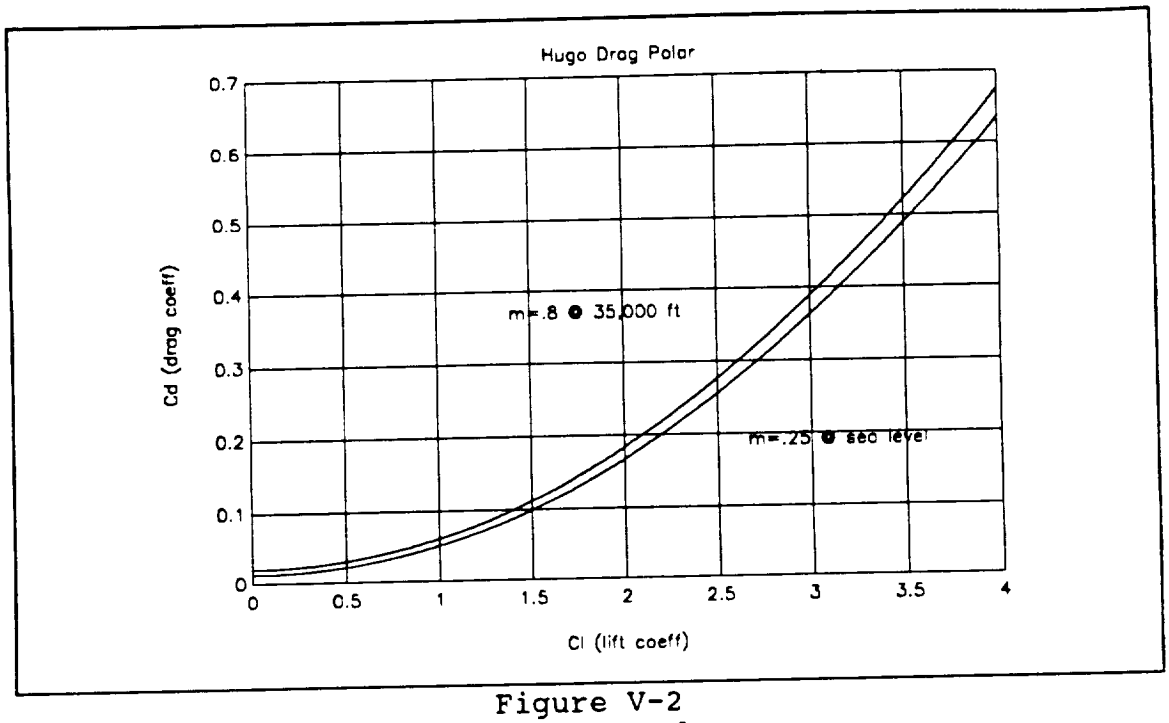

Figure V-2
Hugo Drag Polar

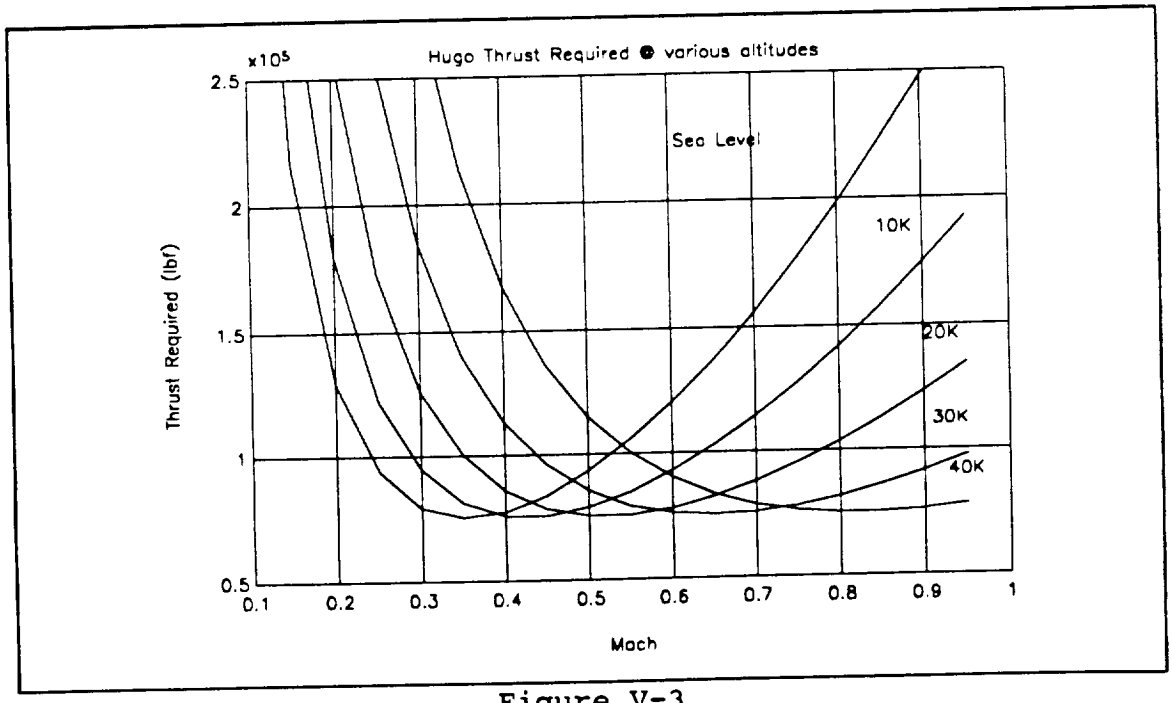

Figure V-3
Hugo Thrust Required

The equation form of the drag polar used for the cruise calculations is:

$$C_D = .02 + .041C_L^2 \qquad \text{V-1}$$

3. Thrust Required

The thrust required for Hugo at four different altitudes versus Mach number were calculated and plotted and can be seen in Figure V-3. The thrust required was calculated using the cruise drag polar and equating thrust required to drag for a particular altitude and Mach number.

4. Climb Performance

The climb performance was calculated using the equation:

$$\frac{R}{C} = \frac{V_\infty \left(THRUST\text{-}DRAG \right)}{WEIGHT} \qquad \text{V-2}$$

where thrust was the sea level thrust multiplied by the density ratio. The drag was calculated from the cruise drag polar and was plotted versus altitude and Mach number as seen in Figure V-4.

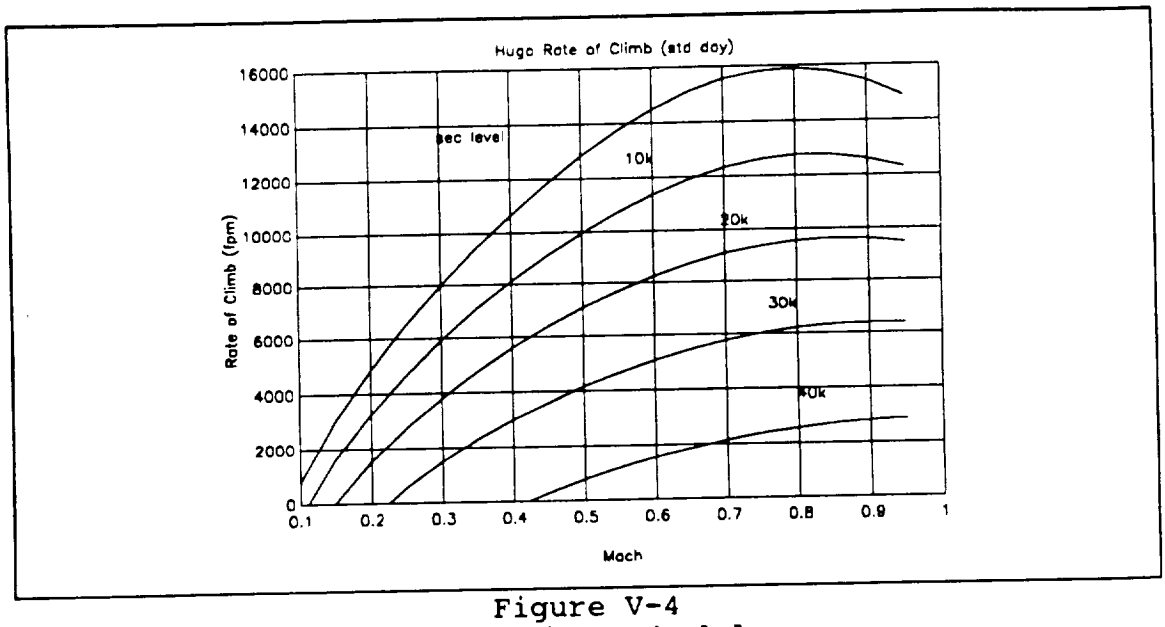

Figure V-4
Hugo Climb Schedule

5. Range and Endurance

The range and endurance were calculated using the Breguet range and endurance equations. The range and endurance were plotted versus payload and Mach number at the cruise altitude of 35,000 feet. The range plot shown in Figure V-5 shows that Hugo meets the range and payload requirements with a range of 6273 NM with a payload of 450,000 pounds.

It is interesting to note that if the advanced technology of boundary layer control were utilized, the lift over drag (L/D) ratio increases by approximately twenty-five percent and our range increases to over 7600 NM. Although

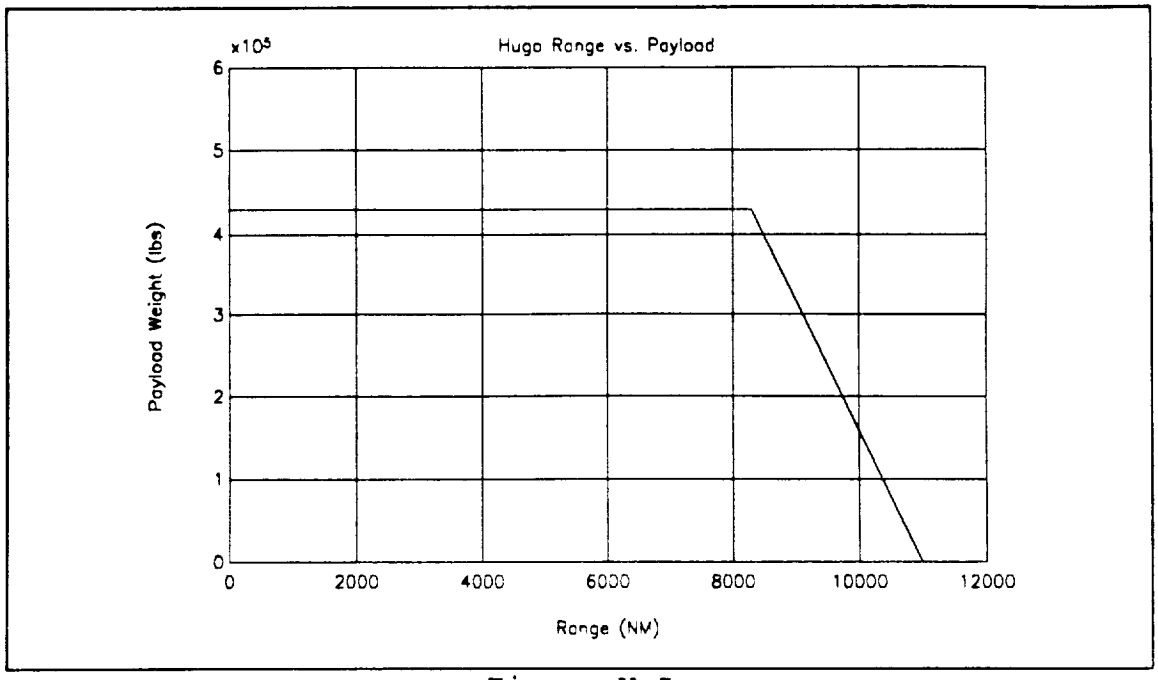

Figure V-5
HUGO Range

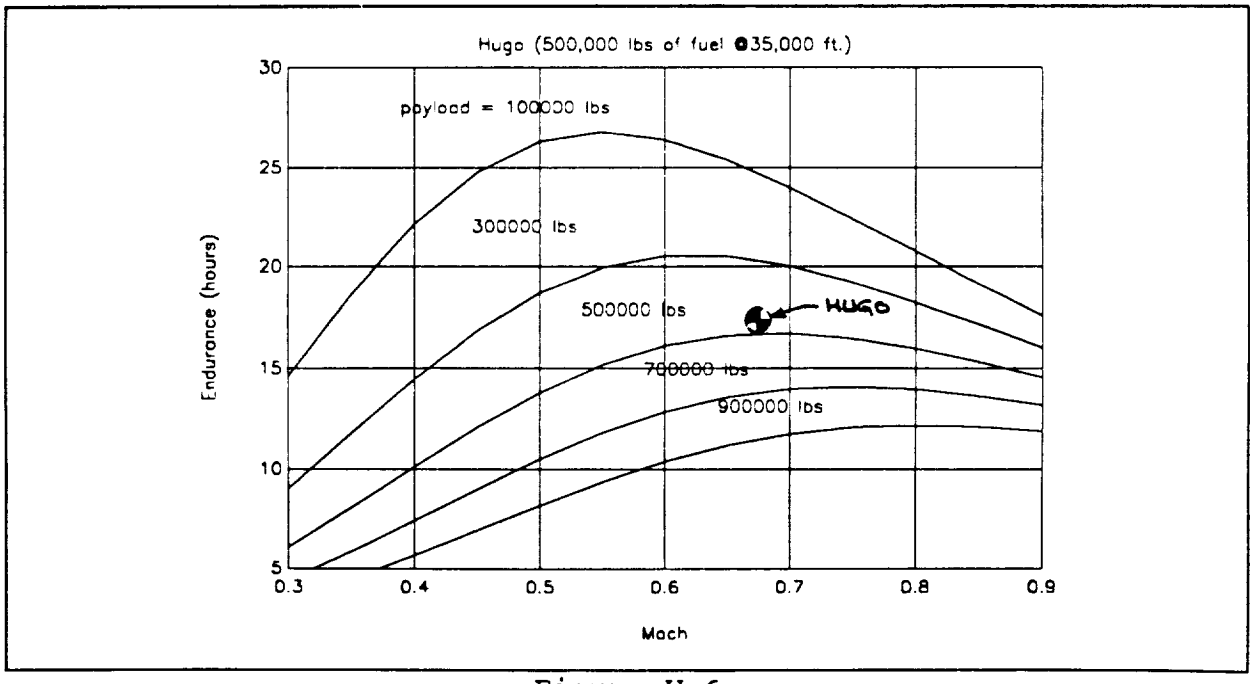

Figure V-6
HUGO Endurance

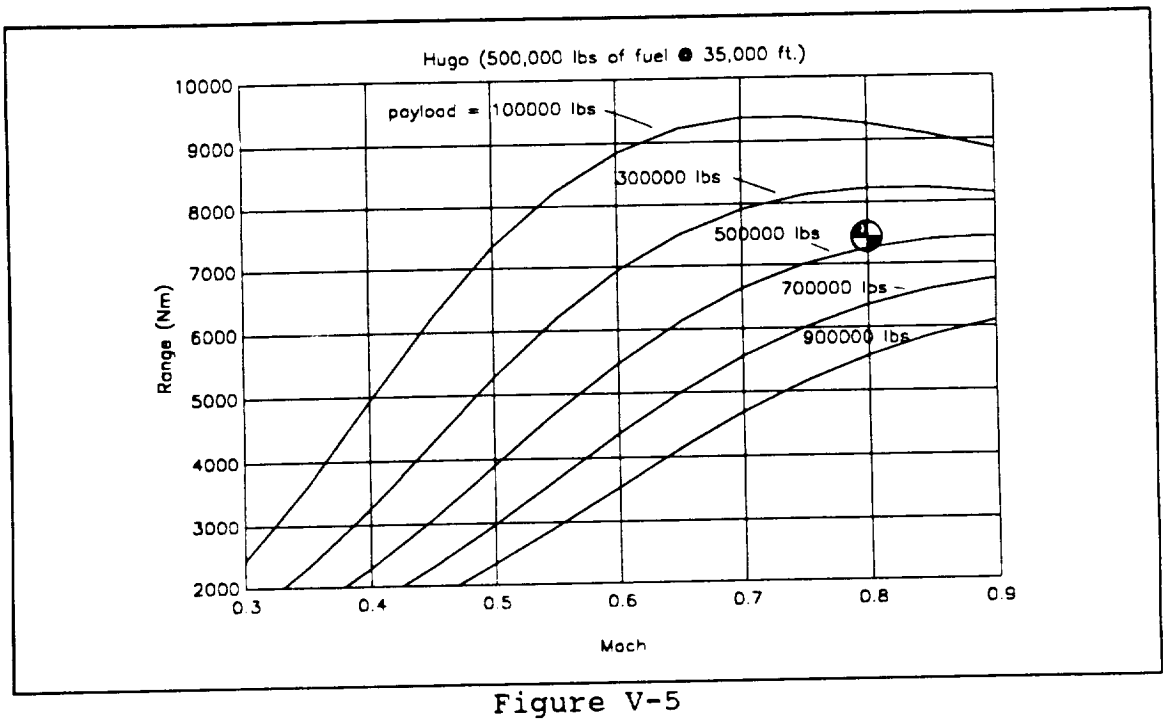

Figure V-5
HUGO Range

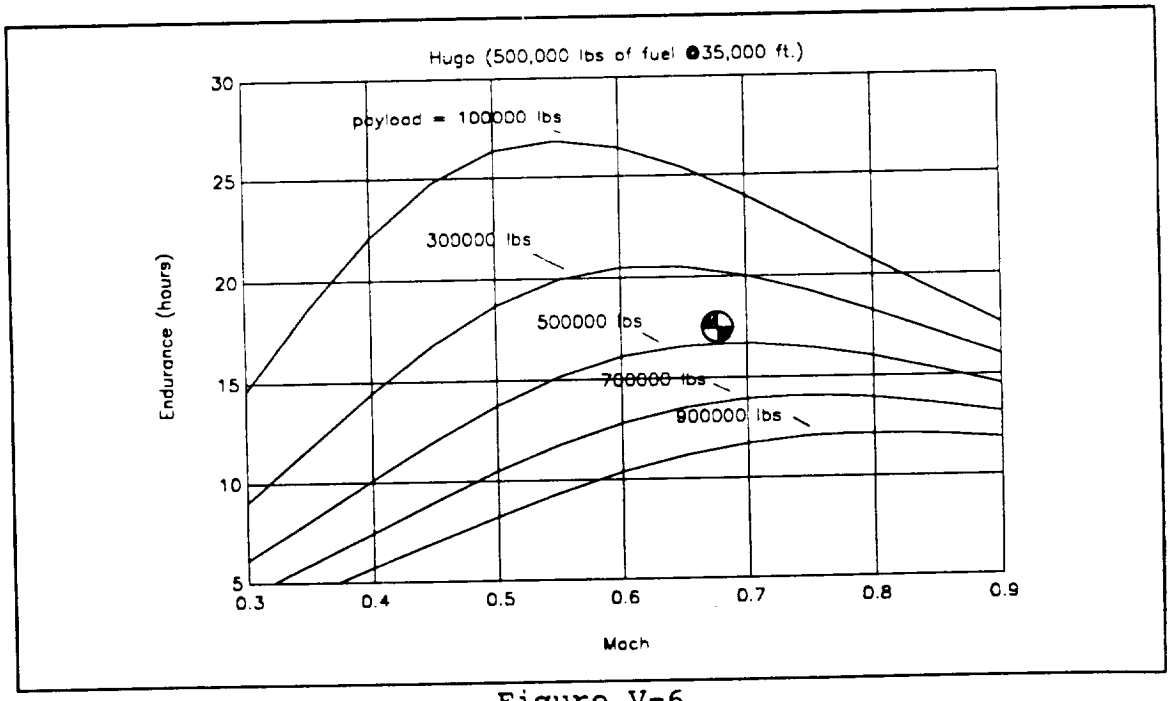

Figure V-6
HUGO Endurance

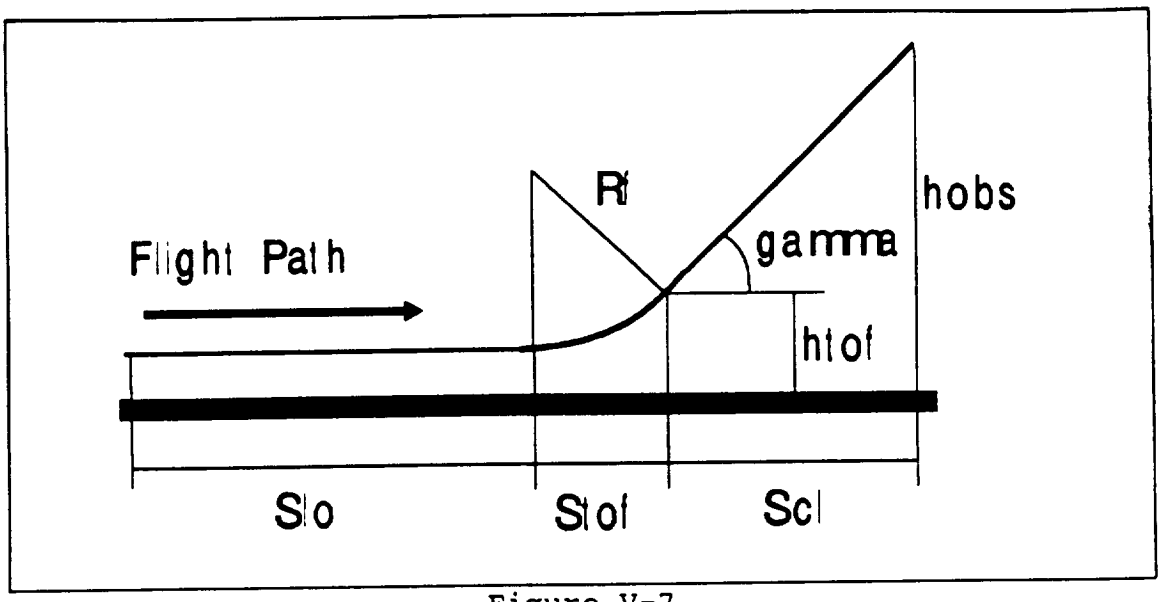

Figure V-7
Takeoff Schematic

this technology adds cost and weight to the aircraft both of which are critical parameters, the enormous benefits mentioned earlier justify the cost and weight penalties. The endurance plot can be seen in Figure V-6.

6. Takeoff Performance

Takeoff performance was calculated using a dry runway with a coefficient of friction of .025 and was divided into three distinct phases, ground roll (Slo), the takeoff rotation (Stof) and climbout (Scl) as seen in Figure V-7. Additionally, a climbout angle of 20 degrees was used for the obstacle clearance. Figure V-8 shows the various takeoff distances for both the ground roll and the 50 foot obstacle

clearance. Standard, tropical and hot day data were used at various altitudes for the calculations.

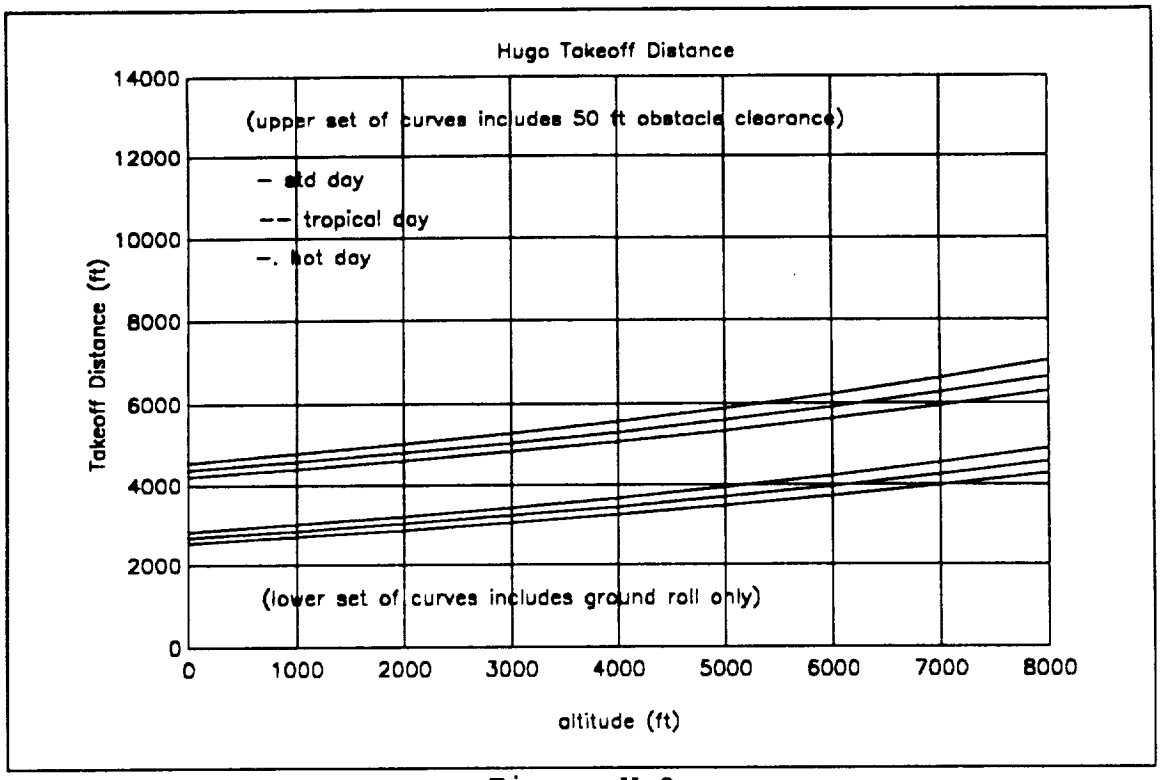

Figure V-8
HUGO Takeoff Distance

7. Landing Distance

In a similar manner, the landing data was calculated using a dry runway coefficient of friction of .3 and were divided into three distinct phases, approach (Sgl), landing flare (Slf) and landing rollout (Slr). An approach angle of five degrees was used for the obstacle clearance as seen in Figure V-9.

Figure V-10 shows various landing distances for both the ground roll and the 50 foot obstacle clearance. Standard, tropical and hot days at various altitudes were used for the curves in Figure V-10.

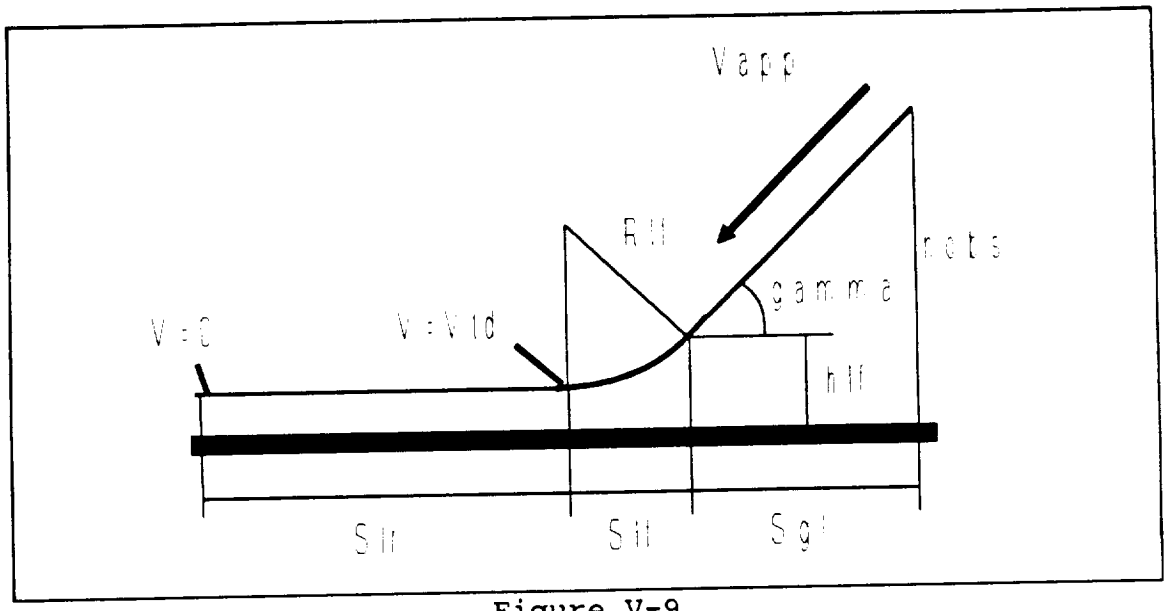

Figure V-9
Landing Schematic

8. Maneuverability

The sea level maneuvering envelope shown in Figure V-11 shows a sea level maneuvering speed of about 180 KIAS in a cruise configuration. Additional requirements as stated in the request for proposal for a 2.5 g positive maneuvering limit (V_{man} = 185 KIAS) and -1.0 g negative maneuvering limit are shown as well as the maximum speed at sea level (V_{max} = 450 KIAS).

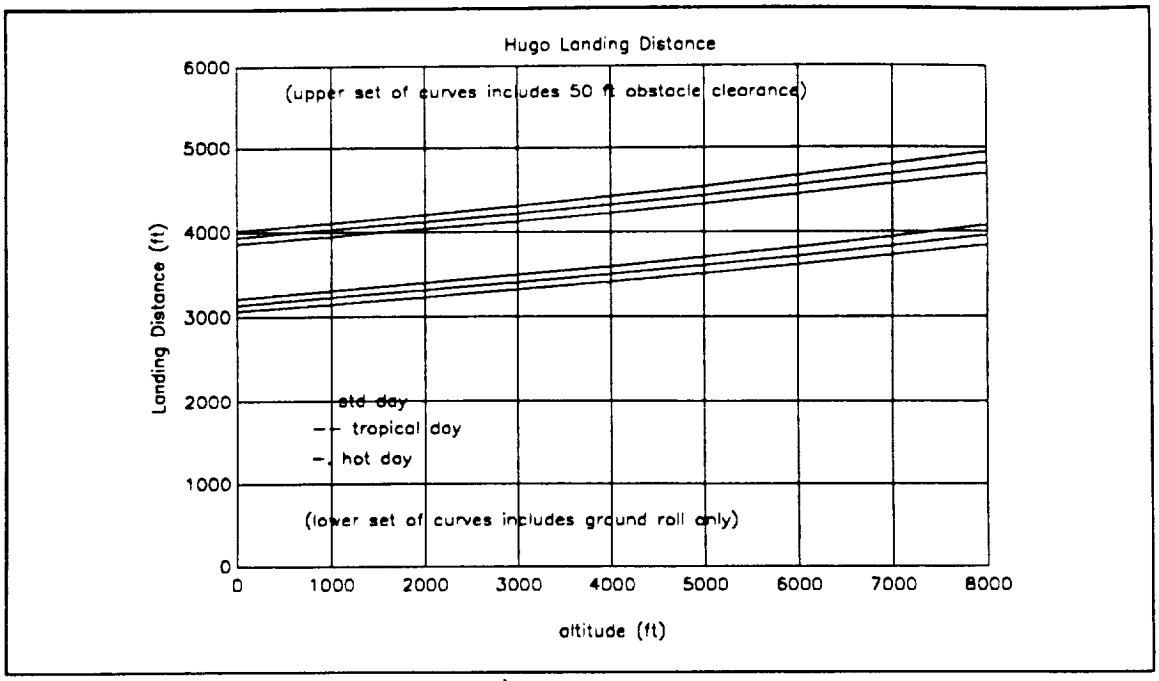

Figure V-10
HUGO Landing Distance

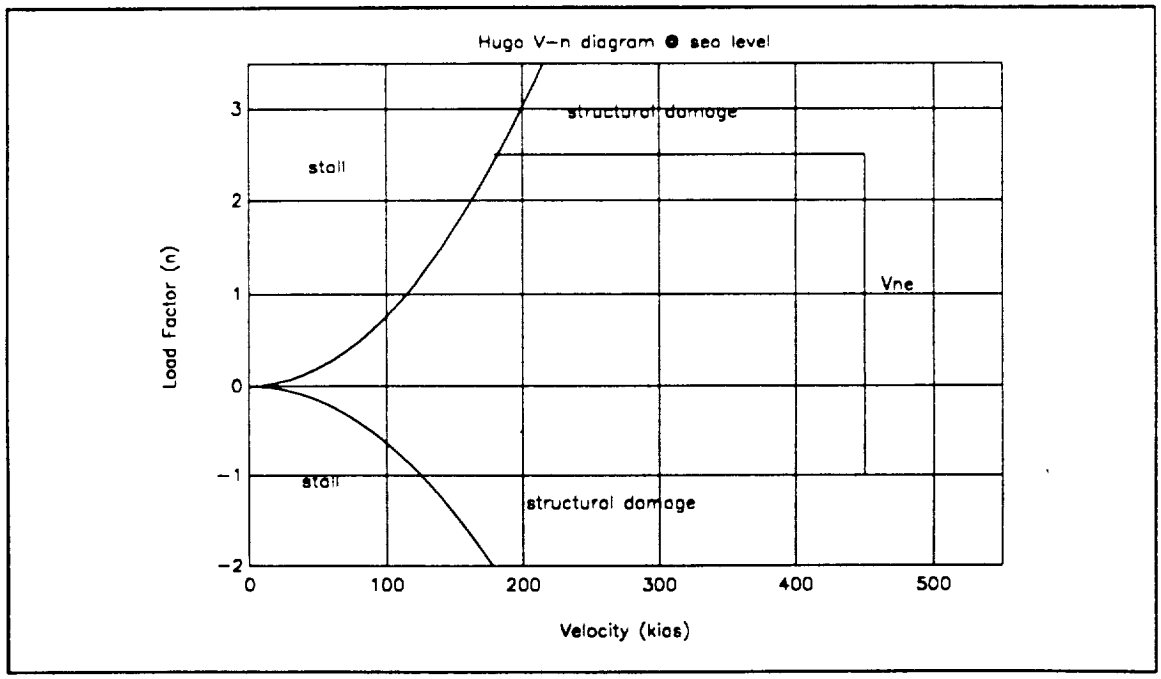

Figure V-11
HUGO Maneuvering Envelope

9. Critical Field Length

The critical field length is defined as the distance covered by an aircraft accelerating to the refusal speed and either continuing the takeoff, or after a three-second delay, applying maximum braking. The refusal speed is the speed at which the distance required to continue the takeoff or delay three seconds and apply maximum braking is equal. For Hugo the sea level critical field length for a standard day was found to be 4900 feet. For a hot day, at 4000 feet elevation, the critical field length was found to be 6100 feet. These distances at first glance appear short but when one considers that the sea level thrust is 600,000 pounds these values seem more reasonable. These short critical field lengths make Hugo capable of landing at a variety of fields further increasing its versatility.

VI. STABILITY AND CONTROL

A. INTRODUCTION

The Hugo design was planned to be a Class III transport which would normally operate in category B/C flight phase as defined by MIL-F-8785C, Reference 20. It was also desired that the aircraft meet level I flying qualities. The stability and control analysis was done using the methods outlined in Torenbeek, Reference 27, and Schmidt, Reference 26. Assumptions made during the analysis included:

- Linearized, small perturbation theory.
- Small deviations about a steady flight condition.
- No coupling between lateral and longitudinal stability derivatives.

The dynamic analysis was conducted at two flight conditions, M = .2 at sea level and M = .8 at 35,000 feet.

B. STATIC STABILITY

1. Longitudinal

The horizontal tail was sized to provide a positive C_{M_0} with a tail setting angle of 3 degrees. At flight conditions 1 and 2, C_{M_0} = .820 and .116, respectively. C_{M_α} was negative for both flight conditions which ensured a longitudinally stable and balanced aircraft. By maintaining the payload

center of gravity at approximately 1.33% MAC, the static margin was 13.5%.

2. Lateral

The aircraft displayed lateral static stability at both flight conditions with a negative C_{l_β} and a positive C_{n_β}. Several iterations of sizing the vertical tail area were required until acceptable values were achieved.

C. DYNAMIC STABILITY

1. Longitudinal

Table VI-1 lists the stability derivatives of the aircraft and shows values of the Lockheed C-5A and Boeing 747 in similar flight regimes. The aircraft longitudinal dynamics were analyzed for both flight conditions and are shown in Table VI-2 along with MIL-F-8785C requirements for level I flying qualities. The short period was stable at both flight conditions while the phugoid was unstable. Figure VI-1 shows the long period response to a longitudinal impulse.

2. Lateral

Listed in table VI-3 are the lateral stability results. At Mach .8, the Dutch-Roll damping did not meet level I flying qualities, but all other parameters were within limits. Figure VI-2 shows the Dutch-Roll response to a rudder impulse.

TABLE VI-1
Stability Derivatives

	HUGO		Lockheed C-5A		Boeing 747	
	M=.2	M=.8	M=.22	M=.8	M=.25	M=.8
C_l	3.2	.61	1.29	.5	1.11	.6
C_D	.4398	.035	.145	.035	.102	.06
$C_{L\alpha}$	4.62	4.71	6.08	6.2	5.70	4.9
$C_{D\alpha}$	1.97	.732	.622	.57	.66	.4
$C_{M\alpha}$	-.923	-.896	-.827	-1.3	-1.26	-1.1
$C_{L\dot{\alpha}}$	-4.315	-4.315			-6.7	
$C_{M\dot{\alpha}}$	-4.185	-3.275	-8.3	-7.6	-3.2	-6
C_{Lq}	3.831	3.63			5.4	
C_{Mq}	-24.114	-25.98	-23.2	-26.5	-20.8	-23.9
C_{LM}	-.982	.00901	-.09	.08	-.81	.2
C_{MM}	.41	.361	-.1	-.36	.27	.2
$C_{L\delta e}$	.396	.382	.385	.39	.338	.36
$C_{M\delta e}$	-1.72	-1.68	-1.6	-1.6	-1.34	-1.55
$C_{Y\beta}$	-.293	-.27	-.77	-.92	-.96	-.9
$C_{l\beta}$	-.0041	-.0018	-.123	-.15	-.221	-.28
$C_{n\beta}$	.0023	.01	.075	.08	.150	.19
C_{lp}	-.326	-.426	-.458	-.58	-.45	-.35
C_{np}	-.0390	-.023	-.098	-.06	-.121	-.5
C_{lr}	.00225	.00225	.290	.24	.101	.3
C_{nr}	-.00104	-.00104	-.293	-.2	-.30	-.33
C_{Yr}	.0247	.0247				
C_{Yp}	.01561	.01561				
$C_{l\delta a}$	.0912	.083	.089	.03	.0461	.014
$C_{n\delta a}$	.01001	.0090	.0091	-.005	.0064	0.0

TABLE VI-1
(continued)
Stability Derivatives

	HUGO		Lockheed C-5A		Boeing 747	
	M=.2	M=.8	M=.22	M=.8	M=.25	M=.8
$C_{Y\delta a}$	-.005	-.005	-.0044			
$C_{Y\delta r}$	.23	.23	.211	.2	.175	.12
$C_{L\delta r}$	.025	.025	.0209	.012	.007	.01
$C_{n\delta r}$	-.111	-.111	-.106	-.08	-.109	-.109

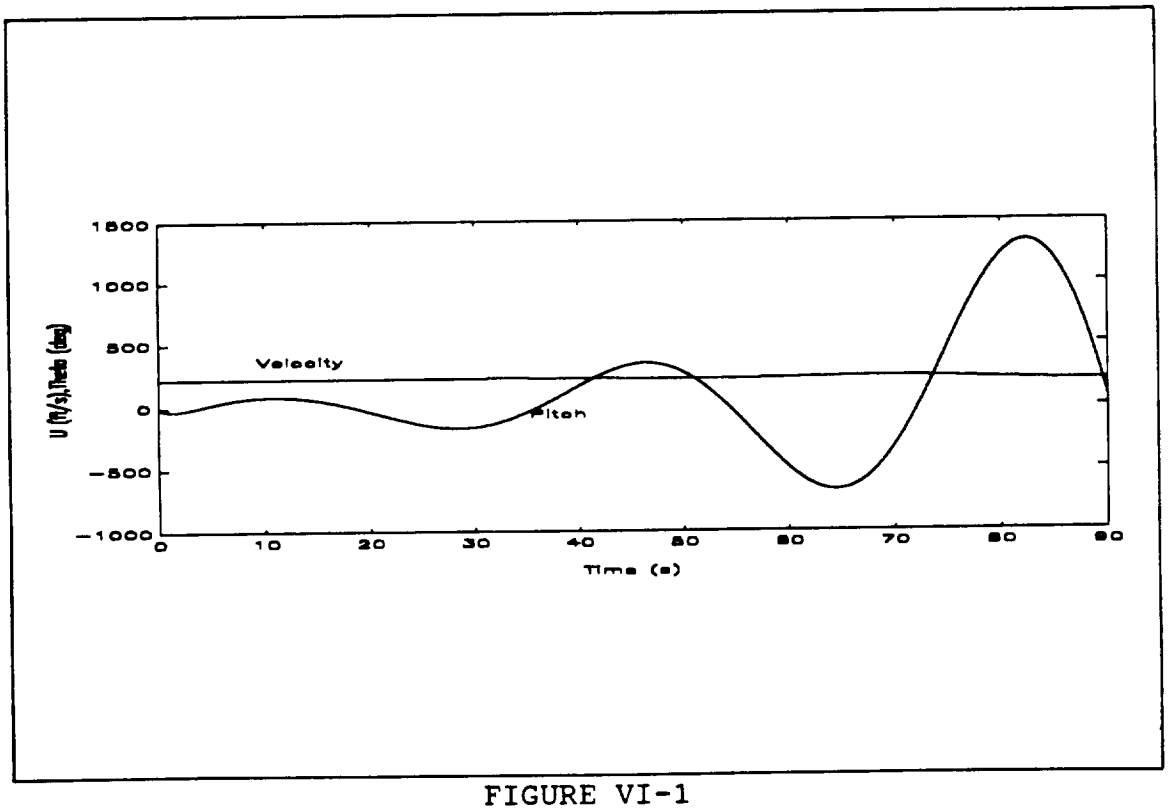

FIGURE VI-1
Unaugmented Phugoid Response

TABLE VI-2
Unaugmented Longitudinal Stability Results

	MACH =.2	MACH = .8	MIL-F-8785C
Short Period Roots	-.401±.226i	-.405±1.051i	Negative
Short Period Damping	.870	.360	.35-1.30
Short Period Natural Frequency	.461	1.126	NA
Phugoid Roots	.039±.181i	.009±.069i	Negative
Phugoid Damping	-.213	-.134	> .04
Phugoid Natural Frequency	.185	.069	NA

TABLE VI-3
Unaugmented Lateral Stability Results

	MACH = .2	MACH = .8	MIL-F-8785C
Dutch Roll Roots	-.0087±.096i	-.0099±.292i	Negative
Dutch Roll Damping	.091	.0341	Minimum .08
Dutch Roll Natural Frequency	.096	.292	
Roll Root	-.897	-1.223	Negative
Roll Natural Frequency	.897	.0341	
Roll Mode Time Constant	1.114	.817	Maximum of 1.4
Spiral Response Roots	.0001	.0002	NA
Spiral Natural Frequency	.0001	.0002	
Minimum Time to Double Amplitude	6930	3465	Minimum of 12

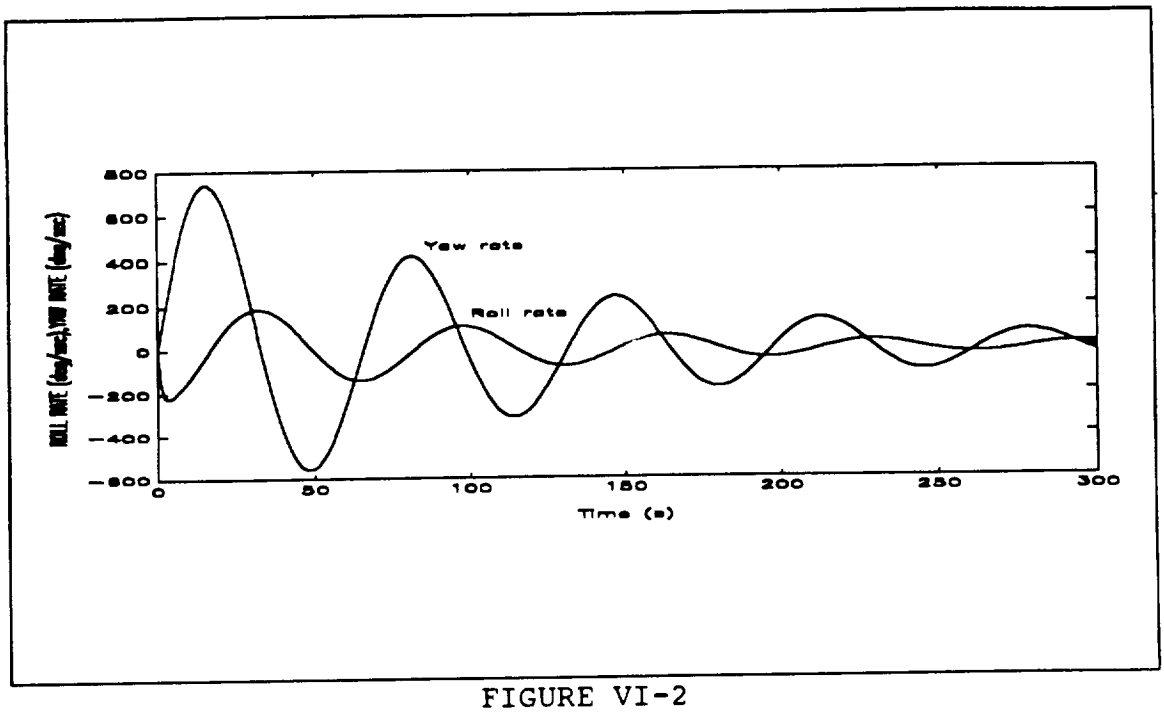

FIGURE VI-2
Unaugmented Dutch-Roll Response

D. STABILITY AUGMENTATION

1. SAS

To bring the aircraft up to Level I flying qualities, stability augmentation about all axes was used. Sensor noise was assumed minimal in order to estimate the pole placement. Table VI-4 and Table VI-5 show the results of the augmented aircraft. All requirements were met for Level I flying qualities with the exception of the Dutch-Roll damping at Mach .8. The Dutch-Roll damping of .0405 meets the requirements for Level II. Figure VI-3 shows the Augmented Phugoid Response and figure VI-4 shows the Dutch-Roll Response.

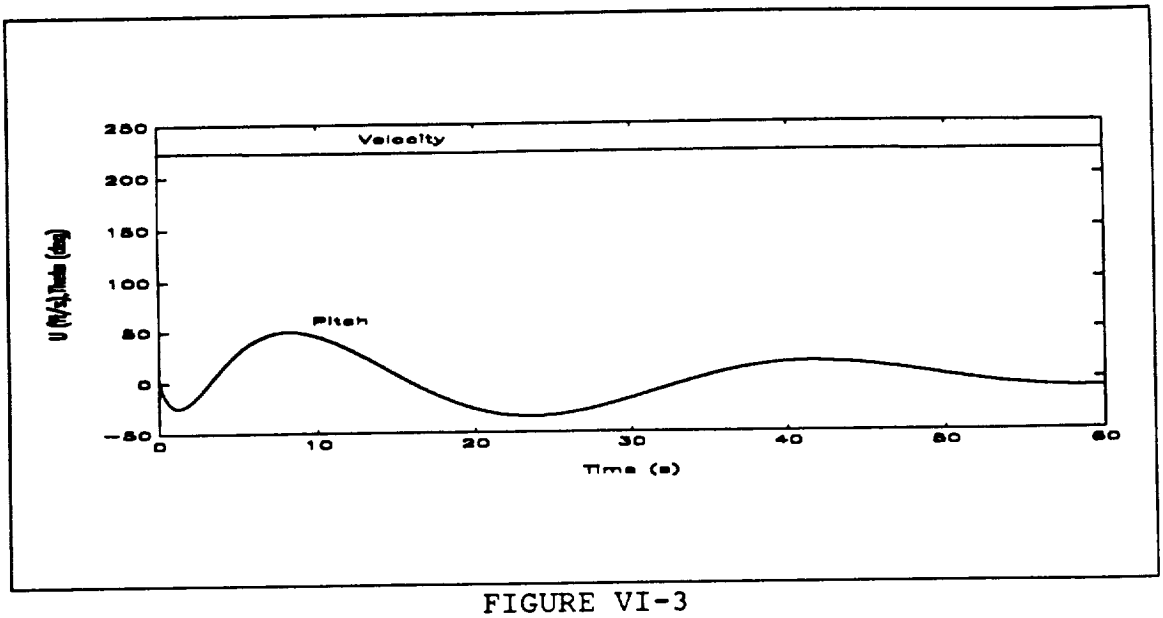

FIGURE VI-3
Augmented Phugoid Response

TABLE VI-4
Augmented Longitudinal Stability Results

	MACH =.2	MACH = .8	MIL-F-8785C
Short Period Roots	-.401±.226i	-.405±1.051i	Negative
Short Period Damping	.870	.360	.35-1.30
Short Period Natural Frequency	.461	1.126	NA
Phugoid Roots	-.039±.181i	-.009±.069i	Negative
Phugoid Damping	.213	.134	> .04
Phugoid Natural Frequency	.185	.069	NA

TABLE VI-5
Augmented Lateral Stability Results

	MACH = .2	MACH = .8	MIL-F-8785C
Dutch Roll Roots	-.0202±.097	-.0118±.292i	Negative
Dutch Roll Damping	.2041	.0405	Minimum .08
Dutch Roll Natural Frequency	.0988	.2918	
Roll Root	-.8977	-1.223	Negative
Roll Natural Frequency	.898	1.223	
Roll Mode Time Constant	1.114	.818	Maximum of 1.4
Spiral Response Roots	-.0091	-.0439	NA
Spiral Natural Frequency	.0091	.0439	
Minimum Time to Double Amplitude	76	15.8	Minimum of 12

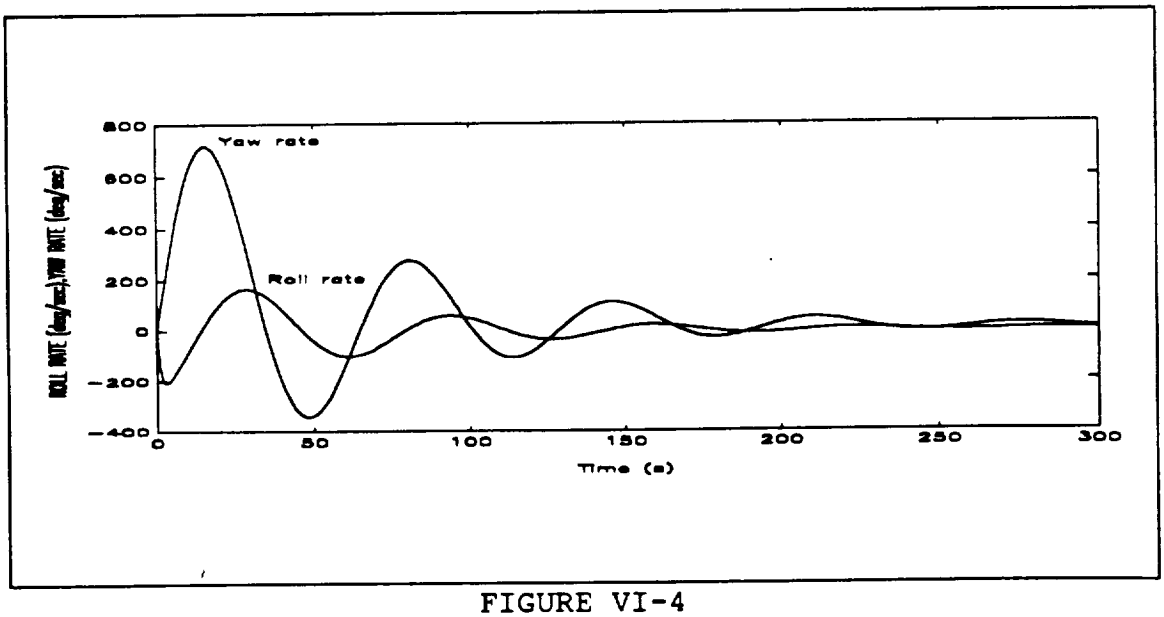

FIGURE VI-4
Augmented Dutch-Roll Response

VII. AIRCRAFT SYSTEMS

A. FLIGHT CONTROLS

The flight control system is divided into three major sections: flight control surfaces, flight control computers, and the hydraulic system. The design of the flight control system was based largely on existing technology thereby reducing Development, Test, and Engineering (DT&E) costs.

The primary flight control surfaces consist of right and left high and low speed ailerons, a two-surface rudder split into upper and lower segments, and right and left elevators. Additional flight controls consist of spoilers, full-span leading-edge slats, and Triple-slotted Fowler type trailing edge flaps. A quadruple redundant, all digital, Fly By Wire (FBW) control system is used to provide inputs to the control surfaces via electrical links and hydraulic actuators. A mechanical backup provides primary flight control inputs in the event of a total electrical failure. Mechanical failure or a total loss of hydraulic fluid will cause the primary flight controls to configure to a fail safe position.

HUGO's hydraulic system consists of three independent and redundant systems operating at 5000 psi. A trade study was performed to measure maintenance costs versus weight savings

as system pressure was varied. 5000 psi was the optimum. It allowed decreased system size and weight over lower pressured systems and decreased maintenance costs over higher pressure systems.

System number one, flight control one (FC1), is powered by engine driven pumps on the number 1, 3, and 5 engines. System number two, flight control two (FC2), is powered by engine driven pumps on the number 2, 4, and 6 engines. System number three, utility one (UT1), is powered by the number 1 and 2 electric pumps or either auxiliary power unit. Hydraulic power distribution is shown in Table VII-1.

TABLE VII-1
Hydraulic Power Distribution

FCI	FC2	UT1
LEFT AILERON	LEFT AILERON	NOSE GEAR
RIGHT AILERON	RIGHT AILERON	MAIN GEAR
RUDDER	RUDDER	LEFT SPOILER
LEFT ELEVATOR	LEFT ELEVATOR	RIGHT SPOILERS
RIGHT ELEVATOR	RIGHT ELEVATOR	AFT RAMP
NOSE GEAR	MAIN GEAR	AFT RAMP DOOR
INBOARD BRAKES	OUTBOARD BRAKES	NOSE VISOR
LEFT SPOILERS	RIGHT SPOILERS	NOSE RAMP
		GEAR KNEELING
		BRAKES
		NOSE WHEEL STEER

FC1 and FC2 provide power to all primary flight controls through dual tandem actuators. UT1 provides power to all utility functions and secondary flight controls. FC1 and FC2 are designed to operate on a minimum of two engine driven pumps. UT1 is capable of operating with a single electric pump. Isolation valves allow any of the three systems to be switched to flight essential only (primary flight controls, landing gear, and brakes).

The hydraulic pumps, electric and engine driven, are demand flow, variable delivery, pressure compensated, piston type. Each system has it's own self pressurizing reservoir to insure positive feed at altitude and it's own hydro-pneumatic accumulator to provide shock damping and emergency power. Nitrogen is used as a precharge gas in the accumulators. Fluid cooling is accomplished by heat exchangers using ram air supplemented by electric fans. The hydraulic system automatically monitors pressure, temperature, and fluid levels. Low pressure or fluid levels will cause each system to switch to alternate power sources or activate isolation valves to maintain control of the flight essential functions. Manual control and monitoring is accomplished by the flight crew through the hydraulic system control panel which displays the pressure, fluid level, and temperature of each system and controls the electric pumps, fire wall shutoff valves, and isolation valves. Low level, High temperature, and low

pressure caution lights are located on the pilot's master caution panel (Green, Reference 11).

The system uses SKY 500 type synthetic fluid that is non flammable and capable of operating over a wide temperature range. The increased hydraulic pressure reduces the volume of the system which increases survivability. Ground servicing of hydraulic fluid and nitrogen is accomplished through the ground servicing panel located on the exterior of the aircraft.

B. FUEL SYSTEM

The design of Hugo's fuel system was initially based on the total amount of fuel needed to meet mission requirements defined by the RFP. Once the capacity of the system was determined, further design decisions on size, number, location, and types of fuel cells were made. The final stage of the design effort focused on associated equipment such as pumps, lines, transferring and monitoring mechanisms, and refueling ports.

Hugo's fuel system is capable of holding 500,000 pounds(75,000 gallons) of usable fuel. This is, for comparison purposes, approximately five times the capacity of the Boeing 767 transport aircraft. The available volume for fuel storage in Hugo's wing was determined to be 20,000 cubic feet from Torenbeek, Reference 27, which is twice the volume needed to hold the required 75,000 gallons. Eight 1250 cubic foot cells

are located symmetrically in the center wing section as shown in Figure VII-1. A wet center wing section was used to meet the capacity requirements while maintaining low structural loading during ground operations.

Submerged electric boost pumps in each fuel cell provide positive pressure from the tanks at all times. Engine driven fuel pumps on each engine are capable of suction feed in the event of boost pump failure. The boost pump and engine driven pump size and configuration are designed to provide 1.5 times the maximum required amount of fuel flow to the engines (Roskam, Reference 25). Engine bleed air is utilized by the pressurization and vent system to maintain tank pressure during flight and prevent excess pressure build up during ground operations. Cross-feed valves are located as shown in Figure VII-1 to provide a means for fuel load balancing. The transfer system can be run automatically or manually and will degrade to a manual gravity transfer mode in the event of multiple transfer pump failure.

Hugo has four high pressure refueling ports to facilitate rapid refueling and each port is capable of single point refueling. In addition, each cell has a gravity refueling port on the upper wing in the event that pressure refueling is not available. Fuel dump capability is provided by two dump valves and two dump ports which are capable of discharging up to 80% of the total fuel load.

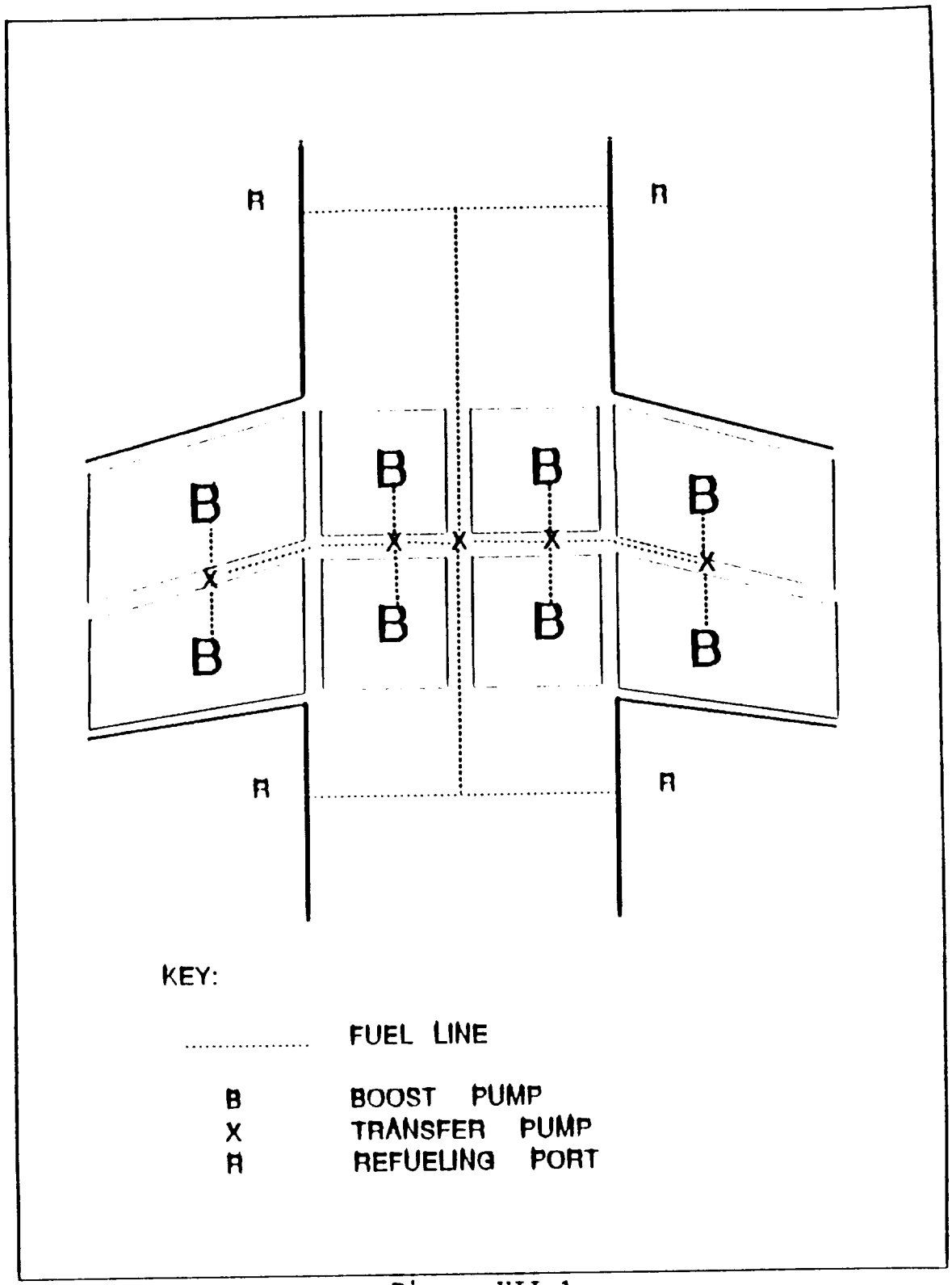

Figure VII-1
Fuel System

Hugo's fuel cells are self sealing and crash resistant to increase survivability. Reticulated foam is installed in each cell to increase survivability. Dry bays and fire walls are used to increase separation between the fuel cells and the engine, passenger, and cargo compartments. Fire wall shut off valves and fire detection/extinguishing systems are installed in each engine.

C. ELECTRICAL SYSTEM

Hugo's electric power is provided by two systems for redundancy: The primary system that supplies essential power under normal operating conditions, and the secondary system which supplies power during ground operations or upon primary system failure. An electric power load profile (Roskam, Reference 25) was constructed to determine the maximum amount of electrical power needed during a typical mission profile. The electrical system was designed to meet the needs of the load profile while operating in a degraded mode (partial electrical failure).

Primary power is produced by six 100 KVA engine driven generators. Six transformer rectifiers convert AC power to DC power. Total AC power requirements can be met by any three generators and total DC power requirements can be met by any three transformer rectifiers.

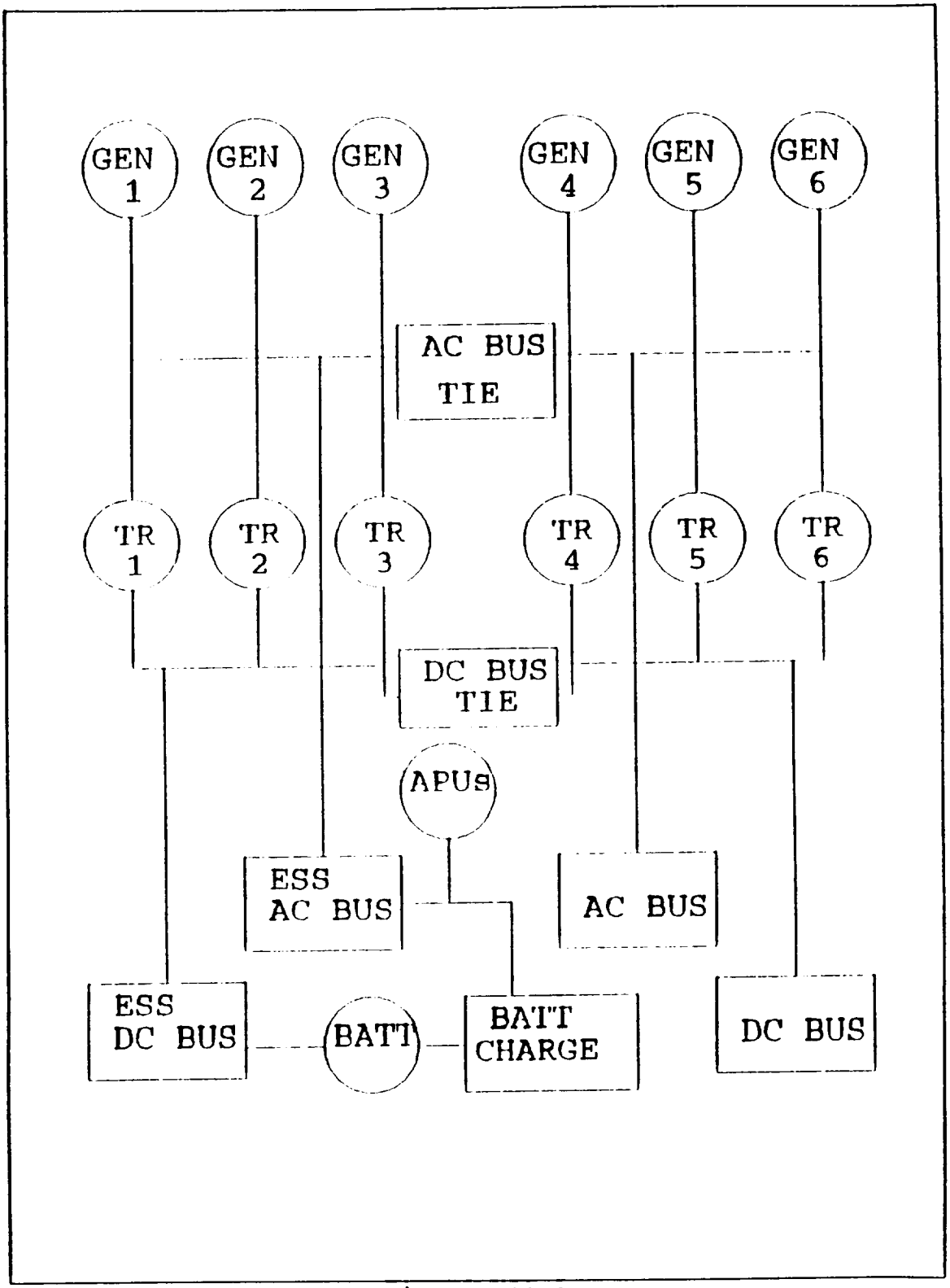

Figure VII-2
Electrical System

Power distributions are shown in Figure VII-2. AC and DC bus tie relays automatically prevent loss of power to AC and DC buses. Power is distributed through four separate electrical buses. The power to each bus is continuously monitored for over/under voltage. A system fault is automatically corrected by switching the faulty source out of the system. Non essential items are automatically shed when electrical power demands exceed the available power. Flight essential buses and wiring bundles are widely separated to avoid electrical system failures due to localized damage. Also, electrical system components are carefully shielded to reduce lightning strike damage and electrical interference.

Secondary power is produced by batteries or the APUs. Redundancy in the electrical system and the ability to independently operate at remote sights is an essential design parameter. The batteries can provide power to the essential DC buses in the event of a total electrical failure. The primary function of the batteries is to start the APUs during normal ground operations or emergency in flight operations. The batteries are continuously charged in flight. One 100 KVA generator on each APU provides emergency power to the essential AC bus and normal AC power during ground operations. Power can also be provided during ground operations through an external power receptacle.

D. ENVIRONMENTAL SYSTEM

The primary functions of the environmental system are pressurization, air conditioning, anti-icing, de-icing, and oxygen supply. Pressurized air is supplied to the system by tapping compressor bleed air from all six engines. This air is pressure controlled by using diffusers and temperature controlled by using heat exchangers, ram air, and additional bleed air. The air is then routed through duct systems for various uses within the environmental system (Roskam, Reference 25).

The pressurization system automatically follows a preset schedule on climb out and maintains cabin altitude below 10,000 feet while at cruise altitude. The climb schedule may also be manually selected and set by the flight crew. Pressurization is maintained by inflatable seals around the cabin doors, nose visor, and aft ramp doors. All seals are automatically inflated after takeoff but can be manually over ridden in flight. Pressure relief valves provide positive and negative pressure relief to protect the aircraft structure.

Cooled bleed air is mixed with ram air for cooling and additional bleed air for heating. Air is distributed in the cabin and cargo areas through ducting with the use of electric fans. The design point for the air conditioning system is flight idle descent since this flight condition leads to minimal bleed air availability (Roskam, Reference 25).

Heating and cooling can be separately controlled for cabin and cargo compartment.

Anti-icing systems, which prevent the formation of ice, include windshield heat, engine inlet and cowling heat, and windshield defog. De-icing systems, which remove ice, include electric impulse devices installed on thee wing and tail leading edges (Roskam, Reference 25).

Two liquid oxygen bottles provide oxygen to crew and passengers in case of intentional or unintentional depressurization. Pressure breathing delator demand regulators with quick donning masks are available in the crew station. Commercial type masks which deploy automatically are installed in the passenger area.

E. AVIONICS

The design of the avionics system included cockpit layout as well as the selection of avionic components and flight management equipment. Again, the goal of the design was to use as much existing technology and off the shelf equipment as possible. Modular type components were extensively used to reduce repair complexity, maintenance costs, and down time.

Cockpit instrumentation layout is uncluttered and extremely functional consisting almost exclusively of advanced flat panel multifunction displays. Dual air data computers with digital avionics are used together with four multifunction color displays to present the flight crew with

essential information. Primary flight data is presented on full flight regime Heads-Up Displays (HWD). The multifunction displays can be selected to present primary flight data, secondary flight data, or computer generated flight plan and weather radar overlays. Frequency tuning for all navigation and communication equipment is accomplished from a glare shield control panel.

The master warning and annunciator panel automatically monitors major systems provides visual, aural, and voice alerts. Dual flight control computers are tied into the Global Positioning System (GPS) and inertial navigation system to provide advanced autopilot control including auto throttle and thrust management.

F. AUXILIARY POWER UNITS

Hugo has two APUs located on opposite sides of the aircraft belly, aft of the nose visor. Their primary function is to provide electrical power, hydraulic pressure, and bleed air. These functions allow engine start and normal ground operations. Both APUs are fed from the main fuel supply and can be started using Hugo's batteries or by external power connection. In flight, the APUs can be used to provide emergency power. Each APU is equipped with a 100 KVA

generator and hydraulic pump similar to the type used in the electrical and hydraulic systems. Intakes for the APUs are located on each side of the fuselage and exhausts are located on the bottom of the aircraft. Normal ground operations can be accomplished using a single APU.

VIII. SURVIVABILITY

A. OVERVIEW

History has shown that when an aircraft has not been designed to survive in its operational environment, it will not be able to accomplish its mission with any regularity. Operational commanders will be forced to cancel raids, to change tactics, or even to remove aircraft from the area. Morale will be significantly reduced due to the lack of capable aircraft and crews. The increasing intensity and sophistication of air-defense systems will exacerbate this situation. Survivability cannot be ignored - its importance will not go away. The following vulnerability reduction concept was generated using Ball, Reference 2.

B. THE THREAT

The primary threat against HUGO was assumed to be small arms fire in the vicinity of the landing field. The design goal is that the aircraft should be capable of continued operation for at least 30 min after a single hit by a 7.62mm API projectile striking anywhere on the aircraft, fully tumbled at zero degree obliquity. (Zero vulnerable area for a B level attrition kill.) Surface-to-air missiles (SAMs) will be avoided by choosing a flight path to fly over friendly territory. One IR missile hit to an engine would not kill the

aircraft. Wollaston, Reference 28, concluded that the SA-12 was the most severe high altitude SAM threat, and that the SA-11 was the most severe low altitude threat. Wollaston also concluded that both could be avoided by remaining outside 35 NM from the launcher while at altitude; and remaining outside 8 NM from the launcher while flying at 500 feet above the ground (AGL), and remaining outside 6 NM while flying at 300 feet AGL.

C. VULNERABILITY REDUCTION

1. Fuel System

The fuel tankage and distribution subsystems represent the largest subsystems of the aircraft and are vulnerable to most damage mechanisms. If unprotected, the fuel system is likely to be the primary contributor to aircraft vulnerability. However, proper design of the fuel system will provide a significant degree of system protection. A high priority assigned to the design of the fuel system to reduce vulnerability will therefore be extremely effective in increasing the survivability of the aircraft.

The fuel tanks are located to minimize presented area to the primary threat direction. The fuel tanks, fuel lines, and other fuel system components are located so damage to one element will not cascade into other systems. The fuel tanks are located such that potential leakage from combat damage

will not flow nor be drawn into engine inlet ducts or into contact with possible ignition sources. Fuel lines are run through the fuel tanks to minimize this problem.

Self-sealing tanks are incorporated on HUGO to minimize the probability of fires, explosions, and engine fuel ingestion as a result of ballistic and hydraulic ram damage. A suction fuel feed system also is incorporated to reduce leakage if a fuel line is hit.

Flexible lightweight foam is installed in the ullage areas of the wing tanks, to minimize the possibility of fire or explosion. This will add very little weight, but reduces the vulnerable area of the fuel tanks by a factor of three. As the fuel tanks are the system with the highest vulnerable area, this one item greatly reduces the vulnerability of the aircraft.

2. Propulsion System

Since HUGO is a multi-engine aircraft, the vulnerability of the propulsion system is quite low. Some vulnerability reduction features are:

- Engines are not in line.
- Fire suppression in each engine.
- Separate fuel and oil tankage.
- Ability to feed any engine from any tank.
- Engines mounted high enough to avoid FOD damage.

- The lubrication system is fail safe to avoid oil starvation.

3. Flight Control System

Hugo's flight control systems is designed to ensure there will be no unacceptable degradation of functional capabilities due to one or more component failures. Many of the safety of flight features, such as independent hydraulic subsystems and backup controls, cause a reduction in vulnerability. Two independent hydraulic subsystems with hydraulic lines separated physically will provide redundancy with separation.

The flight control system was also designed to prevent loss of flight control due to a single hit by a damage mechanism anywhere on the system; that is, there will be no single point failure possibilities. To accomplish this, techniques such as multiple, independent, and widely separated control signal paths, motion sensors, control surfaces, and control power systems are used. No component failure should result in a hard-over signal to a control surface actuator. Jam protection and override capability are included in the design. Heat-resistant materials are used to protect those control components located in areas where fires or hot gas impingement could occur.

Steps have been taken to ensure there is no reduction of control power resulting from a loss of hydraulic fluid.

This is accomplished by using reservoir level sensors, and hydraulic fuzes. The servoactuators are made ballistically resistant by using electroslag remelt steel for the power barrel.

Since HUGO is a fly by wire flight control system, the motion sensors are located on opposite sides of the fuselage to avoid the possibility of a single hit kill of the system, which could kill the aircraft.

The control surfaces and hinges are made fail-safe, by making the control surfaces damage-tolerant, and using multiple hinges.

IX. MANAGEMENT

A. PRODUCTION

Hugo's production plan is based on previous manufacturing experience integrated into a planned framework to insure quality and efficiency. Production cost is specifically addressed due to the low quantity production and the high cost of test aircraft. The production plan consists of four areas; manufacturing organization, aircraft sectional breakdown, subcontracting plan, and production planning outline. The aircraft sectional breakdown of HUGO consists of six major areas: nose section/cockpit, fuselage, tail section, landing gear, engines, and wing. The final assembly line where two HUGOs are produced, is based on this breakdown. The production plan calls for numerous components to be subcontracted to companies where cost efficiency and expertise prove advantageous. The production planning outline translates the engineering design and specifications into completed hardware and components.

Subassembly sections are supported by specialty shops such as tooling, composites, machine, or plastics. Extensive use of computer aided design and manufacturing (CADCAM) integrates airframe design functions to machine control systems. This provides a greater utilization of machines, closer control of

production, improved balance between machining and assembly operations, and reduced labor costs. Also, design data stored in computer memory, can be used to produce production planning information and form a close link between engineering and manufacturing. (Hornk, Reference 13). Quality assurance representatives conduct rigorous final inspections and checks of all subsystem integration and major assembly points.

B. MAINTAINABILITY

Hugo is designed to perform over a 20-year life cycle with minimum costs and maximum availability. Five fundamental maintainability principles (standardization, modularization, functional packaging, interchangeability, and accessibility) are incorporated into every area of Hugo's design to assure sustained performance with minimum expenditure of money and effort.

Standardization assures compatibility between mating parts, common tools, and test equipment while minimizing spare parts inventory. Modularization enforces conformance of assembly configurations to dimensional standards and simplifies assembly and disassembly procedures. Functional packaging assures that all components performing a specific function are located in readily removable and replaceable units so that replacement of a single unit can completely correct a particular failure. Interchangeability controls dimensional and functional tolerances and minimizes

adjustments needed to achieve proper functioning. Accessibility controls spatial arrangements of equipment and parts to allow replacement or repair in place. Accessibility also limits the amount of material removed to gain access to critical equipment thereby reducing down time. (Moss, Reference 21).

Hugo also has an aircraft monitoring system (AMS) designed to provide fault isolation and annunciation. The system uses built in test (BIT) equipment integrated into each individual system or subsystem to allow flight crew or maintenance personnel to display failure and system status information and perform in flight and ground tests on critical equipment. The AMS continuously monitors systems performance, limitations, and discrepancies and notifies the flight crew of any abnormalities or system degradation.

Table IX-1 compares Hugo's predicted mean flight hours between failure (MFHBF) and maintenance man hours per flight hour (MMH/FH) to a variety of aircraft. MFHBF and MMH/FH for HUGO were estimated using multiple functions relating parameters such as thrust to weight, wing loading, and aspect ratio to maintainability. The functions used were developed from existing aircraft maintenance data. The incorporation of rigorous maintainability principles into the design phase and the availability of an extensive AMS system is factored into the calculations of Hugo's MFHBF and MMH/FH figures. Also contributing to HUGO's maintainability is its high sortie

length and high utilization rate. All other aircraft data was taken from 3-M data records and Nicolai, Reference 22.

TABLE IX-1
MFHBF & MMH/FH COMPARISON

	MFHBF	MMH/FH
FA-18	2.3	24
F-14D	0.6	61
C141	0.8	21
KC-135	0.9	27
C-5	0.8	40
HUGO	3.0	25

C. SUPPORTABILITY

Hugo is designed to adapt easily into existing ground support systems. Standard external power connections, hydraulic service units, refueling ports, and liquid oxygen servicing units allow required supportability without specialized equipment. Also, the requirement for specialized tools has been kept to a minimum.

D. LIFE CYCLE COST ANALYSIS

Life cycle cost (LCC) analysis was completed using methods outlined by Nicolai, Reference 22, and Earles, Reference 5, parameter design techniques. LCC estimates cover the cost of the aircraft from "cradle to grave" which includes development test and evaluation (DT&E), production, and operations and maintenance (O&M) phases. Hugo was designed from existing technology and will be manufactured at existing facilities. Therefore, costs for research, test facilities, and manufacturing facilities were omitted from the analysis.

Nicolai's methods utilize basic cost estimate relationships (CER) based on the development, test and evaluation, and production costs for 29 aircraft built between 1945 and 1970. The CERs relate cost to weight, speed, and quantity of aircraft produced. Monetary amounts were adjusted to 1993 dollars by an economic escalation factor. Basic principles and CERs associated with the Earle's methods were utilized to estimate LCC as a comparison to Nicolai's methods.

Two parametric studies were performed to optimize the cost of Hugo. The first study related operating cost to block time and payload for a fixed operating range. The purpose of this study was to determine how cost per ton-mile would vary as payload and block time were varied around design constraints. The second parametric study related cost to payload delivered within a fixed period of time. This study was performed

specifically to examine Hugo's ability to meet the logistic requirements of the RFP. The goal of the design team was to maximize the amount of payload delivered within a 72 hour period while minimizing the cost. The results of the parametric studies indicated that a fleet of 37 aircraft with a payload capability of 450,000 pounds was optimal for a continuous logistic operation over the range specified by the RFP. Once these basic parameters of the design were established, a LCC comparison was made between several design choices (Twin fuselage subsonic, single fuselage subsonic, single fuselage supersonic) to determine the optimum design.

Tables XI-2, XI-3, and XI-4 show Hugo's DT&E, production, and O&M costs estimated from Nicolai's methods. Table XI-5 shows Hugo's DT&E, investment, and operating and support (O&S) costs estimated from Earles' methods. Table XI-6 compares the LCC derived from each method. The LCC using Nicolai's CERs produced a value that was 33% lower than the LCC calculated from Earles' methods. Each technique used different approaches with varying degrees of complexity which points out the need to apply several techniques when estimating LCC. A best estimate for LCC for the HUGO is most probably a combination of both methods. Table IX-7 shows a final comparison of cost per pound between Hugo and several aircraft based on Hugo's estimated unit cost and the actual unit cost of other aircraft.

TABLE IX-2
DT&E COSTS (NICOLAI METHODS)

AIRFRAME ENGINEERING	$ 1067 million
DEVELOPMENT SUPPORT	$ 419 million
FLIGHT TEST AIRCRAFT	$ 2012 million
FLIGHT TEST OPERATIONS	$ 197 million
PROFIT	$ 369 million
TOTAL DT&E COSTS	**$ 4.07 billion**

TABLE IX-3
Production Costs (Nicolai Methods)

ENGINE AND AVIONICS	$ 1197 million
MANUFACTURING LABOR	$ 3044 million
MATERIAL AND EQUIPMENT	$ 603 million
SUSTAINING ENGINEERING	$ 1751 million
TOOLING	$ 1732 million
QUALITY CONTROL	$ 541 million
PROFIT	$ 887 million
TOTAL PRODUCTION COSTS	**$ 9.76 billion**

TABLE IX-4
O&M Costs (Nicolai Methods)

YEARLY FUEL COSTS	$ 261 million
YEARLY MAINTENANCE COSTS	$ 25 million
YEARLY CREW COSTS	$ 15 million
YEARLY O&M COSTS	**$ 302 million**
LIFE CYCLE O&M COSTS	**$ 6.04 billion**

Table IX-5
LCC Analysis (Earles Methods)

DT&E	
AIRFRAME	**$ 5.86 billion**
PROPULSION	
AVIONICS	
INVESTMENT	
SUPPORT EQUIPMENT	**$ 14.55 billion**
INITIAL SPARES	
TECHNICAL DATA	
TRAINING	
OPERATIONS	
FUEL	**$ 10.03 billion**
MAINTENANCE	
OTHER	

Table IX-6
Life Cycle Cost Analysis
Earles vs. Nicolai

	EARLES	**NICOLAI**
TOTAL LCC	$ 30.44 billion	$ 19.87 billion
COST PER PRODUCTION A/C	$ 485 million	$ 325 million

TABLE IX-7
HUGO Cost per Pound Comparison

	COST PER POUND
C-17A	$ 506 / lb
C-5	$ 425 / lb
HUGO	$ 303 / lb

X. SUMMARY

As the United States enters the new century, it must have the required resources to rapidly respond to United Nations' requests for peace enforcement and other national interests. The **best solution** to meet these needs and that will guarantee an effective platform is HUGO. **HUGO** is the **optimum choice** that meets or exceeds all AIAA RFP requirements and restraints. **High reliability, maintainability, and supportability** ensure significantly improved availability and increased sortie generation capability during peak/extended periods of demand over any previous or planned platform. Ideal HUGO secondary missions would include: Airborne C^3, Air refueling tanker, and aeromedical evacuations. HUGO is cost effective and highly survivable. Mission effectiveness has been maximized through software intensive, multifunction systems. Extensive use of composite materials has decreased time consuming corrosion control measures. **U. S. procurement** of **HUGO** would **guarantee** the **most effective global range transport platform for global mobility.**

REFERENCES

1. Anderson, John D., Introduction to Flight, Third Edition, McGraw-Hill, Inc., New York, 1989.

2. Ball, Robert E., The Fundamentals of Aircraft Combat Survivability: Analysis and Design, American Institute of Aeronautics and Astronautics, New York, 1985.

3. Barber, E., Noggle, L., and Rettie, I., Preliminary Design and Analysis of Advanced Military Transports (AIAA-77-1224), American Institute of Aeronautics and Astronautics, Inc. 1977.

4. Currey, Norman S., Aircraft Landing Gear Design: Principles and Practices, American Institute of Aeronautics and Astronautics, Washington, D. C., 1988.

5. Earles, M. E., Factors, Formulas, and Structures for Life Cycle Costing, Eddins-Earles, Concord, Massachusetts, 1981.

6. Etkin, Bernard, Dynamics of Flight, Stability and Control, Second Edition, John Wiley and Sons, Inc., New York, 1958, 1982.

7. Federal Aviation Regulations Part 25, Air Worthiness Standards: Transport Aircraft.

8. Forsch, Hans, Structures and Material Selection, American Institute of Aeronautics and Astronautics/University of Dayton, Aircraft Design Short Course, 1977.

9. Garrard, Wilfred C., The Lockheed C-5 Case Study in Aircraft Design, American Institute of Aeronautics and Astronautics, 1961.

10. Gouhin, Patrick, 1992/1993 AIAA Team Aircraft & Individual Aircraft Competition Engine Data Packages, American Institute of Aeronautics and Astronautics, Washington, D.C., 1992.

11. Green, W. L., Aircraft Hydraulic Systems, Wiley-Interscience, New York, 1985.

12. Harris, Charles D., NASA Supercritical Airfoils, NASA Technical Paper 6932, Langley Research Center, Hampton, Virginia, 1991.

13. Hornk, D. F., Aircraft Production Technology, Cambridge University Press, 1986.

14. Kirkpatrick, D. L. I., Review of Two Methods of Optimizing Aircraft Design, Royal Aircraft Establishment, Farnborough, Hamshire, United Kingdom.

15. Kuchemann, D., The Aerodynamic Design of Aircraft, Pergamon Press, Oxford, United Kingdom, 1978.

16. Lange, R. and Bradley, E., Parametric Study of Advanced Long Range Military/Commercial Cargo Transports (AIAA-77-1221), American Institute of Aeronautics and Astronautics, Inc. 1977.

17. Martin, C. L., Taguchi's Parameter Design Optimization Method Applied to Aircraft Systems, Georgia Institute of Technology, 1989.

18. Mattingly, Jack D., Heiser, William H. and Dailey, and Daneil H., Aircraft Engine Design, American Institute of Aeronautics and Astronautics, New York, 1987.

19. Meese, J. R. and Millett, M. L., The 21st Century Tactical Airlifter, Society of Automotive Engineers, Inc., 1988.

20. MIL-F-8785C, Flying Qualities of Piloted Aircraft, Military Specifications, Nov 1980.

21. Moss, Marvin A., Designing For Minimal Maintenance Expense, Marcel Dekker Inc., New York, 1985.

22. Nicolai, Leland M. , Fundamentals of Aircraft Design, METS, Inc., San Jose, California, 1984.

23. Raymer, Daniel P., Aircraft Design: A Conceptual Approach, American Institute of Aeronautics and Astronautics, Washington, D. C., 1989.

24. Roberts, R., Fiorentino, A. J., and Greene, W., NASA/Pratt & Whitney Experimental Clean Combustor Program - Engine Test Results, NASA Conference Publication 2021, Aircraft Engine Emissions, Lewis Research Center, 1977.

25. Roskam, Jan, Airplane Design, Part IV: Layout Design of Landing Gear and Systems, Roskam Aviation and Engineering Corp., Ottawa, Kansas, 1986.

26. Schmidt, L. V., Introduction to Aircraft Flight Mechanics, Naval Postgraduate School, Monterey, California, 1992.

27. Torenbeek, Egbert, Synthesis of Subsonic Airplane Design, Delft University Press, Delft, The Netherlands, 1976.

28. Wollaston, James W. and Brown, Derrell L., VSTOL Design Implications for Tactical Transports, Society of Automotive Engineers, Inc., 1988.